D Y N A M I C E F F E C T S
O N T H E G A S E X C H A N G E P R O C E S S
I N T W O S T R O K E C Y C L E E N G I N E S

Thesis by

Peter Kyropoulos

In Partial Fulfillment of the Requirements

For the Degree of

Doctor of Philosophy

California Institute of Technology

Pasadena, California

1948

ACKNOWLEDGMENT

The author is greatly indebted to Professor Robert L. Daugherty and Dr. Frederick C. Lindvall for their untiring help, suggestions and patience in supervising this research.

The help of Dr. Donald E. Hudson in questions of instrumentation is gratefully acknowledged.

Thanks go to Messrs. Donald Laird, Ray Kingan and Jack Kingan of the Mechanical Engineering Shop for their help in making the many alterations necessary in the test engine.

TABLE OF CONTENTS

I ABSTRACT

Recent investigations of fuel injection in spark ignition engines have aroused new interest in two stroke cycle engines. The performance of such engines is very much affected by the dynamic behaviour of the fresh air introduced and the exhaust leaving the cylinder through ports, receivers and silencers. The present investigation has as its aim the clarification and establishment of trends in the performance of two stroke engines with particular reference to crank case scavenged engines.

The basic relations governing the flow of air and gas through the whole system are investigated one by one and their interdependence is established. The investigation covers: pulsations in the cylinder, accelerations in the ducts, effect of variable port area, effect of throttling in the ports. The basic differential equation for free oscillation of the exhaust gas in the system comprising receiver, exhaust pipe, and silencer is set up and a method is developed which allows calculation of an equivalent length for the system. With this equivalent length, the natural frequency of the system can be calculated.

An experimental investigation is presented which was carried out on a single cylinder compression ignition engine with crank case scavenging. The volumetric efficiency of the engine was determined as a function of exhaust system configuration at various brake mean effective pressures and at constant engine speed. The pressure in the exhaust near the port was measured (by means of a quartz and crystal pickup) as a function of crank angle.

The results are presented in the form of plots of volumetric efficiencies as function of brake mean effective pressure for various configurations and as photographic records of pressure as a function of

crank angle.

It is concluded that a simple frequency analysis is insufficient for the determination of the exhaust behaviour. Criteria for good exhaust systems are established. The trends predicted in the theoretical analysis of the report are, in general, well verified.

The need for further investigation is indicated and an outline of research is presented.

II. INTRODUCTION AND OUTLINE OF INVESTIGATION

The development of the reciprocating internal combustion engine has reached a stage in which major improvements of output per unit displacement or specific fuel consumption are no longer to be expected. Any further improvement in the future must come from small gains obtained by painstaking development of numerous details.

The conventional gasoline engine with carburetor has been developed exclusively on the four-stroke cycle principle, since the two-stroke cycle results in poor fuel economy due to scavenging losses.

Compression ignition engines of the two-stroke cycle type are built extensively, since in this type only air is introduced into the cylinder during intake and scavenging. Therefore, no loss of fuel occurs. One of the most highly developed and successful high speed compression ignition engines (General Motors Series 71) is of the two-stroke type. Larger engines use blower scavenging, either directly driven or employing exhaust turbines. Crankcase scavenging is believed to be impracticable. Its limitations have, however, not been investigated. Figure 2 shows the cross section through a typical blower scavenged two-stroke engine (General Motors Series 71). Figure 1 shows the cross section through a crank case scavenged two-stroke engine (Venn Severin).

The advent of direct injection of gasoline in spark ignition engines shows great promise, especially with respect to utilization of low octane fuel in high performance engines.

Fuel injection, taking place near top dead center, removes the main objection--low fuel economy--against the two stroke cycle for gasoline engines (Reference 1).

The advantage of the two-stroke cycle, on the other hand, is, that a larger number of power strokes are performed by an engine of comparable weight and size of a four stroke cycle engine.

In two-stroke engines, the processes of gas exchange, i.e. intake, scavenging, and exhaust, are known to be of considerably greater importance to the overall performance of the engine, than they are in four stroke cycle engines.

Since there has been, in the past, little incentive to study this problem, few investigations of basic nature have been made. The work which has been done has been mostly along the lines of development of exhaust systems for specific engines. In many cases solutions are sought by assuming that steady state conditions prevail in the system, such as e.g. the use of two dimensional models and steady flow of water for the investigation of scavenging processes. The validity of such assumptions is then checked by means of performance tests of the complete engine. There is room for doubt as to whether or not such procedure is entirely satisfactory.

Specifically, the following questions are to be investigated:

(1) In what manner do unsteady flow conditions affect the intake, scavenging, and exhaust process of a two stroke engine?

(2) What is the effect of pressure pulsations on the engine flow?

(3) How do the physical parameters: cylinder volume, port size, speed, and dimensions of the duct system affect the conditions of flow?

(4) What is the effect of scavenging pressure on the flow?

(5) What are the limitations of crankcase scavenging?

None of the questions mentioned are restricted to any one type of engine, or to either spark or compression ignition.

The effect of altitude on two stroke engines has been discussed (Reference 7) and will not be included in detail.

The investigation is made without regard to specific applications. Questions of mechanical design have, therefore, been omitted at the present time.

The experimental work done in connection with the present investigation was carried out on a single cylinder two-stroke compression ignition engine with crank case scavenging.

III. PROBLEMS OF THE SCAVENGING PROCESS IN GENERAL

During the downward stroke of the piston, the exhaust port opens first. The exhaust gases "blow down" during which process they must be accelerated to sonic velocity. When the intake port opens, expansion in the cylinder must be such that the cylinder pressure is equal to or lower than the intake pressure.

When the intake port or ports open, the scavenging period begins.

The scavenging air in the intake duct must be accelerated very quickly. It then enters the cylinder through an opening of varying cross-section formed by the port and the receding piston.

The following dynamic phenomena must then be distinguished:

Opening of ports, both inlet and exhaust, produces sudden pressure waves, which propagate in the cylinder with the velocity of sound. These waves may be reflected at the walls and may lead to reverberation.

The weight of air entering through the inlet port is not necessarily the same as the amount of gas leaving the cylinder through the exhaust port, hence both weight of charge and pressure may vary in the cylinder.

The flow accelerated in inlet and exhaust ports represents inert masses which interact with the mass in the cylinder. These masses represent a second possible oscillating system.

The columns of gas in intake and exhaust ducts may themselves oscillate, representing the third possible vibrating system.

Upon opening of the port, the entering or leaving flow must first be accelerated.

The following questions arise in this connection:

(1) What is the effect of the time required for acceleration?

(2) Is the kinetic energy of the exhaust capable of producing a

pressure decrease in the cylinder, thus aiding scavenging, and how can this be analyzed?

(3) The shape of the flow of scavenging air is significant for the expulsion of the burned gases. Can this shape be determined?

(4) Residual velocity and swirl of the scavenging air is necessary for combustion control. Can this motion be analyzed or predetermined?

IV. PULSATIONS IN THE CYLINDER

Pulsations in the cylinder are produced by pressure disturbances at the ports. These are reflected at the walls. Only low frequency vibrations need concern us here.

The largest distance in the cylinder during scavenging exists between piston and cylinder head. The gas in this space oscillates longitudinally (in direction of the cylinder axis), and the system behaves like a pipe with both ends closed.

For this case the amplitude λ is equal to twice the distance between piston and cylinder head, i.e. twice the stroke.

$$\lambda = 2\,L$$

and the frequency

$$\nu_{gas} = 2\,\pi\,\frac{a}{\lambda} = \frac{\pi\,a}{L}$$

where a = velocity of sound in the gas. Expressing the engine frequency in terms of the mean piston speed C_m

$$\nu_{engine} = \frac{\pi\,n}{30} = \frac{\pi\,C_m}{L}$$

we obtain the ratio of gas to engine frequency

$$\frac{\nu_{gas}}{\nu_{engine}} = \frac{\pi\,a}{L} \times \frac{L}{\pi\,C_m} = \frac{a}{C_m} \qquad \text{- - - - - - - - - - - - - - (1)}$$

We see that the natural frequency of the gas is of the order of 100 times the engine frequency. Resonance is not likely to occur, especially since the pressure waves are excited by only small portions of the cylinder walls, (i.e. the ports). We conclude that the pressure in the cylinder is uniform with respect to space, except for changes which are due to the motion of the gas through the cylinder. It is not uniform with respect to time.

V. ACCELERATIONS IN THE DUCTS

After opening of the inlet port, the air in the scavenging duct and part of the cylinder contents must be accelerated (Figure 3).

The first process is similar to that of flow from a pressure vessel into a pipe as in Figure 4.

Neglecting entrance and discharge effects, we have Euler's equation

$$\frac{\partial w}{\partial t} + w\frac{\partial w}{\partial x} = -\frac{1}{\rho}\frac{\partial p}{\partial x} \qquad \text{----------} \quad (2)$$

Integrating along the pipe

$$\int_0^l \frac{\partial w}{\partial t}\,dx + \frac{w^2}{2} = -\int_{p_o}^{p} \frac{dp}{\rho} \qquad \text{----------} \quad (3)$$

If the flow is already accelerated, we get with the steady state velocity the usual efflux equation

$$\frac{w_o^2}{2} = -\int_{p_o}^{p_1} \frac{dp}{\rho} \qquad \text{----------} \quad (4)$$

with w_o in Equation 3, we get

$$\int_0^l \frac{\partial w}{\partial t}\,dx = \frac{w_o^2 - w^2}{2} \qquad \text{----------} \quad (5)$$

This equation holds also if there is a friction pressure drop in the pipe in which case W_o, the steady state velocity, is smaller than corresponds to the pressure drop $p_1 - p_o$ without pressure drop due to friction.

We concluded before that propagation waves in the cylinder had no effect if the distances traversed were of the order of the stroke.

In dealing with short scavenging ducts, this will be true also for waves in these ducts. (This is not true for long scavenging ducts or exhaust ducts).

Again the acceleration $\partial w/\partial t$ is independent of the station in the pipe x and we have

$$\frac{\partial w}{\partial t}\,dx = \frac{dw}{dt}\int_0^l dx = l\,\frac{dw}{dt} \qquad \text{- - - - - - - - - - - - (6)}$$

$$\therefore \quad \frac{dw}{dt} = \frac{w_o^2 - w^2}{2\,l} \qquad \text{- - - - - - - - - - - - - - - - - - (7)}$$

and the solution

$$\frac{w}{w_o} = \tanh \frac{w_o\,t}{2\,l} \qquad \text{- - - - - - - - - - - - - - - - - - (8)}$$

Boundary conditions

$$w = 0 \text{ at } t = 0$$

Figure 5 shows the behavior of the function tanh. It is seen that the function:

(1) Approaches 1 asymptotically

(2) Starts with slope 1 at origin

The acceleration at the origin, i.e. at the start of motion is:

$$\left(\frac{dw}{dt}\right)_o = \frac{w_o^2}{2\,l} \qquad \text{- - - - - - - - - - - - - - - - - - (9)}$$

This represents an acceleration similar to the free fall. Initial acceleration is such that a particle would attain the velocity w_o after traversing the entire tube. Actually this velocity is reached only asymptotically, since other particles must also be accelerated (steady state term of Euler's equation).

The distance covered by a particle is:

$$S = \int_0^t w\,dt = w_o \int_0^t \tanh \frac{w_o t}{2l}\,dt \qquad \text{----------(10)}$$

$$= 2l \ln \left(\cosh \frac{w_o t}{2l}\right)$$

$$\frac{S}{l} = 2 \ln \left(\cosh \frac{w_o t}{2l}\right) \qquad \text{----------(11)}$$

In Figure 6 S/l is plotted against $w_o t/2l$. We see that the first particle, after traversing the pipe (S/l = 1) has reached only 80% of its final velocity.

∴ A column of gas, accelerated by a constant pressure and flowing through a constant cross-section attains 80% of its final velocity after traversing a distance equal to the length of the column.

VI. EFFECT OF VARIABLE PORT CROSS SECTION

Flow through the inlet port begins as soon as the upper edge of the piston opens the port. The free cross-section of the port varies, therefore, during the opening period. Figure 7 shows the geometry of the system and the notation used.

From the simple continuity equation we have

$$f_x w_x = fw \; ; \qquad w_x = \frac{f}{f_x} w$$

With this equation (6) becomes

$$\int_0^l \frac{\partial w_x}{\partial t} dx = \frac{dw}{dt} \int_0^l \frac{f}{f_x} dx \qquad \text{- - - - - - - - - - - - - - - - (12)}$$

comparing (6) and (12), we see that the integral on the right corresponds to a length

$$\int_0^l \frac{f}{f_x} dx = l_1 \qquad \text{- - - - - - - - - - - - - - - - (13)}$$

i.e. the effect of varying section is replaced by an increase in effective length of the approach duct.

The integral may be evaluated graphically from a plot of f/f_x vs. x, as shown in Figure 8.

The question arises as to the effect of the ratio f/t. From considerations of steady flow, we should conclude that the larger the area, the less restricted the flow.

Consider two cases shown in Figure 9.

In the first case, denoted by (I), the total cross-section of the duct f_1 is opened in time t_o.

In the second case, denoted by (II), half the duct cross-section $f_o/2$ is opened but during twice the period of time. In both cases the product of area and time is the same.

$$f_1 \, t_o = \frac{f_1}{2} \, 2t_o \qquad \text{- - - - - - - - - - - - - - - - - (14)}$$

The flow through the area in Case I is $Q_I = f_1 \int_o^{t_o} w \, dt$

and with $\int_o^{t_o} w \, dt = S$ from equation (10)

$$S = 2 \, l \ln \left(\cosh \frac{w_o \, t_o}{2 \, l}\right.$$

$$Q_I = 2 \, f_o \, l \ln \left(\cosh \frac{w_o \, t_o}{2 \, l}\right) \text{- - - - - - - - - - - - - - - - (14.1)}$$

For case II we have from equation (13)

$$l_1 = \int_o^{l} \frac{f}{fx} \, dx = \int_o^{l} \frac{f_1}{2f_1} \, dx = \frac{l}{2}$$

Equation (7) then becomes

$$\frac{dw}{dt} = \frac{w_o^2 - w^2}{2 \, l_1} = \frac{w_o^2 - w^2}{l} \qquad \text{- - - - - - - - - - - - - - - - (15)}$$

with the solution

$$\frac{w}{w_o} = \tanh \frac{w_o \, t}{l} \qquad \text{- - - - - - - - - - - - - - - - (16)}$$

from which

$$Q_{II} = \frac{f_1}{2} \int_o^{2t_o} w \, dt = \frac{f_1 \, l}{2} \ln \left(\cos h \frac{w_o \, t_o}{2 \, l}\right) \text{- - - - - - - (17)}$$

In order to compare the two cases, Figure 10 was plotted.

Case (I) and (II) are seen to be different.

In spite of the smaller cross-sectional area of Case II, more flow enters the cylinder during the period of unsteady flow.

This result, in itself, does not necessarily mean that Case II results in better scavenging. It indicates, however, that it is necessary to investigate the flow into the engine as a problem of unsteady flow.

Case III

The actual engine cannot have the shape of f_1 vs t relation shown, since all opening and closing processes require a finite length of time.

We, therefore, investigate the case of a triangular function f_1 vs. t as shown in Figure 11.

Actual opening functions can always be approximated by a trapezoid composed of a rectangle as in Case I and II and a triangle as in Case III.

We then have

$$\frac{f}{f_1} = \frac{t}{t_o} \qquad \text{- - - - - - - - - - - - - - - - - - (18)}$$

$$w_x = \frac{fw}{f_x} = \frac{f}{f_1}\,\frac{f_1}{f_x}\,w = \frac{f}{f_1}\,w = \frac{t}{t_o}\,w \qquad \text{- - - - - - - - - - - - (19)}$$

where w_x is the velocity in the duct during the opening period. For equation (6), we get

$$\int_o^1 \frac{\partial w_x}{\partial t}\,dx = \left(\frac{t}{t_o}\frac{dw}{dt} + \frac{w}{t_o}\right)\int_o^1 dx = \frac{1}{t_o}\left(t\frac{dw}{dt} + w\right)$$

$$t\frac{dw}{dt} + w = \frac{t_o}{2\,l}\left(w_o^2 - w^2\right) \qquad \text{- - - - - - - - - - - - - - - - (20)}$$

with

$$\frac{w}{w_o} = W$$

$$\frac{dW}{dt} = \frac{\frac{w_o t_o}{2\,l}\left(1 - W^2\right) - W}{t} \qquad \text{- - - - - - - - - - - - - - - - (21)}$$

The particular integral for the opening period is, with the boundary conditions, $f = 0$ at $f = 0$

Velocity in the port

$$W' = \frac{\alpha}{1 + \sqrt{1 + \alpha^2}} = \frac{\frac{w_o t_o}{l}}{1 + \sqrt{1 + \left(\frac{w_o t_o}{l}\right)^2}} \qquad \text{------- (22)}$$

(prime denotes opening process)

Physically α represents the ratio of the distance traversed at the velocity of steady flow w_o to the length l.

The velocity in the duct

$$W_x' = \frac{t}{t_o} W \qquad \text{(see Equation 19)}$$

$$W_x' = \frac{t}{t_o} \frac{\alpha}{1 + \sqrt{1 + \alpha^2}} \qquad \text{------------------ (23)}$$

For the closing process, we chose a new origin for our coordinates, as shown in Figure 12, and write

$$w_x = \frac{t_o - t}{t_o} w \qquad \text{------------------ (24)}$$

$$\frac{dW}{dt} = \frac{\frac{\alpha}{2}(1 - W^2) - W}{t_o - t} \qquad \text{------------------ (25)}$$

Boundary condition is that at $t = 0$ the velocity in the duct is given by Equation (22).

$$W' = \frac{\alpha}{1 + \sqrt{1 + \alpha^2}}$$

Velocity in the port = $W'' = \dfrac{\alpha t_o (1+\alpha^2)^{1/2} - W'(t_o - t)(1+\alpha^2)^{1/2}}{\alpha W' t_o (1+\alpha^2)^{1/2} + (t_o - t)(1+\alpha^2)^{1/2}}$ - (26)

(during closing process)

The velocity in the duct is

$$W_x'' = W'' \frac{t_o - t}{t_o} \qquad \text{- (27)}$$

These relations, (22), (23), (26), (27), are plotted in Figure 13 for different values of α as parameter.

From the graph we conclude:

(1) In the port, the velocity is constant during the opening period and smaller than the velocity for steady state w_o since both

$$\frac{t}{t_o} < 1 \quad \text{and} \quad \frac{\alpha}{1 + \sqrt{1 + \alpha^2}} < 1$$

(2) In the duct the velocity is zero at $t/t_o = 0$ and increases with t/t_o. For a given t/t_o the velocity is the higher the larger α. For very large α the second part $\frac{\alpha}{1 + \sqrt{1 + \alpha^2}} \rightarrow 1$ and W becomes proportional t/t_o.

(3) During the closing period, the port velocity increases with t/t_o and becomes very large for small α and $t/t_o \rightarrow 1$, i.e. $t \rightarrow t_o$.

In that case, equation (26) becomes

$$W'' = \frac{\alpha t_o (1 + \alpha^2)^{1/2} + 0}{\alpha W' t_o (1 + \alpha^2)^{1/2} + 0} = \frac{1}{W'} \qquad \text{- - - - - - - - - - (28)}$$

The port velocity is always higher than the velocity of steady state.

(4) The duct velocity increases to a maximum and drops to zero. The maximum is lower and nearer closing (with respect to time) for larger l and lower w_o (velocity of steady flow in the duct).

Since the amount of flow Q is proportional to $w\,dt$, the area under

the curves for W' represents flow. It is seen that for large α the flow is approximately equal to the maximum flow, as given by the curve for $\alpha = \infty$,

VII. EFFECT OF THROTTLING IN THE INTAKE PORT

In order to permit flow from the intake (or scavenging system) into the cylinder, an excess pressure must exist in the intake system. The port then represents an orifice restricting the flow and it is in order to ask what effect the throttling in this restriction has on the scavenging process. This throttling effect, in general, includes the effect of all resistances opposing the flow in the system and the following considerations are applicable to the exhaust port and system as well as to the whole engine. The analysis applies both to piston controlled ports of a two stroke engine or the valve controlled ports of the four stroke engine. Figure 14 shows the geometry of the system and the notation used.

The ideal velocity of flow through the port, assuming adiabatic flow and validity of the perfect gas relation is

$$w_o = \left\{ 2g\, J\, C_p\, T_i \left[1 - \left(\frac{P_i}{P_c} \right)^{\frac{k-1}{k}} \right] \right\}^{1/2} \qquad \text{- - - - - - - (29)}$$

Any of the possible approximate forms of this equation may be used if applicable.

P_i = pressure in the intake receiver.

P_c = pressure in the cylinder.

The ideal velocity is proportional to the isentropic enthalpy drop. The actual velocity is smaller due to losses (reheat in turbine terminology).

A port efficiency can now be defined as follows:

$$= \frac{\text{isentropic } \Delta H - \Delta H_{loss}}{\text{isentropic } \Delta H} = \frac{\Delta H_{actual}}{\Delta H_{isentropic}} = 1 - \frac{H_{loss}}{H_{isentropic}}$$

The term $\frac{\Delta H_{loss}}{\Delta H_{isentropic}}$ represents the percent loss due to resistances in the system and shall be denoted by

$$\eta = 1 - \Lambda$$

This expression is related to the efflux velocities since

$$w_1 = \text{actual velocity} \sim \sqrt{\Delta H_{actual}}$$

$$w_o = \text{ideal velocity} \sim \sqrt{\Delta H_{isentropic}}$$

$$\frac{w_1}{w_o} = \sqrt{\frac{\Delta H_{actual}}{\Delta H_{isentropic}}} = \sqrt{1 - \Lambda}$$

Next we define a flow coefficient in the usual manner:

$$K = \frac{\text{actual weight of flow}}{\text{ideal weight of flow}} = \frac{B_{actual}}{B_{ideal}}$$

actual weight of flow $B_a = K\, B_{ideal}$.

Λ and K are interrelated, since

$$\Lambda = \frac{\Delta H_{actual}}{\Delta H_{isentropic}} = \frac{\text{work of isentropic expansion - losses}}{\text{work of isentropic expansion}}$$

$$\text{work of isentropic expansion} = \frac{w\, R\, T_1}{1 - K}\left[\left(\frac{P_i}{P_e}\right)^{\frac{k-1}{k}} - 1\right]$$

$$\frac{w_1}{w_o} = \frac{w_{actual}}{w_{isentropic}} = \sqrt{1 - \Lambda} = K\left\{1 + \Lambda\left[\left(\frac{P_i}{P_e}\right)^{\frac{k-1}{k}} - 1\right]\right\}$$

From which we obtain K in terms of Λ and the pressure ratio through which expansion takes place.

$$K = \frac{\sqrt{1 - \Lambda}}{1 + \Lambda\left[\left(\frac{P_i}{P_e}\right)^{\frac{k-1}{k}} - 1\right]}$$

This expression holds, of course, also for the flow through the engine from inlet to exhaust receiver in which case P_i/P_c is replaced by P_1/P_2, the ratio of intake pressure over exhaust pressure. K is then a volumetric efficiency. However, it is identical with the usually measured volumetric efficiency only if there are no losses in the induction system ahead of the intake port. For this reason, we shall retain the name flow coefficient in order to avoid confusion.

Since both pressures can be measured and K be found from measurement of air flow through the engine, Λ can be calculated.

The relation is plotted in Figure 15 (calculated from the foregoing equation). The effect of pressure ratio is relatively small in the range of pressure ratios which occur in the engine. Even at a pressure ratio of 2:1, i.e. with considerable boost, K is only 6% lower than for a pressure ratio of 1:1.

Remembering that Λ is proportional to the flow losses, we see that even with high losses, the flow coefficient is large. This is born out by the experience that crankcase scavenged engines show good volumetric efficiencies in spite of obviously unfavorable flow conditions (feather valves in the intake, low pressure towards the end of the scavenging period). This conclusion is significant. From the standpoint of engine performance, volumetric efficiency is the important item, since indicated power is directly proportional to the airflow through the engine. The foregoing analysis shows why attempts at improvement of performance by streamlining of ports and valves have not yielded, in general, much improvement in performance. Where such an improvement is found, it is most likely due to changed swirl in the combustion chamber, resulting in better mixing and combustion. This, in itself, is an important factor, but does not concern the present investigation.

On the other hand we conclude that a good volumetric efficiency does not necessarily mean a satisfactory pressure in the cylinder at the beginning of compression. The energy supplied by precompression of the intake air may be largely lost in overcoming resistance.

The losses may be calculated from the foregoing relation if the temperatures are known, since we have a case similar to the calculation of blower losses from T-S diagram shown in Figure 16.

Assuming perfect gas relations

$$\Lambda = \frac{T_2 - T_{2'}}{T_1 - T_{2'}}$$

$$T_2 - T_{2'} = \Lambda\,(T_1 - T_{2'})$$

for isentropic change of state

$$\frac{T_1}{T_{2'}} = \left(\frac{P_1}{P_{2'}}\right)^{\frac{k-1}{k}}$$

$$T_{2'} = T_1\left(\frac{P_{2'}}{P_1}\right)^{\frac{k-1}{k}}$$

$$T_2 - T_1\left(\frac{P_{2'}}{P_1}\right)^{\frac{k-1}{k}} = \Lambda\, T_1\left[1 - \left(\frac{P_{2'}}{P_1}\right)^{\frac{k-1}{k}}\right]$$

$$T_2 = \Lambda\, T_1\left[1 - \left(\frac{P_{2'}}{P_1}\right)^{\frac{k-1}{k}}\right] + T_1\left(\frac{P_{2'}}{P_1}\right)^{\frac{k-1}{k}}$$

$$= T_1\left[\Lambda + (1 - \Lambda)\left(\frac{P_{2'}}{P_1}\right)^{\frac{k-1}{k}}\right]$$

where T_2 is the actual temperature after throttling expansion.

The entropy increase due to irreversibility is a measure of the losses and is given by

$$S_2 - S_{2'} = C_p \ln \frac{T_2}{T_{2'}}$$

In general a detailed analysis will not be worth while and it is sufficient to estimate the magnitude of losses from Figure 15. For instance, a measured K = .75 at a pressure ratio 1.3:1 corresponds to a value of $\Lambda = .4$, i.e. the losses amount to 40% of the isentropic work of expansion. If this quantity is desired in terms of either Btu/lb or power, it can be calculated for any set of given conditions with the aid of Figure 15.

Summarizing it can be said that the velocity of the unsteady flow is unfavorable from the point of view of engine operation. It would be desirable to have high velocities at the beginning of the scavenging process in order to accelerate the flow quickly. This is not actually what happens. At the end of the process (closing) the velocity rises unnecessarily.

It should be noted that, in this respect, crank case scavenging is favorable, since there the pressure at beginning of the port opening is high, resulting in high velocities and rapid acceleration. The pressure drops as closing is approached, without a resulting decrease in velocity of the scavenging medium. This explains the relative efficiency of crankcase scavenging. It should also be noted that the density was considered constant, which is not true for higher Mach numbers. The results are, therefore, of the nature of an estimate. The analysis of throttling effects shows that in spite of energy losses in the ports, high volumetric efficiencies may be obtained.

VIII. THE DYNAMIC BEHAVIOUR OF INTAKE, CYLINDER AND EXHAUST DURING SCAVENGING AND EXHAUSTING.

During the intake process, the air in the duct is accelerated by an essentially constant pressure in the charging system.

During the exhaust process the gases are accelerated by the cylinder pressure, which decreases as the process progresses. Cylinder and exhaust gas represent a system capable of oscillating.

During the scavenging period both intake air and exhaust gas take part in the motion.

In order to estimate the dynamic effect of this process we neglect

(1) the variation in port opening due to piston motion.

(2) the flow inside the cylinder.

(3) the steady state term of the equation of motion

i.e. we consider only an oscillatory motion of intake and exhaust.

From Equation (3) we get for the inlet pipe (subscript i)

$$\rho_i l_i \frac{dw_i}{dt} = P_i - P \qquad \text{- - - - - - - - - - - - - - - - - - (29)}$$

and for the exhaust pipe (subscript e)

$$\rho_e l_e \frac{dw_e}{dt} = P - P_e \qquad \text{- - - - - - - - - - - - - - - - - - (30)}$$

The change with time of the contents of the weight B in the cylinder of volume V

$$\frac{dB}{dt} = \rho_i f_i w_i - \rho_e f_e w_e$$

$$= \frac{B}{V} (\rho_i f_i w_i - \rho_e f_e w_e) \qquad \text{- - - - - - - - - - - - - - - (31)}$$

For an isentropic change of state

$$\frac{dp}{p} = K \frac{dB}{B} \qquad \text{- - - - - - - - - - - - - - - - - - (32)}$$

where B = weight of substance in pounds and with $a = \sqrt{\frac{Kp}{\rho}}$, velocity of sound:

$$a^2 = \frac{Kp}{\rho}$$

$$dp = \frac{Kp\rho}{\rho B}\, dB = \frac{a^2 \rho}{B}\, dB$$

$$\frac{dp}{dt} = \frac{a^2 \rho}{B} \frac{dB}{dt} \qquad \text{- - - - - - - - - - - - - - - - - - (33)}$$

With

$$\frac{dB}{dt} = \frac{B}{\rho V} (\rho_i f_i w_i - \rho_e f_e w_e) \text{ - - - - - - - - - - - - -}$$

$$\frac{dp}{dt} = \frac{a^2}{V} (\rho_i f_i w_i - \rho_e f_e w_e) \qquad \text{- - - - - - - - - - - - - - (34)}$$

$$\frac{d^2p}{dt^2} = \frac{a^2}{V} \rho_i f_i \frac{dw_i}{dt} - \frac{a^2}{V} \rho_e f_e \frac{dw_e}{dt} \qquad \text{- - - - - - - - - - - (35)}$$

from (29) and (30) we get

$$\frac{dw_i}{dt} = \frac{P_i - P}{\rho_i l_i} \quad \text{and} \quad \frac{dw_e}{dt} = \frac{P - P_e}{\rho_e l_e} \qquad \text{- - - - - - - - - - - (36)}$$

and with that

$$\frac{d^2p}{dt^2} = \frac{a^2}{V} \frac{\rho_i f_i}{\rho_i l_i} (P_i - P) - \frac{a^2}{V} \frac{\rho_e f_e}{\rho_e l_e} (P - P_e) \qquad \text{- - - - - (37)}$$

$$\frac{d^2p}{dt^2} = - \frac{a^2}{V} \left[\frac{f_i}{l_i} + \frac{f_e}{l_e} \right] P + \frac{a^2}{V} \left[\frac{f_i}{l_i} P_i + \frac{f_e}{l_e} P_e \right] \qquad \text{- - - - (38)}$$

$$\frac{d^2p}{dt^2} + \frac{a^2}{V} \left[\frac{f_i}{l_i} + \frac{f_e}{l_e} \right] P + C = 0 \qquad \text{- - - - - - - - - - - (39)}$$

or

$$\frac{V}{a^2} \frac{d^2p}{dt^2} + \left[\frac{f_i}{l_i} + \frac{f_e}{l_e} \right] P + C' = 0 \qquad \text{- - - - - - - - - (39a)}$$

This equation is seen to be similar to that for a shaft clamped at the ends, having a disc between the supports, as shown in Figure 17.

$$I \frac{d^2\theta}{dt^2} + (C_1 + C_2)\,\theta = 0 \qquad \text{- - - - - - - - - - - - (40)}$$

$$C_1 = \frac{N J_1}{L_1} \qquad C_2 = \frac{N J_2}{L_2} \qquad \text{coefficient of stiffness} \qquad \text{- - - - - - - - (41)}$$

(see for instance: Reference 8, p. 122)

Coefficient of stiffness = couple required to twist the shaft through unit angular displacement.

N = modulus of rigidity

J = polar moment of inertia of shaft

Identifying terms in the second part of equation (39a) we find

$$C = \frac{f}{I}$$

$$I_m = \frac{V}{a^2} \qquad \text{- - - - - - - - - - - - - - - - - - (42)}$$

From this analogy, we write at once the frequency as

$$\nu = C \sqrt{\frac{C_1 + C_2}{I}} \quad \text{for the shaft} \qquad \text{- - - - - - - - - - - - (43)}$$

and

$$\nu = a \sqrt{\frac{1}{V}\left[\frac{f_i}{l_i} + \frac{f_e}{l_e}\right]} \qquad \text{- - - - - - - - - - - - - - - - - - (44)}$$

In order to estimate the duration of pressure fluctuation, we compare the frequency of pulsation with the engine frequency

$$\nu_{\text{engine}} = \frac{\pi n}{30} = \frac{\pi C_m}{S}$$

where C_m = mean piston speed.

Using f_p = piston area, S = stroke

$$\frac{f_i}{f_p} = F_i \qquad \frac{f_e}{f_p} = F_e$$

$$\frac{l_i}{S} = L_i \qquad \frac{l_e}{S} = L_e \qquad \text{- - - - - - - - - - - - - - - - - - (45)}$$

$$\frac{\nu}{\nu_e} = \frac{a}{\pi C_m}\sqrt{\frac{F_i}{L_i} + \frac{F_e}{L_e}} \qquad \text{- - - - - - - - - - - - - - - - - - (46)}$$

The root is usually of the order of .2 to .7, the ratio a/C_m from 60 to 100 so that approximately

$$\nu / \nu_e = \frac{80}{\pi} \times .45 = 11.5$$

or in degrees $\frac{360}{11.5} = 30^\circ$ crank angle.

Pulsations in the Ducts.

Pulsation in intake and exhaust ducts have been observed. They may affect the flow through the engine materially. As a result the so called "tuning of the exhaust system" is an important step in the development of exhaust duct and silencer systems.

In its simplest form the problem reduces to the oscillation of a gas in a straight pipe, or, similarly the longitudinal vibration of an elastic bar.

IX. THE BASIC DIFFERENTIAL EQUATION FOR THE LONGITUDINAL VIBRATION OF AN ELASTIC BAR.

The notation for the following analysis is shown in Figure 18.

Let a disturbing force act on the section resulting in a stress P. Disturbance produces uniform stress in plane x = 0 which, by continuity, is transmitted to adjacent particles.

If plane B is subjected to stress P, then at C we have

$$-\left(P + \frac{p}{x}\,dx\right) \qquad \text{- - - - - - - - - - - - - - - - - -} \quad (47)$$

The force on the element of cross sectional area A is

$$A \quad p - \left(P + \frac{p}{x}\,dx\right) \quad = -A\,\frac{p}{x}\,dx \qquad \text{- - - - - - - - - - -} \quad (48)$$

This force displaces the particles from their equilibrium position in direction of position x by a shift u in plane B.

Then in plane C, the shift is

$$-\left(u + \frac{u}{x}\,dx\right)$$

(partials, since p and u are both functions of x and f)

If φ = density, we get for the mass of the element

$$\frac{A\varphi}{g}\,dx = \text{mass}$$

$$\frac{\partial^2 u}{\partial t^2} = \text{acceleration} \qquad \text{- - - - - - - - - - - - - - - - - -} \quad (49)$$

Newton's law then gives

$$-\frac{A\varphi}{g}\,dx\,\frac{\partial^2 u}{\partial t^2} = A\,\frac{\partial p}{\partial x}\,dx$$

or

$$-\frac{\varphi}{g}\,\frac{\partial^2 u}{\partial t^2} = \frac{\partial p}{\partial x} \qquad \text{- - - - - - - - - - -} \quad (50)$$

The difference between the displacements (or shifts) for planes B and C is

$$u - \left(u + \frac{\partial u}{\partial x}\,dx\right) = -\frac{\partial u}{\partial x}\,dx \qquad \text{- - - - - - - - - - - - (51)}$$

Writing the stretch of the material

$$e = -\frac{\partial u}{\partial x}\,\frac{dx}{dx} \qquad \text{- - - - - - - - - - - - - - - - - - (52)}$$

and by definition

$$p = Ee = -E\,\frac{\partial u}{\partial x} \qquad \text{- - - - - - - - - - - - - - - - - - (53)}$$

(negative sign indicates that element is under compression)

Differentiating with respect to x

$$\frac{\partial p}{\partial x} = -E\,\frac{\partial^2 u}{\partial x^2} \qquad \text{- - - - - - - - - - - - - - - - - (54)}$$

Substituting this into

$$-\frac{\rho}{g}\,\frac{\partial^2 u}{\partial t^2} = \frac{\partial p}{\partial x} = -E\,\frac{\partial^2 u}{\partial x^2} \qquad \text{- - - - - - - - - - - - (55)}$$

$$\therefore \quad \frac{\partial^2 u}{\partial t^2} = \frac{Eg}{\rho}\,\frac{\partial^2 u}{\partial x^2} \qquad \text{- - - - - - - - - - - - - - - - - - (56)}$$

$$\frac{\partial^2 u}{\partial t^2} = a^2\,\frac{\partial^2 u}{\partial x^2} \qquad \text{- - - - - - - - - - - - - - - - - - (56a)}$$

$a = \sqrt{\frac{Eg}{\rho}}$ = velocity of propagation of disturbance in bar, as will be shown presently.

A general solution may be taken as being of the form

$$u = f(x - at) + F(x + at) \qquad \text{- - - - - - - - - - - - (57)}$$

where f and F are arbitrary functions.

Let $F = 0$

Then $u = f(x - at)$ - - - - - - - - - - - - - - - - - - (58)

The function $f(x - at)$ has a zero value at $x = at$. From this the rate of propagation is

$$\frac{dx}{dt} = a = \sqrt{\frac{Eg}{\rho}} \qquad \text{- - - - - - - - - - - - - - - - - - (59)}$$

where

$$\rho = \frac{1}{v} \quad \frac{\text{lbs}}{\text{ft}^3}$$

The wave travels in the direction of positive x.

The equation

$$u = F(x + at) \qquad \text{- - - - - - - - - - - - - - - - - - (60)}$$

refers to a progressive plane wave travelling with velocity a in direction of negative x.

Our solution is a complete solution, hence any displacement must be made up of such waves as described.

Note that

"a" is independent of velocity of shift $\frac{\partial u}{\partial t}$

f and F depend on boundary conditions and initial conditions

f is fixed by elastic properties

F is determined by nature of the disturbing forces.

The modulus of elasticity is not commonly used when dealing with gases. We, therefore, express it in terms of thermodynamic parameters.

Modulus of Elasticity for a Gas

A particle of fluid has an initial volume of v = pressure p. Pressure is increased to $p + \Delta p$. Volume is decreased to $v - \Delta v$.

Increment in stress = Δp.

Increment in strain = change in volume per unit, = $-\frac{\Delta v}{v}$

Modulus of elasticity

$$E = -\frac{\Delta pv}{\Delta v} \qquad \text{- - - - - - - - - - - - - - - - - - (61)}$$

$$E = -v\frac{dp}{dv} \qquad \text{- - - - - - - - - - - - - - - - - - (62)}$$

$$= -\frac{v}{dv}\ dp \qquad \text{- - - - - - - - - - - - - - - - - - (63)}$$

For isothermal state change

$$pv = C_1$$

$$\frac{dp}{dv} = -\frac{p}{v}$$

$$\therefore\ E = p \qquad \text{- - - - - - - - - - - - - - - - - - (64)}$$

For an isentropic state change

$$p\ v^k = C_2$$

$$\frac{dp}{dv} = -\frac{k\ p}{v}$$

$$E = kp \qquad \text{- - - - - - - - - - - - - - - - - - (65)}$$

In general

$$\frac{dp}{dv} = \frac{dp}{d\rho}\ \frac{d\rho}{dv}$$

$$v = \frac{1}{\rho g} \qquad \text{where} \quad \rho = \text{density in } \frac{\text{slugs}}{\text{cft}}$$

$$\frac{d\rho}{dv} = -\rho^2 g$$

$$E = \rho\frac{dp}{d\rho} \qquad \text{- - - - - - - - - - - - - - - - - - (66)}$$

With the expression (65) for adiabatic change of state, the velocity of propagation becomes

$$a = \sqrt{\frac{E}{\rho}} = \sqrt{\frac{kp}{\rho}} \qquad \text{where } k = \frac{Cp}{Cv} \qquad \text{- - - - - - - (67)}$$

Example:

Air at 1 atm. or 2116.8 $\frac{\text{lbs}}{\text{ft}^2}$ and 59° F

$$\rho = .07651 \text{ lbs/ft}^3$$

$$a = \sqrt{\frac{1.4 \times 2116 \times 32.2}{.07651}} = 10^3 \sqrt{1.241} = 1115 \text{ fps}$$

The effect of temperature is obtained by

$$pv = RT$$

$$v = \frac{1}{\rho g}$$

$$\frac{p}{\rho} = g\,RT$$

$$a = \sqrt{kgRT} \qquad \text{- - - - - - - - - - - - - - - - - - (68)}$$

X. REMARKS CONCERNING THE LIMITATIONS OF CRANK CASE SCAVENGING

Crank case scavenged engines have been mentioned repeatedly before. Besides, the experimental work reported on later, was done with such an engine.

It is, therefore, of interest to investigate the possibilities of this type and to establish some limiting design criterion.

Air is taken into the crank case through feather valves during the up stroke of the piston. During the down stroke this air is compressed until the piston opens the intake port. In other words, the engine piston acts at the same time as scavenging and charging pump. No mechanical losses are incurred due to the scavenging pump since all parts are basic engine components. The overall mechanical efficiency of a crank case scavenged engine is, therefore, high.

The geometry of the engine determines, within narrow limits, the maximum scavenging pressure which is available. The crankcase must be as small as possible in order to obtain a high scavenging pressure. This in turn limits the amount of air which is available for scavenging.

Due to this limit on available scavenging pressure, high exhaust back-pressure is particularly detrimental to the performance of this type of engine.

The variables involved are:

Engine speed

Port dimensions

Exhaust pressure

Crank case volume is determined by cylinder displacement and exhaust pressure and thus not independent.

A design criterion can be developed in terms of the parameters above, as follows:

The flow of scavenging air from the crank case to the exhaust port is determined by the pressure drop from port to port (intake to exhaust).

$$W = AK \sqrt{\rho} \sqrt{P_i - P_e} \quad \text{(lbs)}$$

$$dW = AK \sqrt{\rho} \sqrt{P_i - P_e} \, dt$$

dt = element of time

A = port area

K = flow coefficient

P_i = crank case or inlet port pressure

P_e = exhaust backpressure

$\rho = \frac{w}{2g}$ density $\quad \frac{\text{lbs} \ \text{s}^2}{\text{ft} \ \text{ft}^3}$

In terms of engine speed and crank angle

$$dt = \frac{d\alpha}{\omega} = \frac{30}{n\pi} \, d\alpha$$

α = crank angle

ω = angular velocity

n = engine speed (Rpm)

With that

$$W = \frac{30 \, K \sqrt{\rho}}{\pi \, n} \int_{\alpha_1}^{\alpha_2} A \sqrt{P_i - P_e} \, d\alpha \qquad \text{(lbs)}$$

α_1 and α_2 denote, respectively, the crank angle at which the inlet port opens and closes.

For adequate scavenging this amount of air W must be a certain ratio of the displacement volume.

The weight flow of air through the engine in terms of displacement and volumetric efficiency is

$$W = \eta_v \frac{\pi D^2}{4} \times \frac{L}{v}$$

η_v = volumetric efficiency

D = bore

L = stroke

v = specific volume of air

Port area A is connected with other engine parameters as follows:

Port width is a linear function of the bore D.

Port height increases linearly with stroke L and is a function of crank angle α.

Hence

$$A = C\, DL\, f(\alpha)$$

where

C is a constant

$f(\alpha)$ means function of α

Equating the two expressions for W and substituting A, we find that, besides constants and the integral expression, D and n are the only engine design quantities which enter into the equation. We may therefore write:

$$Dn = \frac{120}{\pi^2} \frac{K\sqrt{\rho}\, Cv}{v} \int_{\alpha_1}^{\alpha_2} f(\alpha) \sqrt{P_i - P_e}\, d\alpha$$

$$Dn = C' \int_{\alpha_1}^{\alpha_2} f(\alpha) \sqrt{P_i - P_e}\, d\alpha$$

The scavenging airflow is, then, proportional to the parameter Dn. It may be increased by increasing the scavenging pressure, which is, however, limited by the displacement of the engine. For a given engine stroke, it is fixed. There remains the functional relation between port opening and crank angle. Increased port height increases the airflow but also decreases the useful compression space in the cylinder. The foregoing considerations indicate that there must be a practical upper limit of the parameter Dn beyond which crank case scavenged engines cannot operate.

Typical values of Dn are:

Venn Severin Engine:

Bore 7 inches, Stroke 8 inches

Rated speed, 660 Rpm

Dn = 6.4 fps

Humboldt-Deutz:

Bore 12.6 inches, Stroke 15 inches

Rated speed 310 Rpm

Dn = 5.4 fps

For comparison the following values are given for the General Motors blower scavenged engine of the 71 series.

Bore 4.25 inches, Stroke 5.5 inches

Rated speed 2000 Rpm

Dn = 11.8 fps.

The amount of air available for scavenging in the blower scavenged engine is about twice as large as for crank case scavenged engines at comparable dimensions.

XI. ANALYSIS OF THE SYSTEM: RECEIVER, EXHAUST-PIPE, SILENCER

A typical exhaust system consists of a receiver close to the exhaust ports, an exhaust pipe, and a silencer, as shown in Figure 19.

For purposes of analysis, we shall find an equivalent pipe length such that its natural frequency is the same as that of the configuration of V_r and V_s and pipe. Besides the cross sectional area A of actual and equivalent system shall be equal.

The differential equation of this system is, as before, Equation (56a).

$$\frac{\partial^2 u}{\partial t^2} = a^2 \frac{\partial^2 u}{\partial x^2} \qquad \text{- - - - - - - - - - - - - - - - - (56a)}$$

where $a = \sqrt{\frac{Kp}{\rho}}$ = velocity of sound.

Similarly we get an equation for the pressure

$$\frac{\partial^2 p}{\partial t^2} = a^2 \frac{\partial^2 p}{\partial x^2} \qquad \text{- - - - - - - - - - - - - - - - - (69)}$$

with the solutions

$$u = \left(A \sin \frac{\pi a}{l_e} + B \cos \frac{\pi a}{l_e}\right) \sin \frac{\pi}{l_e} x \qquad \text{- - - - - - (70)}$$

$$p = a \rho_o \left(A \cos \frac{\pi a}{e} - B \sin \frac{\pi a}{e}\right) \cos \frac{\pi}{e} \qquad \text{- - - - - - (71)}$$

These solutions are special forms of the general solution Equation (57).

The original system and the equivalent straight pipe are actually equivalent if a velocity at b and c is accompanied by the same pressure rise, i.e.

$\frac{u}{\partial p / \partial t} = \varphi$ = the same value for both systems.

Differentiating (71) we get for $\frac{u}{\partial p / \partial t}$

$$\frac{u}{\partial p/\partial t} = \frac{\left(A \sin \frac{\pi a t}{l_e} + B \cos \frac{\pi a t}{l_e}\right) \sin \frac{\pi}{l_e} x}{-a^2 \rho_o \frac{\pi}{l_e} \left(A \sin \frac{\pi a t}{l_e} + B \cos \frac{\pi a t}{l_e}\right) \cos \frac{\pi x}{l_e}}$$

$$\frac{u}{\partial p/\partial t} = \frac{\sin \frac{\pi x}{l_e}}{\cos \frac{\pi x}{l_e}} \left(- \frac{l_e}{a^2 \rho_o \pi}\right) = - \frac{\cot \frac{\pi x}{l_e}}{a^2 \rho_o \frac{\pi}{l_e}}$$

at b with $x = \frac{l_e}{2} - l_1$

$$\cot \frac{\pi}{l_e} \left(\frac{l_e}{2} - l_1\right) = \cot \frac{l_1}{l_e}$$

$$\frac{u}{\frac{\partial p}{\partial t}} = - \frac{\cot \frac{l_1}{l_e}}{a^2 \rho_o \frac{\pi}{l_e}} \qquad \text{- - - - - - - - - - - - - - - - - (72)}$$

This equation is related to the design parameters of the system as follows:

Assuming that the receiver is large enough compared to the pipe so that the velocities in the receiver may be neglected, then the pressure in the receiver is equal to the pressure at the pipe entrance (station b).

The volume of gas leaving the receiver is

$$- dV = - \frac{V_r}{k P_o} dp_b = u_b A \, dt$$

A = cross section of pipe

$$\left.\frac{\partial p}{\partial t}\right|_b = \frac{u_b A}{\left(- \frac{V_r}{k P_o}\right)}$$

$$-\frac{V_r}{kP_oA} = \frac{u}{\partial p/\partial t}\Bigg|_b \qquad \text{- - - - - - - - - - - - - - - - - (73)}$$

Equating (72) and (73) we get

$$\frac{\cot \pi \frac{l_1}{l_e}}{a^2 \rho_o \frac{\pi}{l_e}} = \frac{V_r}{kP_oA}$$

with

$$a^2 = \frac{kP_o}{\rho_o}$$

$$a^2 \rho_o \frac{\pi}{l_e} = kP_o \frac{\pi}{l_e}$$

$$\cot \pi \frac{l_1}{l_e} = \frac{V_r \pi}{A l_e}$$

and since

$$\operatorname{tg} x = \frac{1}{\cot x}$$

$$\operatorname{tg} \pi \frac{l_1}{l_e} = \frac{A l_e}{V_r \pi} \qquad \text{- - - - - - - - - - - - - - - - - (74)}$$

and similarly for V_s

$$\operatorname{tg} \pi \frac{l_2}{l_e} = \frac{A l_e}{V_s \pi} \qquad \text{- - - - - - - - - - - - - - - - - (75)}$$

Since $l_1 + l_2 = l$, we may now combine both equations (74) and (75) and get

$$\operatorname{tg} \pi \frac{l}{l_e} = \frac{\left(\frac{A}{V_r} + \frac{A}{V_s}\right) \frac{l_e}{\pi}}{1 - \frac{A^2}{V_r V_s} \frac{l_e^2}{\pi^2}} \qquad \text{- - - - - - - - - - - (76)}$$

l_e = equivalent length

l = distance between receiver and silencer

V_r = volume of receiver

V_s = volume of silencer

A = cross section of pipe

Equation (76) can be solved for the equivalent length l_e if the other quantities are known.

For a system with receiver and exhaust pipe only but no silencer $V_s = \infty$ (i.e. the whole atmpsphere serves as silencer volume) and equation (76) becomes

$$\operatorname{tg} \pi \frac{l}{l_e} = \frac{A}{\pi} \frac{l_e}{V_r} \qquad \text{- - - - - - - - - - - - - - - - (77)}$$

where V_r = volume of receiver.

The natural frequency of the system using the effective length is then

$$\nu_o = \frac{a}{4\, l_e} \quad \text{or} \quad \nu_o = \frac{a}{2\, l_e} \qquad \text{- - - - - - - - - - - (78)}$$

where a = velocity of sound.

Which of the two frequency equations is to be used is determined by the behaviour of the system. The former equation holds for a pipe closed at one end and open at the other. The second equation holds for a pipe open at both ends.

The end correction to the pipe length amounts to only an addition of 0.41 D (where D = diameter of pipe). In view of other uncertainties, such as the proper value for the exhaust temperature, this correction is negligible.

With Equation (78) in (77) we obtain

$$\operatorname{tg} \frac{\pi}{a} 4 \nu_o 1 = \frac{A}{\pi} \frac{a}{4 \nu_o V_r} \qquad \text{- - - - - - - - - - - - (79)}$$

$$\operatorname{tg} 4 \frac{\pi}{a} 1 \nu_o = \frac{\left(\frac{A}{V_r} + \frac{A}{V_s}\right) \frac{a}{4\pi \nu_o}}{1 - \frac{A^2}{V_r V_s} \frac{a^2}{16\pi^2 \nu_o^2}} \qquad \text{- - - - - - - - - - - (80)}$$

Figure 21 shows a plot of the relation represented by Equation (77). The actual length 1 is plotted against the effective length 1_e for different values of the parameter V/A, i.e. receiver volume over pipe cross-sectional area.

Figure 22 shows a different presentation of Equation (77). The right hand portion shows the effect of the parameter V/A on effective length.

Since the ultimate object of the analysis is the determination of the natural frequency of the exhaust system, the left hand side of Figure 22 allows us to pick values of frequency ν_o for the configuration in question. Velocity of sound is plotted as parameter.

Equations (76) and (77) must be solved numerically for the effective length 1_e by substituting the given design quantities. This is greatly simplified by assuming values of 1_e and solving for the corresponding actual length 1. Three or four points were found to be sufficient for a solution by this method, whereas solving for 1_e requires approximately ten to twelve points. The sample calculation below shows the method.

Configuration: (See: experimental setup)

Receiver tank volume $V_r = 0.204$ ft^3

Silencer tank volume $V_s = 0.204$ ft^3

Length of pipe (4" diameter) $1 = 12.3$ ft.

$$\frac{A}{V_r} = \frac{A}{V_s} = \frac{.0884}{.204} = .434 \text{ ft}^{-1}$$

$$\text{tg } \pi \frac{l}{l_e} = \frac{\left(\frac{A}{V_r} + \frac{A}{V_s}\right) \frac{l_e}{\pi}}{1 - \frac{A^2}{V_r V_s} \frac{l_e^2}{\pi^2}} = \frac{.277\ l_e}{1 - (.019)\ l_e^2}$$

Assume l_e = 20 feet

$$\text{tg } \frac{\pi\, l}{20} = \text{tg } .157\ l = \frac{5.54}{-6.6} = -.84$$

$$\text{tg}^{-1}\ (-.84) = 139^\circ$$

$$\frac{139}{57.3} = 2.42$$

$$l = \frac{2.42}{.157} = 15.4 \text{ ft}$$

Assume l_e = 15 feet and repeat calculation

Result: l = 10.65

Assume l_e = 17.5 feet and repeat calculation

Result l = 13.05

This example is shown in Figure 20.

It is at times desirable to express the exhaust system dimensions in terms of displacement volume and stroke. The equations then take the following form:

$Z = \frac{\pi D^2}{4}$ = piston area

$aZ = A$ = exhaust pipe area

$Z \times S$ = Displacement volume V_D (where S = stroke)

$b \times V_D = V_r$ = receiver volume

$c\ V_D = V_S$ = silencer volume

$d \times S = l$ = length of pipe

$$\operatorname{tg} \pi \frac{l}{l_e} = \frac{a\, l_e}{\pi\, b\, S} \qquad \text{- - - - - - - - - - - - - - - - - (79.1)}$$

$$\operatorname{tg} \pi \frac{l}{l_e} = \frac{\frac{1}{\pi}\left(\frac{a}{b} + \frac{a}{c}\right) l_e}{1 - \frac{a^2}{bc}\,\frac{l_e^2}{\pi^2}} \qquad \text{- - - - - - - - - - - (80.1)}$$

XII. QUALITATIVE EFFECTS OF EXHAUST SYSTEM CONFIGURATION PRESSURE DEVELOPMENT AND ENGINE BEHAVIOR

Summarizing the foregoing discussions, the following effects will influence exhaust conditions:

(1) Inertia of the accelerated gas column. After the port is closed, the inertia of the gas will tend to maintain the velocity in the exhaust duct which, in turn will lower the pressure at the port. Sudden expansions in the duct, such as receiver or silencer volumes decrease the velocity and increase the losses. It is to be expected that large volumes are unfavorable from this point of view.

(2) Free oscillation of the gas in the duct, excited by the pressure wave from the port.

Several cases of oscillation are, in principle, possible.

(1) The exhaust system behaves like a pipe open at both ends. The wave length is equal to twice the length (or effective length) of the duct, and the frequency is

$$\nu = \frac{a}{2\,l}$$

a = velocity of sound

l = length of duct

At both ends there is a node. Since the pressure at one end is approximately atmospheric or higher, the pressure in front of the port will also be high. Such a system will be quite unfavorable. This case might be obtained with large volumes near the exhaust port.

(2) The exhaust system behaves like a pipe with one open and one closed end. The wave length is then four times the length of the duct and the frequency is

$$\nu = \frac{a}{4 l_e}$$

The pressure at the open end is near atmospheric and higher at the closed end. This is unfavorable. Since this condition exists in the case of a simple exhaust pipe, it is to be expected that this configuration is poor.

In either case, a standing wave of engine frequency or multiple of engine frequency will result in high pressure at the port. This will be reflected in a low volumetric efficiency of the engine, which is a quantity which can be measured without difficulty.

It must be concluded that the exhaust system should not be in resonance with the engine. If not in resonance, there will be two cases possible.

(1) The pressure due to free oscillation in the pipe is increasing at the time when the port is opening. This will increase the pressure rise in the port over and above the value caused by the exhaust blowdown and amounts to an increased resistance and hence decreased volumetric efficiency.

(2) The pressure in front of the port is decreasing due to the free oscillation at the time when the port opens, thus aiding exhaust and increasing volumetric efficiency.

It seems immaterial by what natural frequency of the duct this effect is brought about. It must, therefore, be concluded that it is important to know and control the pressure development due to exhaust oscillation, rather than to know and control the frequency. Since the expected effect is a combination of inertia and resonance effect, great sensitivity to changes in frequency of either engine or exhaust system is not to be expected.

The analysis shows that system frequency alone is not the determining factor. The following other factors may influence exhaust behavior:

(1) Functional relation between crank angle and port opening.

(2) Flow coefficient of the ports.

(3) Sudden expansion losses in the transitions of duct to receiver or silencer.

(4) Secondary oscillations in cylinder or tanks.

XIII. EXPERIMENTAL SETUP

In order to investigate some of the conclusions experimentally, a single-cylinder, two-stroke Diesel engine with crankcase scavenging was adapted for such use.

Figure 23 shows a schematic diagram of the mechanical equipment used.

Air is supplied to the outer crankcase of the engine (See Figure 1 for principle of operation) by a Roots type blower. Airflow is measured by means of a Rotameter type flowmeter, placed between surge tanks.

All tests were run with atmospheric pressure in the outer crankcase. The pressure was adjusted by controlling the speed of the blower motor.

The exhaust system consisted of the exhaust elbow supplied with the engine, a series of receiver tanks and silencers, and a flexible duct, three feet in length, which prevented damage to the engine by thermal expansion, vibration, or weight of the exhaust system.

The dimensions of the exhaust components tested are shown in Figure 24. Figure 25 shows the receiver and silencer tanks. Tank 1 and 1A are identical. All tanks were fabricated in the shop of the Mechanical Engineering Department.

Engine output was measured by means of a General Electric, Sprague type electric dynamometer.

Exhaust temperatures were measured by means of a shielded iron-constantan thermocouple and a potentiometer.

A schematic diagram of the electronic equipment used is shown in Figure 26. The instrumentation consisted of standard items commonly used in engine studies (See Table A, "List of Data Concerning the Test Equipment").

The pressure fluctuations in the exhaust were picked up by a quartz crystal element attached to a low pressure multiplier. This multiplier consists of a diaphragm which, exposed to the pressure to be measured, increases the sensitivity of the quartz element by a factor seventeen. Figure 26 shows a schematic diagram of the instrumentation used.

The crystal signal was fed into an amplifier and from there into an oscilloscope. The amplifier included a calibrating circuit.

A synchronizer and marker was driven from the engine governor shaft and used to synchronize the sweep of the oscilloscope with the engine speed. The marker produced a pip on the trace of the oscilloscope to indicate top dead center.

A camera was used to photograph the screen.

A zero line on the screen was obtained by shorting out the oscilloscope signal input for a short period by means of a manually operated microswitch.

All terminals and leads were carefully shielded to prevent disturbances of the trace.

It was found necessary to provide a separate ground for the indicator equipment. This was accomplished by driving a pipe into the ground through a hole in the floor near the test setup.

Figure 27 shows the remaining disturbance of the trace due to vibration and pickup. Elimination of this irregularity would have required complete rebuilding of the amplifier and was not considered worthwhile.

Considerable difficulty was encountered in eliminating the effect of engine vibrations on the electronic equipment. It was found necessary to mount the cabinet, on which the apparatus rested, on tennis balls. The

oscilloscope, camera-mount and amplifier were, in addition, mounted on shock mounts.

Figure 28 shows the engine on the dynamometer bed plate. Intake and exhaust are on the opposite side.

Figure 29 shows the intake and exhaust side of the engine as well as the dynamometer (left) and the variable speed drive for the blower and one of the surge tanks. The thermocouple galvanometer can be seen resting on a stool. Receiver number one and the flexible connection are mounted on the exhaust elbow.

Figure 30 shows the dynamometer and control panel with the test engine flywheel barely visible at the left hand edge of the picture.

Figure 31 shows the air supply system: blower, two tanks and a flow meter.

In the foreground the instrument table can be seen resting on tennis balls (lower right hand edge of the cabinet). On the table (from right to left) are seen: constant voltage transformer, amplifier, camera mount, and oscilloscope.

At the right edge of the picture, the synchronizer and marker unit can be seen (on stool) connected to the engine governor by an extension shaft.

Figure 32 shows a closeup of the amplifier. The selector switch (lower left) is in the calibrating position, the meter range selector switch (lower right) is in the position: Meter Factor 1. In this setting a sine wave of known voltage is put into the oscilloscope. The calibration is shown in Figure 33. This voltage is read on the millivolt meter, upper center, of the amplifier panel. In the test a calibration of 1 mV per inch

deflection on the oscilloscope was used throughout. The calibration constant of the quartz element is 3.1 mV per 100 lbs/in^2 pressure. The low pressure multiplier divides this pressure by a factor 17 so that the resulting calibration is

$$\frac{100 \text{ psi}}{3.1 \text{ mV} \times 17} = 1.9 \text{ psi/mV}$$

Hence a deflection of one inch on the oscilloscope corresponds to 1.9 lbs/in^2. There are ten divisions to the inch on the oscilloscope screen scale. Each small division, then, corresponds to a pressure of .19 lbs/in^2.

The quartz element was calibrated by applying a constant hydrostatic pressure of known magnitude and observing the oscilloscope deflection when the pressure was suddenly released. The calibration was performed by Mr. Chi-nan Hsu in the course of his investigation of the behavior of pressure indicating elements. The calibration curve for the low pressure range is shown in Figure 34.

The oscilloscope gain was kept constant throughout: Range: under 250 rms, gain Y-axis 30, x-axis 20. This x-axis setting resulted in a trace length such that each 1/10 division on the screen corresponded to 10 degrees crank angle.

Figure 35 shows the marker and synchronizer unit. The left hand protractor allows the marker pip to be adjusted to any desired crank angle. Throughout the tests the marker was set to indicate top dead center. The pip was about one quarter of an inch wide. Its left hand edge indicates the desired position.

Figure 36 shows the cylinder and exhaust port. The intake ports

can be seen, inside the cylinder, opposite the exhaust ports.

Figure 37 shows a view into the cylinder through the exhaust port. The port dimensions are as follows:

Intake: 1-1/8 x 1-7/16, 1-1/8 x 1-1/2, 1-1/8 x 1-9/16, 1-1/8 x 1-7/16 inches, (4 ports).

Total port area: 6.3 $in.^3$

Exhaust: 1-7/8 x 1-1/2, 1-7/8 x 1-1/8, 1-7/8 x 1-1/4, 1-7/8 x 1-1/2 inches, (4 ports).

Total port area: 11 $in.^2$

Figure 38 shows the piston. The piston crown serves as a deflector baffle, directing the incoming air upwards.

Figure 39 shows a closeup of the quartz element mounted in the exhaust elbow.

Figure 40 shows details of the quartz element. From right to left: quartz element, low pressure multiplier body, diaphragm, retaining nut.

Assembly of the complete unit as seen in Figure 39 is as follows:

The retaining unit is screwed into the exhaust elbow by means of a special spanner wrench. The diaphragm is then placed inside the nut and rests against a shoulder. The body is then screwed in place with a spanner wrench until it firmly clamps the diaphragm. The crystal element is then screwed in until the pressure piston (top in Figure 40) is in contact with the small hex-unit of the diaphragm. The shielded cable is then screwed on. The cooling connection in the multiplier body was not used during the present experiment.

Operation

Both engine and electronic equipment were warmed up for 30 minutes

before each series of runs.

All components were checked for proper operation and the amplifier calibrated.

For each configuration three runs were made, one at idling load, half load and full load. The speed of the engine was kept constant by the integral engine governor.

After setting the dynamometer field to give the desired engine output, the blower speed was adjusted such that the outer crank case pressure was atmospheric, as indicated by a water U-tube manometer attached to the crankcase.

The engine speed was then read with counter and stop watch.

After this the trace on the oscilloscope was adjusted so as to fall exactly on the center portion of the screen. The frequency and synchronizer adjustment was turned until the trace remained stationary on the screen. A picture was then taken exposing approximately for one half second with the pressure trace, and an equal period with the signal shorted out, which gave the zero line. Both lines were thus photographed on the same negative.

Since all records look similar, it was important to have a reliable system of identifying each photographic record.

The following scheme was used:

Before each run, the run was entered into the test log and assigned a serial number. This number was written on a file card (3 x 4 inches) on which were recorded:

(1) Serial number

(2) Dark slide number

(3) Configuration (e.g. Receiver No. 1, Silencer No. 4)

(4) Air consumption

(5) Amplifier calibration

(6) Engine setting (e.g. No Load, 1/2 Load, Full Load)

(7) Dynamometer load (lbs)

(8) Counter reading at start and finish

On the same card, engine speed and brake mean effective pressure were computed.

The card was fastened to the appropriate side of the film holder (4 x 5 inch cut film). In the dark room, film and card were put together and punched with a small hand punch like two streetcar tickets. Since no two punch patterns were apt to be alike, this afforded a positive way of identifying record card and film. After drying, the serial number was marked on the film with india ink and card and film filed in a card file box.

The film used was Arrow Pan, D-19, high contrast developer.

Brake mean effective pressure was used to denote engine output since this parameter is proportional to the power delivered per cycle. It is, of course, independent of engine speed. In comparing the values of brake mean effective pressures, it must be remembered that the test engine is a two stroke engine. The mean effective pressure is, therefore, only half that customarily expected of four stroke engines. The average values were as follows:

Idling brake mean effective pressure	1.4 lbs/in^2
Half power brake mean effective pressure	17.0 lbs/in^2
Full power brake mean effective pressure	30.0 lbs/in^2

The engine speed was held constant by the engine governor. The speed was from 638 to 661 revolutions per minute. The constant speed operation was the one seriously limiting factor of the test engine. It was not possible, at the present time, to remedy this situation.

The engine air flow was measured by means of a rotameter reading directly in cubic feet per minute. The surge tanks successfully eliminated any fluctuation in the system in spite of the low frequency and large displacement volume of the engine. It was found, in preliminary studies, that a blower is necessary with any rotameter measuring engine airflow. Without an external source of energy the pressure drop across the measuring element is so large that the float remains seated until considerable vacuum is produced above it. It then flies from its seat and performs oscillations between the two extreme positions.

XIV. CALCULATION OF DATA AND PRESENTATION OF RESULTS

A sample calculation of the evaluation of engine data (Bmep, volumetric efficiency, engine efficiendy) and frequency of the exhaust system is shown in Table (C).

Values of the velocity of sound are based on measurements of exhaust temperatures taken at the port and at the discharge to atmosphere, plotted in Figure 41. The mean temperature and values of K (ratio of specific heats) are listed in Table (B). The gas constant R was taken as that of air, which is permissible for Diesel engines because of the large amount of excess air.

Observed and calculated data are collected in Table (D). In the last column, the ratio of exhaust system frequency over engine frequency is listed.

The volumetric efficiencies for each series of configurations are plotted as a function of brake mean effective pressure in Figure 42 to 47.

The important photographic records of pressure in the exhaust near the port as a function of crank angle are appended. The basis for selection is described below. On each record the zero pressure line and top dead center mark was recorded photographically together with the pressure curve. Crank angle marks were drawn into the negative with india ink and thus show up on the print.

The cycle progresses, on all records, from left to right.

Top or bottom dead center is indicated by the left hand edge of the marker pip. The letter code used is as follows:

B = bottom dead center

T = top dead center

EO = exhaust port opens

IO = inlet port opens

EC = exhaust port closes

IC = inlet port closes

In terms of crank angle the points occur (See Table A)

EO = 84.5° BBC (before bottom dead center)

IO = 66.5° BBC

IC = 66.5° ABC (after bottom dead center)

EC = 84.5° ABC

On each photograph the serial number of the test run is shown which allows quick cross reference with Table (D) in which all pertinent data for each run are collected.

XV. DISCUSSION OF TEST RESULTS

The following data were obtained:

(1) From dynamometer:

Brake mean effective pressure

Engine speed

(2) From air flowmeter:

Engine air consumption

(3) From electronic pressure pickup and oscilloscope:

Photographic record of exhaust pressure near the port as a function of crank angle.

These data were taken at three different brake mean effective pressures and approximately constant engine speed. Exhaust temperatures were measured as function of brake mean effective pressure (see Figure 41) and used to evaluate velocity of sound for use in the frequency equation. Results are tabulated in Table B.

Sample calculations are shown in Table (C).

Experimental and calculated data are summarized in Table (D).

The table shows volumetric efficiency, effective length, and natural frequency of the exhaust configuration as calculated by the method outlined before. The frequency is based on the equation for the pipe closed at one end, open at the other.

Volumetric efficiencies are plotted for all configurations investigated as a function of brake mean effective pressure in Figure 42 to 47.

Table (E) shows the reproducibility of values of volumetric efficiency. In view of the fact that measurement of air flow into single cylinder engines of large displacements are difficult, the results are quite satisfactory.

All plots show that the effect of brake mean effective pressure is relatively small. There are, however, definite trends discernible.

An exhaust pipe without receiver or silencer (Figure (42) shows a slight increase in volumetric efficiency with increasing brake mean effective pressure. The absolute value of volumetric efficiency is of the order of .75.

Addition of a silencer, but no receiver, produces a marked sensitivity to changes in bmep, and a rising characteristic.

A comparison of calculated exhaust system and engine frequencies (Table D) Serial No. 44 to 52, shows that the volumetric efficiencies increase with decreasing system frequencies. Maximum values of volumetric efficiencies are found when the exhaust system frequency is approximately one half engine frequency. These optimum values are obtained with silencer No. 4 with a ratio of silencer volume to engine displacement of 1 to 11.6 which is in agreement with recommended practice. The result indicates that the necessarily high velocities in the exhaust pipe near the port are not detrimental to the volumetric efficiency if the system frequency is near engine frequency. The mere effect of gas inertia is not sufficient to produce good volumetric efficiencies.

The great sensitivity of the system to changes in bmep makes this configuration undesirable.

The configurations with receiver 1, 2 and 5 give consistently high volumetric efficiencies (Figures 43, 44, 46), and relatively little change with mean effective pressure.

Configurations of pipe and silencer (Figure 42) receiver 3 and 4, Figure 45 and 47 show low volumetric efficiencies throughout, accompanied by falling characteristics.

It becomes at once apparent that two configurations, made up of identical components, but in interchanged positions (e.g. receiver 1 and silencer 4 do not have the same characteristics. To facilitate comparison, Table G has been prepared. Included in this table is the ratio of volumetric efficiency for the configuration to that of the pipe alone. This number indicates the relative improvement. It is seen that addition of a silencer to the pipe always results in an improvement. This was to be expected since the silencer reduces the frequency of the exhaust system. A large receiver near the port may, on the other hand, produce a high back pressure due to the sudden expansion of flow. The most striking example of this effect is presented by the configurations: receiver 1 and silencer 3 as compared with receiver 3 and silencer 1. The former configuration has volumetric efficiencies of the order of .9 to .92, i.e. high and increasing with mean effective pressure. The latter configuration has efficiencies from .67 to .62, i.e. materially lower and decreasing with increasing mean effective pressure. This behavior is not at all predicted by the analysis of system frequencies, since in the calculation the two systems are identical. The case in hand illustrates well the limitation of the concept of "tuning" an exhaust system on the basis of frequencies only.

It is in order at this point to inspect the records of measurement of pressure as a function of crank angle. The case under discussion is represented by serial number 31 and 82 of the collection of photographic records. Each photograph represents several cycles. The trace, therefore, appears blurred. The cycles give essentially the same trace.

The straight horizontal line represents zero pressure (atmospheric). The vertical lines indicate crank position and port timing.

Following through the cycle, beginning with top dead center and moving towards the right we find on Serial No. 31 (receiver 1 and silencer 3) positive pressure near top center. In serial No. 82 the pressure is equal in magnitude, but negative. In No. 31, the pressure is decreasing as exhaust opening is approached, in No. 82 the pressure is rising. Inspection of all other records shows that the behavior of the pressure curve prior to exhaust port opening determines to a large extent the volumetric efficiency. If the pressure caused by free oscillation in the exhaust system is increasing before the exhaust and scavenging period, the pressure throughout the scavenging period is high and the volumetric efficiency low. The absolute amount of pressure at the time of port opening does not affect conditions materially. This was expected and explained before.

An attempt was made to determine the actual frequencies of the free oscillation, from the photographic records. The results are listed in Tables (F) and (G). Agreement is, as a rule, not very good. This is due to the difficulty in evaluation of the photographs. The small scale fluctuations make extrapolation of the free oscillation hard and often impossible, especially in case of low frequencies.

The discrepancy between the calculated frequencies, which are the same for a given configuration, irrespective of interchange of tanks, and the measured frequencies can be explained as follows:

In the present setup, receiver and silencer tanks were installed with their long axis normal to the exhaust pipe, (see Figure 25). The tank itself represents a pipe capable of oscillations perpendicular to the oscillation of the exhaust line. Because of their short length, the natural frequencies are relatively high (approximately 250 cycles per

second for receiver 1, 91 c.p.s. for receiver 5).

This oscillation in the tanks may materially change the behavior of the exhaust system by affecting the pressure at the point where the exhaust enters and leaves the tank. This effect is superimposed on the pressure rise due to sudden expansion. Depending on the resultant pressure, a configuration may show a behavior not predicted by frequency analysis. It is interesting to note the frequency of the small scale fluctuation during the period of closed exhaust port is of the same order of magnitude as the natural frequency of the receiver tank. No such fluctuations are observed for the pipe alone or pipe and silencer. (Due to a malfunction of the photographic setup, no photographic records are available of the bulk of the runs of pipe and silencers. What records exist show the effect as indicated).

The difference in behavior of the configurations discussed is certain indication that the described effect was present. Since it influences both pressure and phase relations, it seems worthwhile to investigate the possibilities of exhaust control in this manner. It is likely that the interference between oscillations in the system is also the key to the adaptation of the present single cylinder analysis to multicylinder problems.

Further study of the photographic records brings out additional points of interest.

For the sake of simplicity and in order to facilitate cross reference with Table D, the photographs are identified by their serial number rather than individual figure numbers.

Serial No. 26, 27, 28 show configuration receiver 1, silencer 2, at three mean effective pressures. The records support the statement that the effect of this parameter is moderate. The configuration is favorable,

as indicated by the high volumetric efficiency. From a practical point of view, the configuration is attractive since an appreciable gain in volumetric efficiency is obtained with relatively little addition in weight. It is well known to operators of two-stroke motor cycles that elimination of the muffler and, worse yet, the tail pipe, results in great decrease in performance and that only relatively small mufflers are sufficient.

Serial No. 107, 108, 109, configuration: silencer 5 and pipe shows a case of decreasing volumetric efficiency with increasing mean effective pressure. The large receiver results in very small pressure fluctuations. This in itself is seen to be of little importance. Other configuration show higher efficiencies in spite of high pressure peaks.

Serial No. 51 and 52 show the same components but interchanged pipe and silencer No. 5. The large pressure peaks characteristic for the pipe alone or small receiver is clearly visible (compare with Serial No. 40, 38 for receiver 1 and pipe, Serial No. 44, 45, 46 for pipe only).

Serial No. 44, 45, 46 show pressure against crank angle for the pipe alone, without silencer or receiver. Pressure fluctuations are very large and the pressure is positive and high throughout the scavenging period. For high mean effective pressure (Serial No. 46) exhaust blow-down accelerates the flow in the pipe very rapidly (note steep pressure peak immediately after opening of the intake). This, in conjunction with the high scavenging pressure at beginning of scavenging, results in inertia scavenging, as described before. As a result, the pressure becomes negative well before the intake closes, with a resulting slight improvement in volumetric efficiency.

The following conclusions can be drawn:

The frequency of the exhaust system is much higher than the engine frequency, roughly four times.

The exhaust pressure due to free oscillation in the pipe is increasing just when the exhaust port opens. This always results in poor volumetric efficiency.

Low pressure towards the end of scavenging is rather ineffective in improving volumetric efficiency and is unable to counteract the high pressure during scavenging.

Serial No. 59, 60, 61 represents configuration receiver 2 and pipe only. This arrangement shows the highest volumetric efficiencies of all investigated cases. Exhaust frequency is of 70 percent of engine frequency. The pressure is low throughout, even though negative only during the last portions of scavenging. The frequency of the receiver is high and does not interfere with the system. At high mean effective pressure (Serial No. 61) a sharp short oscillation after bottom center is probably due to receiver oscillation and aids scavenging.

Serial No. 65 and 67, receiver 2 and silencer 3, shows that the general character of pressure development is maintained, except for somewhat stronger high frequency oscillations near bottom center. System frequency is equal to engine frequency. The volumetric efficiency is decreased, as compared with the previous case.

Serial No. 61 (receiver 2 and pipe only) and 70 (receiver 2 and silencer 4) are compared to show that there is not necessarily a definite ratio of exhaust system frequency to engine frequency, which results in good or bad performance. Both cases have approximately the same

volumetric efficiency (.96 and .95). The frequency ratios are .72 and .98 respectively. The general character of pressure development is the same in both cases and hence the volumetric efficiency.

Serial No. 70 (receiver 2, silencer 4) and 73 (receiver 2 and silencer 5) show still the same general appearance. The large silencer, however, raises the pressure slightly throughout scavenging, most likely due to increased losses of sudden expansion in the silencer transition. As a result, the volumetric efficiency is lowered.

From the practical point of view, this permits an important conclusion:

Installation engineers tend to be conservative and, in case of doubt, select oversize equipment according to the principle that much helps much. In the case of silencers, as is seen, that may not be the right thing to do.

Serial No. 77, 78, 79, receiver 3, pipe only, for three mean effective pressures, is presented to show again that generalizations are not permissible: receiver and pipe only must not be considered a good installation purely on the basis of similarity in the geometry. The present configuration shows a pressure curve more similar to the case of a pipe without receiver and has the correspondingly low values of volumetric efficiency (.65 to .73).

All combinations involving receiver 3 are poor. This cannot be due to sudden expansion losses since larger receivers show better performance. The pressure is high throughout scavenging, rising already before opening of the exhaust to positive values. At high mean effective pressure, low pressure develops near the end of scavenging, resulting in a noticeable increase in efficiency. It is also conspicuous that the efficiency is

the higher, the smaller the amplitude of high frequency oscillation, again verifying the contention that transverse oscillations of the receiver have a powerful effect.

Serial No. 112, 115, 118, configuration: receiver 5 with silencer 1, 2, 4 respectively show again that the receiver controls the general characteristic of the pressure curve. From the practical point of view, large receivers are, of course, undesirable, and the present investigation shows that they are unnecessary.

Serial No. 25, 28, 31, 34, etc to 120 show the pressure curves for all configurations investigated for maximum brake mean effective pressures. They are presented to complete the record. Detailed discussion does not bring out new points and is, therefore, omitted. For the same reason, not all photographic records, representing other values of mean effective pressures, are included in the report.

XVI. SUMMARY OF CONCLUSIONS

Comparison of analysis and experiment shows clearly that exhaust behavior cannot be predicted on the basis of any one analysis, such as frequency analysis, alone. The order of magnitude of various effects is similar and the interaction of these effects determines the result.

Two basic conclusions stand out:

(1) The receiver controls the behavior of the exhaust system.

(2) The overall pressure characteristic is not determined alone by system frequency and its relation to engine frequency.

The present investigation has shown in many cases what trends are to be expected and has shown the need of more information on a number of phases of the problem. Future research must clarify the following points:

(1) Effect of engine speed, i.e. investigation of high speeds and variable speeds.

(2) Effect of orientation of receiver and silencer tanks, i.e. effect of secondary oscillations and their interaction with engine and system oscillations. This requires also an investigation of pressure development along the axis of the exhaust system.

(3) Investigation of multicylinder effects. This probably is closely related to the problem outlined under (2).

(4) Development of better instrumentation for investigations of this nature.

XVII. REFERENCES

1. E. M. Barker, J. B. Maline and J. J. Mikita, The Elimination of Combustion Knock, Journal of the Franklin Institute, (April 1946) Volume 241, No. 4.

2. O. Holm, Die Kurbelkastenspülung eines Zweitaktmotors, Zeitschrift des Vereines Deutscher Ingenieure, Volume 71, No. 24 (June 11, 1927) page 847.

3. F. Trendelenburg, Akustik, J. Springer, Berlin, 1939.

4. T. Warming, Polar Diagram for Tuning of Exhaust Pipes, Transactions, American Society of Mechanical Engineers, (January, 1946), Volume 68, page 31.

5. H. Helmholtz, Theorie der Luftschwingungen in Rohren mit offenen Enden, Ostwald's Klassiker der exakten Wissenschaften, No. 80, 1896.

6. R. C. Binder and A. S. Hall, Jr., An Introduction to an Analysis of Gas Vibrations in Engine Manifolds, Journal of Applied Mechanics, September, 1947, Volume 14 No. 3, page A-183.

7. H. Kühl and F. A. F. Schmidt, Die Eignung verschiedener motorischer Arbeitsverfahren fur Höhen und Weitflug, Jahrbuch der D.V.L., 1937, page 433.

8. D. L. Thornton, Mechanics Applied to Vibrations and Balancing, Wiley and Sons, New York, 1942.

LIST OF TABLES

TABLE A

LIST OF DATA CONCERNING THE TEST EQUIPMENT

ENGINE:

MAKE: VENN SEVERIN, MODEL HC, SERIAL NO. S5767

TYPE: SINGLE CYLINDER, TWO STROKE, CRANKCASE SCAVENGED

BORE: 7 INCHES, STROKE: 8 INCHES, DISPLACEMENT VOLUME: 308 IN^3 = .178 FT^3

RATED POWER: 20 BHP AT 650 RPM

SPEED: GOVERNOR CONTROLLED, 650 RPM

EXHAUST PORT OPENS: 34.5^0 BEFORE BOTTOM DEAD CENTER

INLET OPENS: 66.5^0 BEFORE BOTTOM DEAD CENTER

INLET CLOSES: 66.5^0 AFTER BOTTOM DEAD CENTER

EXHAUST CLOSES: 34.5^0 AFTER BOTTOM DEAD CENTER

INTAKE SYSTEM: (NOT PART OF ENGINE)

BLOWER: SUTORBUILT MODEL 6H, POSITIVE DISPLACEMENT ROTARY BLOWER

DRIVE: STERLING SPEEDTROL, MODEL KFE, VARIABLE SPEED: 600 TO 1200 RPM

FLOWMETER: FISHER PORTER FLOWRATOR, SER. #J9-2925, CALIBRATED IN CUBIC FEET PER MINUTE OF AIR.

SURGE TANKS: STANDARD (ASME) AIR PRESSURE TANKS

DYNAMOMETER: GENERAL ELECTRIC (SPRAGUE TYPE), CAPACITY 150 BHP AT 3600 RPM

BEAM SCALE, REVOLUTION COUNTER, STOPWATCH

EXHAUST THERMOMETER:

ALNOR SHIELDED THERMOCOUPLE

(IRON-CONSTANTAN) WITH LEEDS NORTHRUP GALVANOMETER, SERIAL NO. 515588

ELECTRONIC PRESSURE INDICATOR

MANUFACTURER: COMMERCIAL RESEARCH LABORATORIES, DETROIT, MICHIGAN

PRESSURE ELEMENT: COX TYPE 3, SERIAL NO. 1306 (PIEZO-QUARTZ ELEMENT)

AMPLIFIER: COX TYPE 2, SERIAL NO. 1061 AMPLIFIER

SYNCHRONIZER: MULTIPLE CONTACTOR, TYPE VI, SERIAL NO. 149

OSCILLOSCOPE: DUMONT TYPE 208B, SERIAL NO. 6967

CONSTANT VOLTAGE TRANSFORMER: SOLA TYPE 30, SERIAL NO. C91082

RECORDING CAMERA: SPEED GRAPHIC, KODAK EKTAR F 4.7, 128 MM.

TABLE (B)

MEAN EXHAUST TEMPERATURES AND VELOCITIES OF SOUND USED IN EVALUATION OF EXHAUST SYSTEM FREQUENCIES

EXHAUST IS ASSUMED TO HAVE THE GAS CONSTANT R FOR AIR = 53.3.

TEMPERATURES FROM FIGURE (41)

BMEP δ	T $^{o}_{R}$	K	a FPS	ν_{1_e} CPS
1.6	650	1.270	1190	297
17.0	725	1.250	1250	312
31.0	790	1.245	1300	324

TABLE (C)

SAMPLE CALCULATION

$$BMEP = \frac{33000 \times BHP}{LAN}$$

$$BHP = \frac{\text{SCALE FORCE} \times RPM}{\frac{8}{12}\frac{\pi 7^2}{4} \times 3000}$$

L = STROKE = 8 INCHES

A = PISTON AREA $\frac{\pi D^2}{4}$

D = 7 INCHES

DYNAMOMETER CONSTANT = 3000

BMEP = 0.431 SCALE FORCE

$$\eta_v = \frac{CFM}{V_D\ RPM} = \frac{CFM}{.178\ RPM}$$

CFM = AIR CONSUMPTION FROM FLOW METER

V_D = DISPLACEMENT VOLUME OF ENGINE = $.178\ FT^3$

FREQUENCY OF ENGINE

$$\nu_e = \frac{RPM}{60}$$

FREQUENCY OF EXHAUST SYSTEM

$$\nu_o = \frac{a}{4 l_e}$$

a = VELOCITY OF SOUND = $\sqrt{k\ g\ R\ T}$ = $41.4\sqrt{k\ T}$

a IS CALCULATED IN TABLE (B) FOR OBSERVED EXHAUST TEMPERATURES.

l_e FROM EQUATION (76) AND DIMENSIONS FROM FIGURE (24)

TABLE (D)

COLLECTED EXPERIMENTAL AND CALCULATED DATA

V_R = RECEIVER TANK η_v = VOLUMETRIC EFFICIENCY ν_e = ENGINE FREQUENCY

V_S = SILENCER TANK l_e = EFFECTIVE LENGTH ν_o = EXHAUST SYSTEM FREQUENCY

SERIAL NO.	CONFIGURATION V_R NO.	CONFIGURATION V_S NO.	BMEP LBS/IN^2	AIR CONSUMPTION FT^3/MIN	RPM	ν_e CPS	η_v	l_e FT	ν_o CPS	ν_o/ν_e
44	PIPE ONLY		1.4	82.5	650	10.82	.711	12.3	24.2	2.24
45	"	"	16.9	82.0	648	10.3	.710	12.3	25.4	2.35
46	"	"	30.2	83.0	641	10.7	.725	12.3	26.4	2.46
47	"	"	1.3	85.5	654	10.88	.735	12.3	24.2	2.23
48	"	"	17.0	86.0	639	10.62	.756	12.3	25.4	2.49
49	"	"	30.0	86.0	640	10.65	.755	12.3	26.4	2.48
137	PIPE	& 1	1.2	91.0	649	10.8	.788	32.0	9.28	0.860
138	"	& 1	15.9	95.0	646	10.78	.325	32.0	9.75	0.916
139	"	& 1	27.5	101.5	640	10.65	.890	32.0	10.11	0.950
134	PIPE	& 2	1.3	91.0	650	10.82	.785	42.0	7.06	0.652
135	"	& 2	16.3	95.5	646	10.78	.830	42.0	7.44	0.691
136	"	& 2	27.0	102.0	641	10.7	.890	42.0	7.72	0.721
131	PIPE	& 3	1.2	94.5	646	10.78	.820	54.0	5.50	0.510
132	"	& 3	16.3	98.0	645	10.75	.855	54.0	5.78	0.537
133	"	& 3	27.1	106.0	635	10.6	.935	54.0	6.00	0.566
128	PIPE	& 4	1.3	91.0	650	10.82	.786	62.0	4.79	0.446
129	"	& 4	16.7	96.5	649	10.8	.835	62.0	5.04	0.466
130	"	& 4	27.5	110.0	631	10.5	.977	62.0	5.23	0.498
50	PIPE	& 5	1.3	95.5	646	10.78	.830	76.0	3.91	0.363
51	"	& 5	17.5	94.5	646	10.78	.820	76.0	4.11	0.382
52	"	& 5	29.5	94.5	645	10.75	.820	76.0	4.26	0.396

THESE DATA ARE PLOTTED IN FIGURE (42)

TABLE (D) - CONTINUED

SERIAL NO.	CONFIGURATION V_R NO.	V_S NO.	BMEP $\frac{Lbs}{IN^2}$	AIR CONSUMPTION $FT^3/MIN.$	RPM	ν_e CPS	η_v	l_e FT	ν_o CPS	ν_o/ν_e
38	1	& PIPE	1.1	101.0	659	11.0	.850	32.0	9.28	0.844
39	1	& "	16.4	101.0	648	10.8	.875	32.0	9.75	0.903
40	1	& "	30.8	101.0	645	10.75	.880	32.0	10.11	0.941
23	1	1	1.3	111.0	655	10.9	.951	17.0	17.47	1.60
24	1	1	17.1	111.0	659	11.0	.946	17.0	18.35	1.67
25	1	1	31.6	111.0	641	10.7	.967	17.0	19.08	1.76
25	1	2	1.6	109.5	654	10.83	.941	21.0	14.13	1.30
27	1	2	16.6	109.5	649	10.8	.950	21.0	14.89	1.378
28	1	2	30.2	111.0	645	10.78	.965	21.0	15.42	1.432
29	1	3	1.5	104.5	651	10.86	.903	24.0	12.38	1.140
30	1	3	16.1	104.5	647	10.79	.906	24.0	13.00	1.202
31	1	3	30.1	104.5	639	10.62	.920	24.0	13.50	1.270
32	1	4	1.5	105.0	654	10.89	.900	24.6	12.08	1.110
33	1	4	16.8	105.0	649	10.8	.909	24.6	12.70	1.165
34	1	4	30.2	105.0	648	10.8	.910	24.6	13.19	1.220
37	1	5	1.7	111.0	656	10.92	.950	26.2	11.80	1.080
36	1	5	17.0	111.0	650	10.82	.960	26.2	12.40	1.143
35	1	5	30.0	111.0	649	10.8	.960	26.2	12.84	1.190

THESE DATA ARE PLOTTED IN FIGURE (43)

TABLE (D) - CONTINUED

SERIAL NO.	CONFIGURATION V_R NO.	V_S NO.	BMEP $\frac{LBS}{IN^2}$	AIR CONSUMPTION FT^3/MIN	RPM	ν_e CPS	η_v	l_e FT	ν_o CPS	ν_o/ν_e
59	2	& PIPE	1.5	107.0	651	10.86	.921	42.0	7.06	0.650
60	2	"	16.0	109.0	649	10.8	.944	42.0	7.42	0.686
61	2	"	30.2	110.0	643	10.7	.960	42.0	7.72	0.721
62	2	1	1.4	101.0	661	11.0	.856	21.0	14.13	1.236
63	2	1	16.5	104.0	648	10.8	.900	21.0	14.89	1.380
64	2	1	30.2	106.0	647	10.79	.920	21.0	15.42	1.432
65	2	3	1.4	99.0	654	10.89	.850	30.5	9.74	0.895
66	2	3	16.7	99.0	650	10.82	.855	30.5	10.20	0.942
67	2	3	29.8	103.0	644	10.72	.900	30.5	10.61	0.990
68	2	4	1.4	101.5	645	10.75	.879	31.5	9.43	0.887
69	2	4	16.7	102.5	654	10.88	.880	31.5	9.91	0.913
70	2	4	30.3	107.0	633	10.33	.950	31.5	10.30	0.977
71	2	5	1.4	101.0	650	10.82	.871	34.5	8.61	0.795
72	2	5	17.0	101.0	646	10.77	.876	34.5	9.04	0.840
73	2	5	29.3	104.0	642	10.70	.910	34.5	9.40	0.878

THESE DATA ARE PLOTTED IN FIGURE (44)

TABLE (D) - CONTINUED

SERIAL NO.	CONFIGURATION V_R NO.	V_S NO.	BMEP LBS/IN^2	AIR CONSUMPTION FT^3/MIN	RPM	ν_e CPS	η_v	l_e FT	ν_o CPS	ν_o/ν_e
74	3	& PIPE	1.4	77.0	653	10.88	.661	54.0	5.50	0.506
75	3	"	16.5	79.5	645	10.75	.691	54.0	5.78	0.537
76	3	"	30.7	83.0	645	10.75	.723	54.0	6.00	0.558
77	3	"	1.4	75.0	651	10.86	.646	54.0	5.50	0.497
78	3	"	17.6	78.5	642	10.70	.686	54.0	5.78	0.540
79	3	"	30.2	84.0	645	10.75	.730	54.0	6.00	0.558
80	3	1	1.3	77.0	649	10.80	.666	24.0	12.38	1.145
81	3	1	17.4	71.5	647	10.79	.620	24.0	13.00	1.206
82	3	1	30.5	69.0	629	10.49	.616	24.0	13.50	1.290
83	3	2	1.3	78.5	655	10.90	.674	30.5	9.74	0.894
84	3	2	17.1	75.5	659	11.0	.644	30.5	10.20	0.927
85	3	2	30.2	73.0	639	10.62	.644	30.5	10.61	1.00
86	3	4	1.3	83.0	652	10.87	.713	37.0	8.04	0.740
87	3	4	16.6	79.0	648	10.8	.685	37.0	8.43	0.780
88	3	4	28.6	76.5	642	10.70	.667	37.0	8.71	0.815
89	3	5	1.3	57.0	650	10.82	.491	41.3	7.20	0.665
90	3	5	17.0	55.5	646	10.78	.481	41.3	7.56	0.703
91	3	5	29.5	54.0	652	10.86	.465	41.3	7.80	0.718

THESE DATA ARE PLOTTED IN FIGURE (45)

TABLE (D) - CONTINUED

SERIAL NO.	CONFIGURATION V_R NO.	V_S NO.	BMEP $\frac{LBS}{IN^2}$	AIR CONSUMPTION FT^3/MIN	RPM	ν_e CPS	η_v	l_e FT	ν_o CPS	ν_o/ν_e
92	4	& PIPE	1.3	82.0	655	10.9	.705	62.0	4.79	0.440
93	4	"	16.9	77.0	645	10.78	.670	62.0	5.04	0.468
94	4	"	29.9	75.5	639	10.62	.665	62.0	5.23	0.487
95	4	1	1.3	92.0	650	10.82	.795	24.6	12.08	1.114
96	4	1	16.5	82.5	644	10.72	.720	24.6	12.70	1.182
97	4	1	30.3	80.0	638	10.62	.705	24.6	13.19	1.230
98	4	2	1.3	92.5	652	10.88	.796	31.5	9.43	0.879
99	4	2	16.5	87.0	645	10.73	.758	31.5	9.91	0.924
100	4	2	29.5	80.0	652	10.88	.690	31.5	10.30	0.947
101	4	3	1.3	94.5	662	11.02	.801	37.0	8.04	0.729
102	4	3	17.3	88.0	646	10.78	.765	37.0	8.43	0.782
103	4	3	30.6	80.5	632	10.53	.715	37.0	8.71	0.828
104	4	5	1.3	93.0	657	10.96	.795	44.8	6.64	0.606
105	4	5	16.9	87.0	648	10.80	.755	44.8	6.96	0.645
106	4	5	30.2	83.0	644	10.71	.725	44.8	7.20	0.671

THESE DATA ARE PLOTTED IN FIGURE (46)

TABLE (D) - CONTINUED

SERIAL NO.	CONFIGURATION V_R NO.	V_S NO.	BMEP $\frac{LBS}{IN^2}$	AIR CONSUMPTION FT^3/MIN	RPM	ν_e CPS	η_V	l_e FT	ν_o CPS	ν_o/ν_e
107	5	& PIPE	1.2	106.0	651	10.85	.914	76.0	3.91	0.360
108	5	& "	16.4	103.0	648	10.80	.894	76.0	4.11	0.381
109	5	& "	30.7	100.0	642	10.70	.875	76.0	4.26	0.398
110	5	1	1.3	108.0	647	10.79	.935	26.2	11.80	1.092
111	5	1	16.7	105.0	647	10.79	.910	26.2	12.40	1.150
112	5	1	30.2	102.0	643	10.71	.891	26.2	12.84	1.198
113	5	2	1.2	107.0	664	11.07	.906	34.5	8.61	0.780
114	5	2	17.0	102.5	648	10.80	.890	34.5	9.04	0.836
115	5	2	29.0	102.0	655	10.90	.872	34.5	9.40	0.862
119	5	3	1.3	106.0	651	10.86	.914	41.3	7.20	0.664
120	5	3	17.4	104.0	652	10.89	.895	41.3	7.56	0.695
121	5	3	29.1	102.0	640	10.68	.895	41.3	7.80	0.730
116	5	4	1.4	100.0	652	10.89	.862	44.3	6.64	0.610
117	5	4	16.4	106.0	645	10.75	.921	44.8	6.96	0.648
118	5	4	30.4	108.0	639	10.62	.950	44.8	7.20	0.670

THESE DATA ARE PLOTTED IN FIGURE (47)

TABLE (E)

COMPARISON OF VOLUMETRIC EFFICIENCIES OF DUPLICATE RUNS MADE AT DIFFERENT TIMES.

SERIAL NO.	CONFIGURATION V_R	CONFIGURATION V_S	BMEP	η_v	Δ	%
44	PIPE ONLY		1.4	.711	+	
47	"	"	1.3	.735	+.025	+3.4
45	"	"	16.9	.710		
48	"	"	17.0	.756	+.046	+6.1
46	"	"	30.2	.725		
49	"	"	30.0	.755	+.030	+4.0
74	3	NONE	1.4	.661		
77	3	"	1.4	.646	-.015	-2.3
75	3	"	16.5	.691		
78	3	"	17.6	.686	-.015	-2.2
76	3	"	30.7	.723		
79	3	"	30.2	.730	+.007	+0.96
107	4	NONE	1.2	.914		
122	4	"	1.3	.940	+.026	+2.0
108	4	"	16.4	.894		
123	4	"	16.3	.916	+.022	+2.4
109	4	"	30.7	.875		
124	4	"	25.9	.865	+.010	+1.1

V_R = VOLUME OF RECEIVER

V_S = VOLUME OF SILENCER

η_v = VOLUMETRIC EFFICIENCY

Δ = DIFFERENCE

TABLE (F)

COMPARISON OF CALCULATED AND MEASURED FREQUENCIES

(ALL DATA FOR MAXIMUM BMEP)

SERIAL NO.	CONFIGURATION V_R	CONFIGURATION V_S	η_v	ν_o CALCULATED	$\nu_{o'}$ MEASURED	$\nu_{o'}/\nu_o$
46	PIPE ONLY		.725	26.4	42.7	1.62
38	1 + PIPE ONLY		.86	9.3	16.5	1.78
23	1	1	.95	17.5	14.0	.80
25	1	2	.94	14.1	15.9	1.11
28	1	3	.965	12.5	16.6	1.22
34	1	4	.910	13.2	17.0	1.29
37	1	5	.950	11.8	16.6	1.40
61	2	PIPE	.96	7.8	11.9	1.53
64	2	1	.92	15.4	16.0	1.04
67	2	3	.90	10.6	17.0	1.61
70	2	4	.95	10.3	- -	- -
73	2	5	.91	9.4	18.7	1.99
82	3	1	.616	13.5	12.6	.935
85	3	2	.644	10.6	14.5	1.37
88	3	4	.67	8.7	12.0	1.38
91	3	5	.47	7.8	12.6	1.62
79	3	PIPE	.646	5.5	12.2	2.05
97	4	1	.705	13.2	11.8	.9
100	4	2	.69	10.3	10.4	1.01
103	4	3	.70	8.7	11.4	1.31
105	4	5	.725	7.2	10.5	1.46
94	4	PIPE	.665	5.2	11.7	2.24

TABLE (G)

COMPARISON OF SIMILAR CONFIGURATIONS WITH INTERCHANGED TANK POSITIONS

(η_{PIPE} = .755 AT MAXIMUM BMEP)

CONFIGURATION V_R	CONFIGURATION V_S	BMEP LOW	BMEP MEDIUM	BMEP HIGH	ν_o CALCULATED	η/η_{PIPE}	V/A	ν_o' MEASURED
-	1	.788	.825	.890	10	1.18	2.3	16.5
1	-	.860	.875	.880	10	1.17		11.9
-	2	.785	.830	.890	7.5	1.18	9.5	
2	-	.921	.944	.960	7.5	1.27		11.9
-	3	.820	.855	.935	5.8	1.24	17.8	
3	-	.646	.686	.730	5.8	.97		12.2
-	4	.786	.835	.977	5.0	1.29	23.5	
4	-	.705	.670	.665	5.0	.88		11.7
-	5	.830	.820	.820	4.1	1.08	41.5	16.1
5	-	.914	.894	.875	4.1	1.16		
1	2	.941	.950	.965	14.9	1.28		15.9
2	1	.856	.900	.920	14.9	1.22		16.0
1	3	.900	.906	.920	13.0	1.22		16.6
3	1	.666	.620	.616	13.0	.82		12.6
1	4	.900	.909	.910	12.7	1.20		17.0
4	1	.795	.720	.705	12.7	.935		11.8
1	5	.950	.960	.960	12.4	1.27		16.6
5	1	.935	.910	.891	12.4	1.18		10.2

CONTINUED NEXT PAGE

TABLE (G) - CONTINUED

CONFIGURATION V_R	V_S	BMEP LOW	BMEP MEDIUM	BMEP HIGH	η_0 CALCULATED	η/η_{PIPE}	V/A	η_0 MEASURED
5	2	.906	.890	.872	9.0			
2	5	.871	.876	.910	9.0			
5	3	.914	.895	.895	7.6			
3	5	.491	.481	.485	7.6	.615		12.6
4	1	.795	.720	.705	12.7	.93		11.8
1	4	.900	.909	.910	12.7	1.20		17.0
4	2	.796	.758	.690	9.9	.915		10.4
2	4	.879	.880	.950	9.9	1.26		
3	2	.674	.544	.644	10.2	.85		14.5
2	3	.850	.855	.900	10.2	1.19		17.0

LIST OF FIGURES

LIST OF FIGURES - continued.

LIST OF FIGURES - continued.

LIST OF FIGURES - continued

Photographic records are identified by serial numbers to facilitate cross reference with Table D.

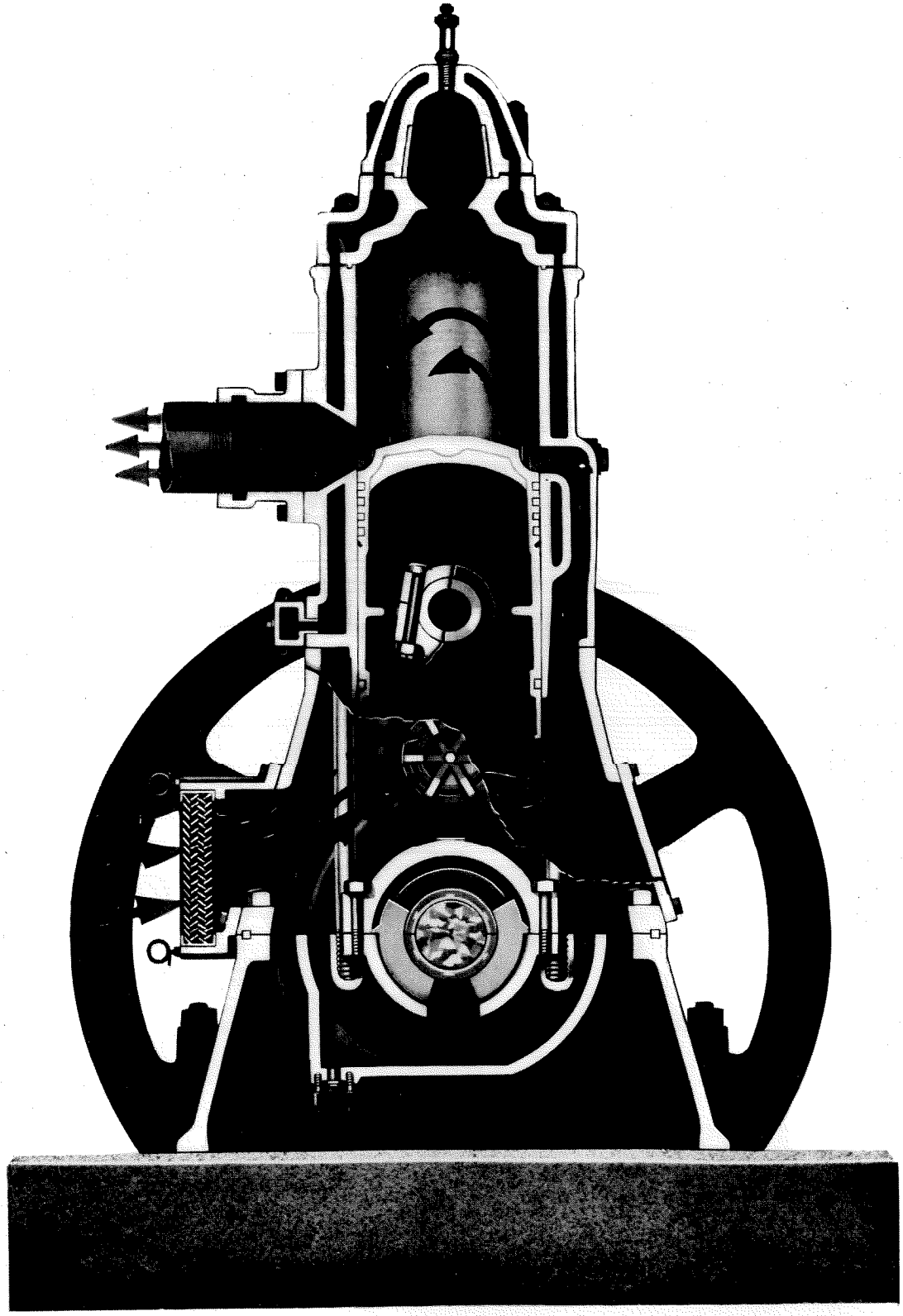

FIGURE (1)

CROSS SECTION THROUGH CRANK CASE SCAVENGED TWO STROKE ENGINE (VENN SEVERIN).

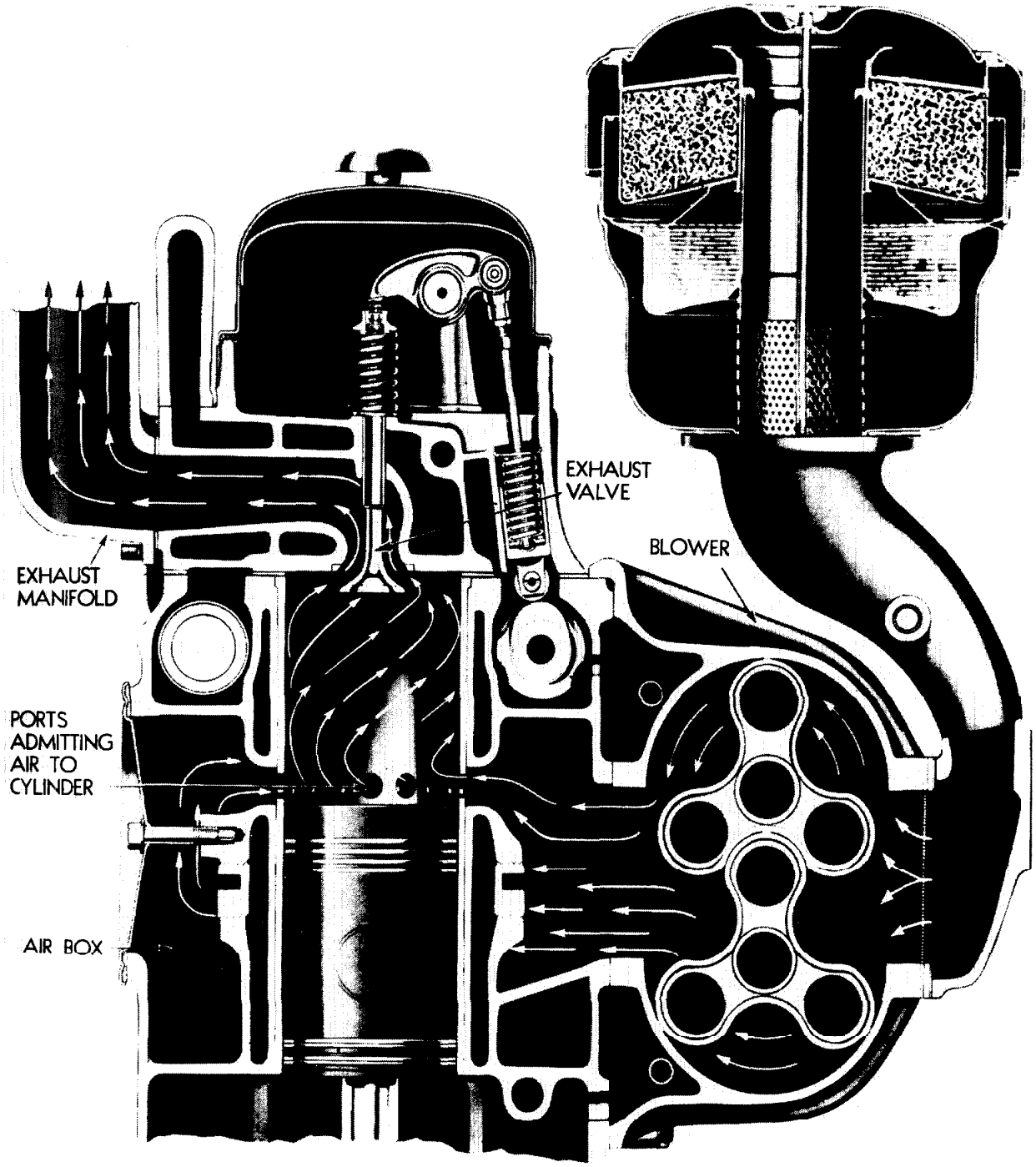

AIR INTAKE AND EXHAUST SYSTEM

FIGURE (2)

CROSS SECTION THROUGH BLOWER SCAVENGED TWO STROKE ENGINE (GENERAL MOTORS SERIES 71)

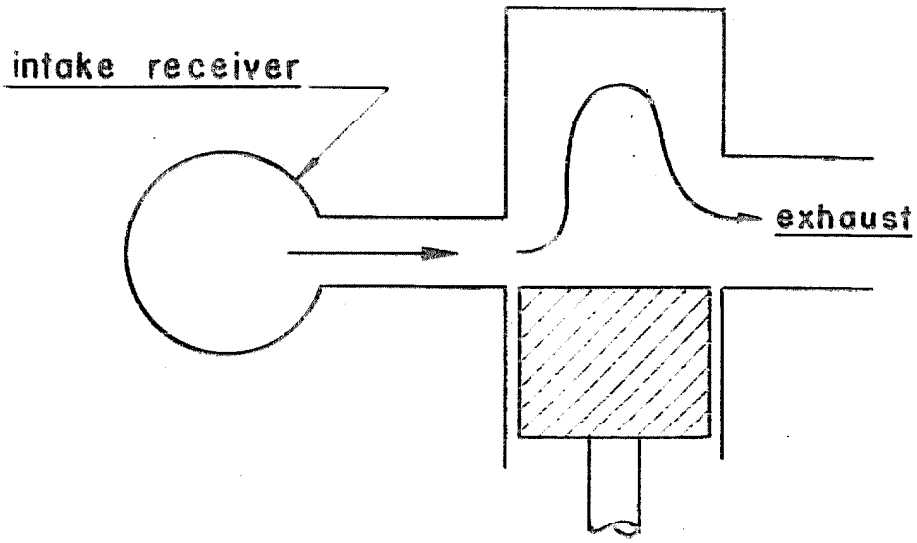

Fig. (3) Schematic diagram of scavenging blower through a two stroke engine

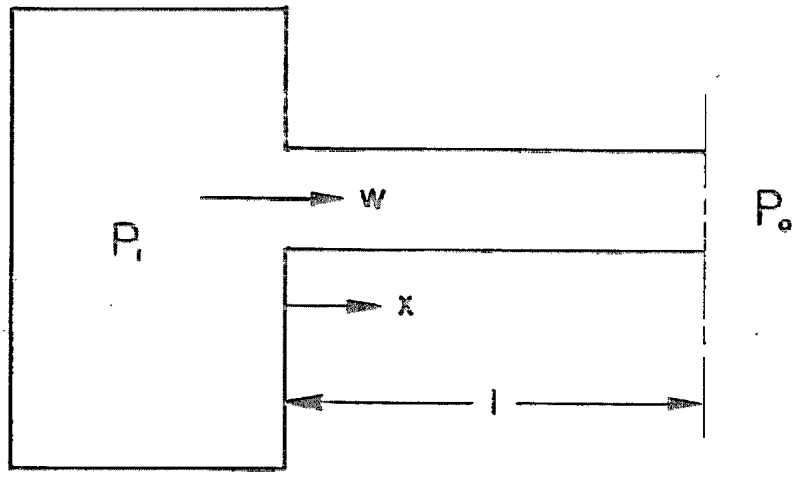

Fig. (4) Efflux from a pressure tank through a pipe (accelerated flow)

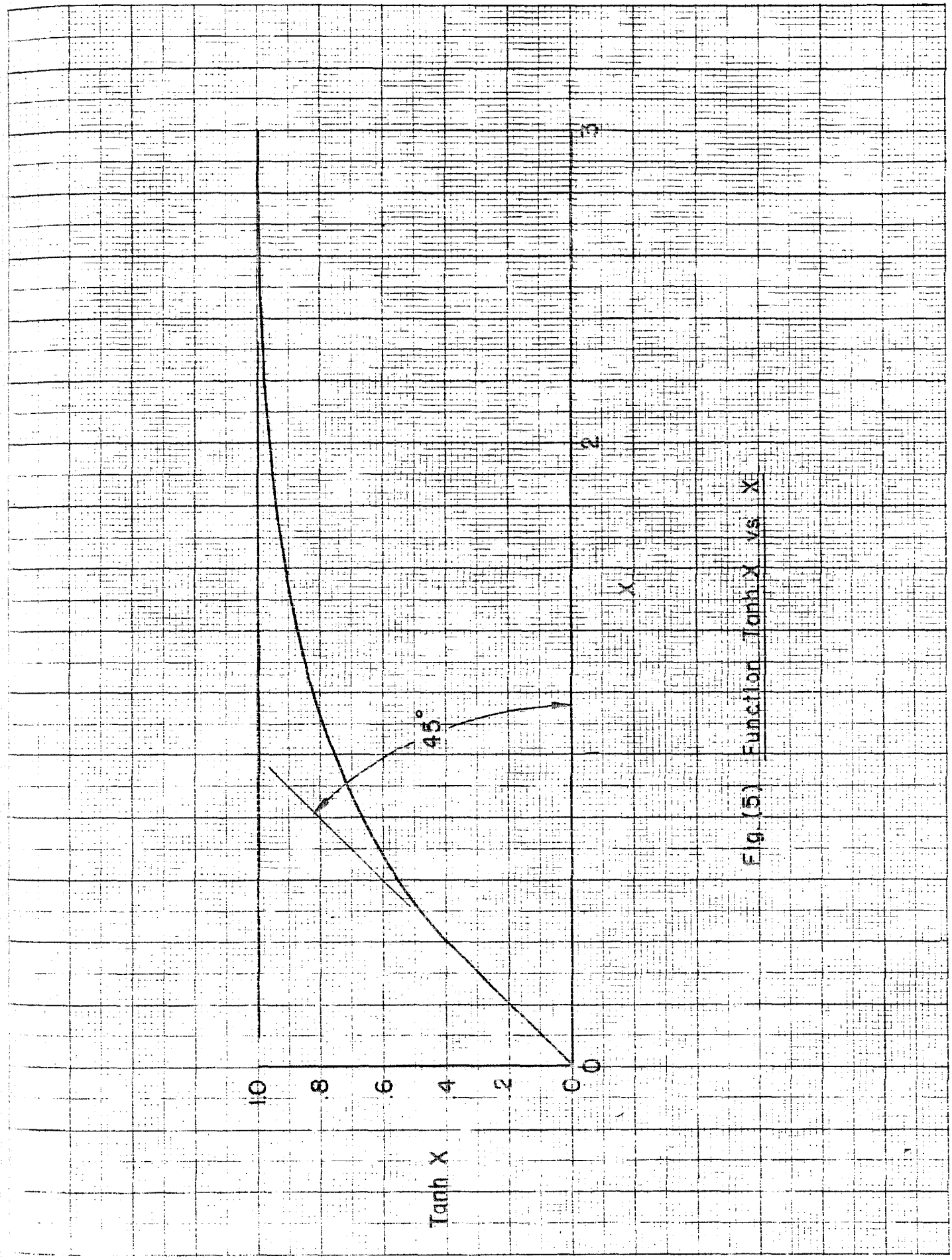

Fig. (5) Function Tanh X vs X

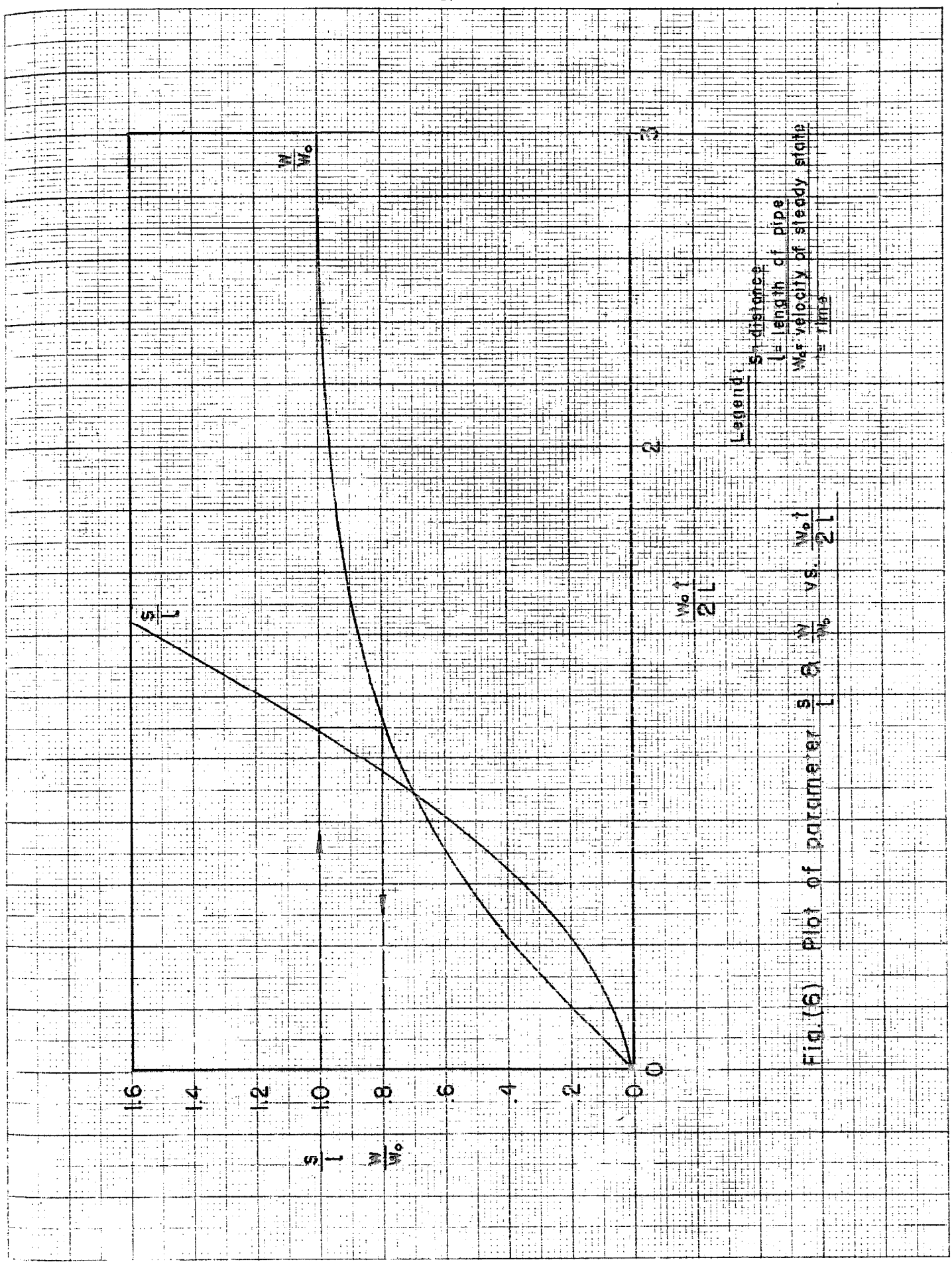

Fig. (6) Plot of parameter $\frac{s}{l}$ & $\frac{W}{W_o}$ vs. $\frac{W_o t}{2L}$

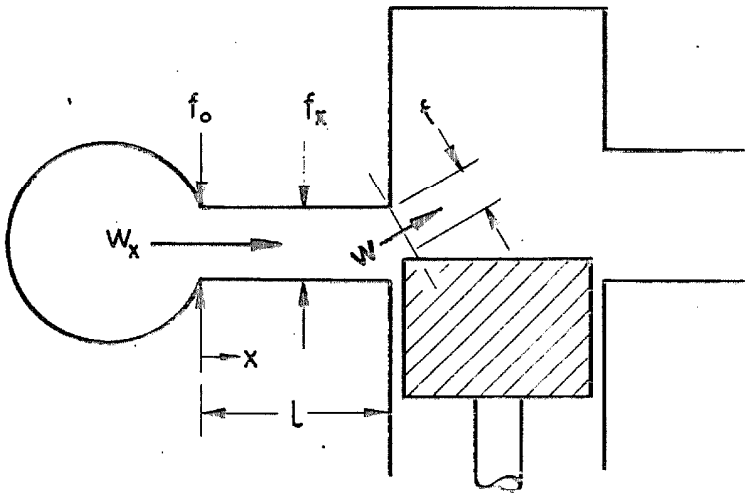

Fig. (7) Notation used in analysis of flow from intake receiver to cylinder.

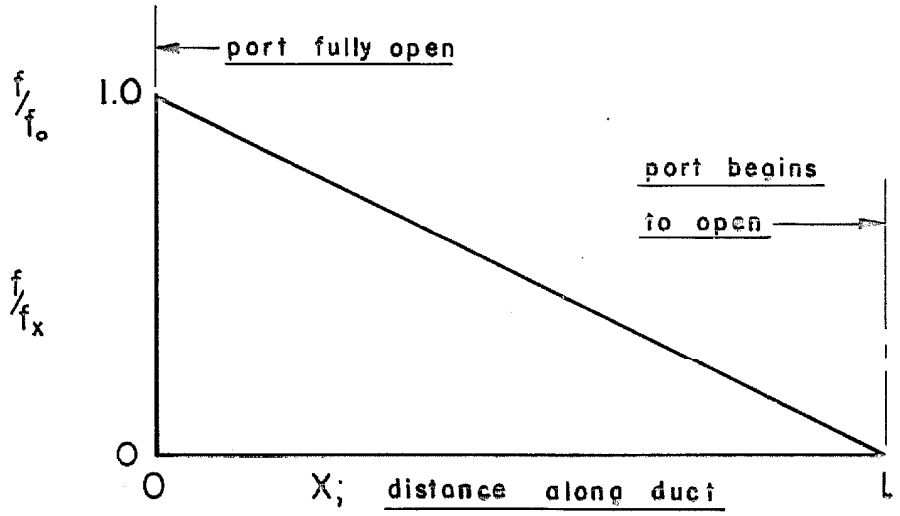

Fig. (8) Plot of f/f_x vs. X

Legend:

f = port opening

f_o = cross sectional area of duct at any station

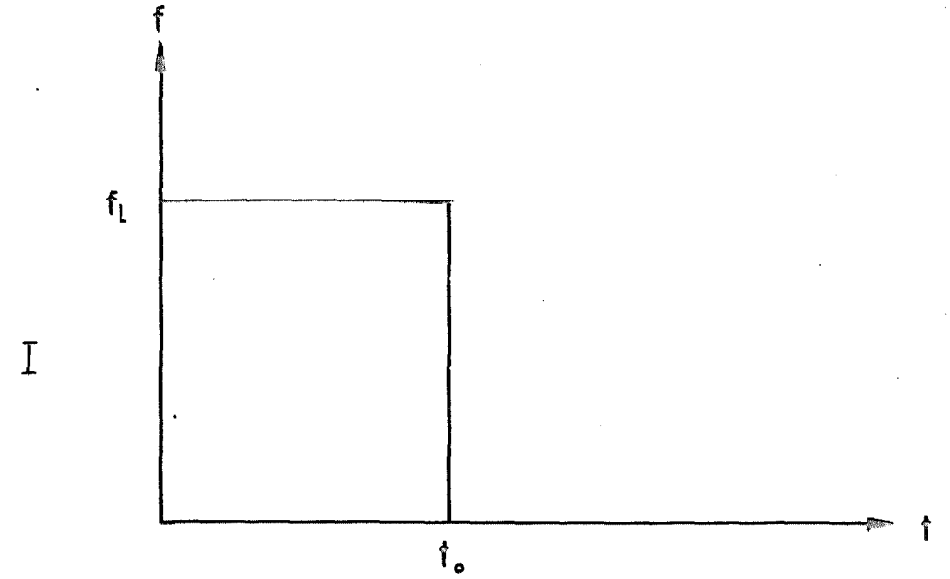

Area f_o is open for period t_o

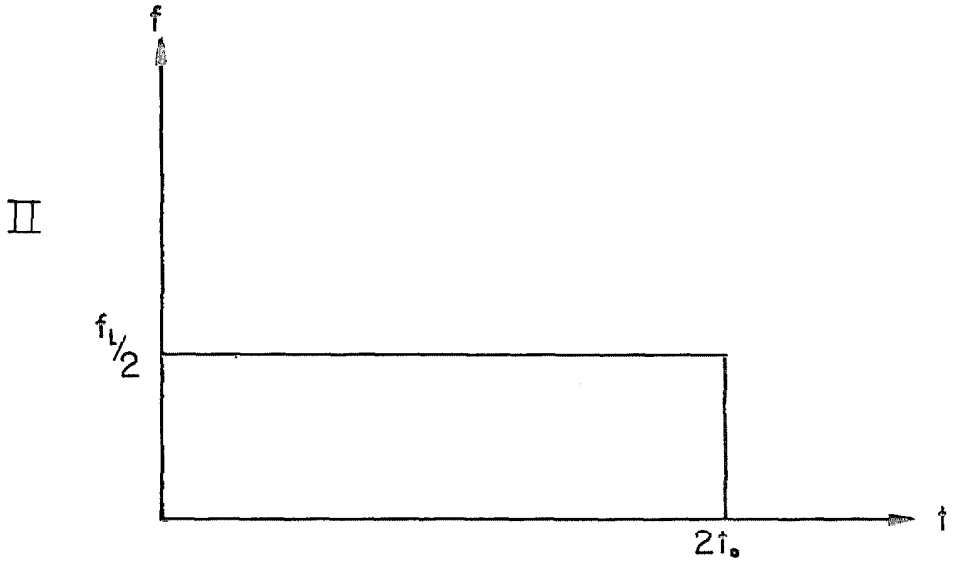

Area $f_L/2$ is open for period $2t_o$

Fig. (9) Two cases of the relationship between port area and time

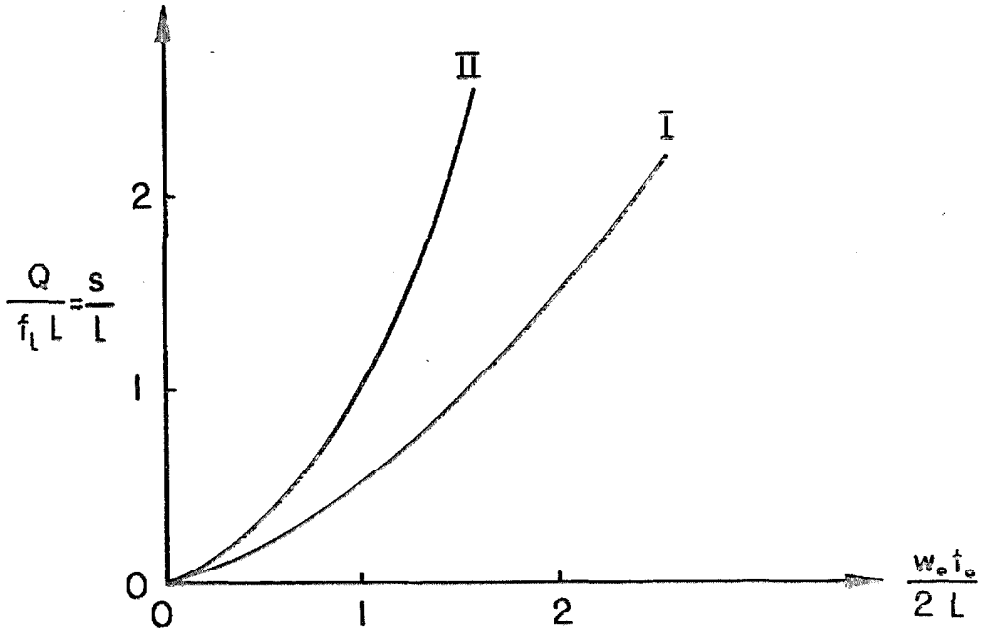

Fig. (10) Plot of $Q/f_L L$ vs. $w_o t/2L$ for case I & II

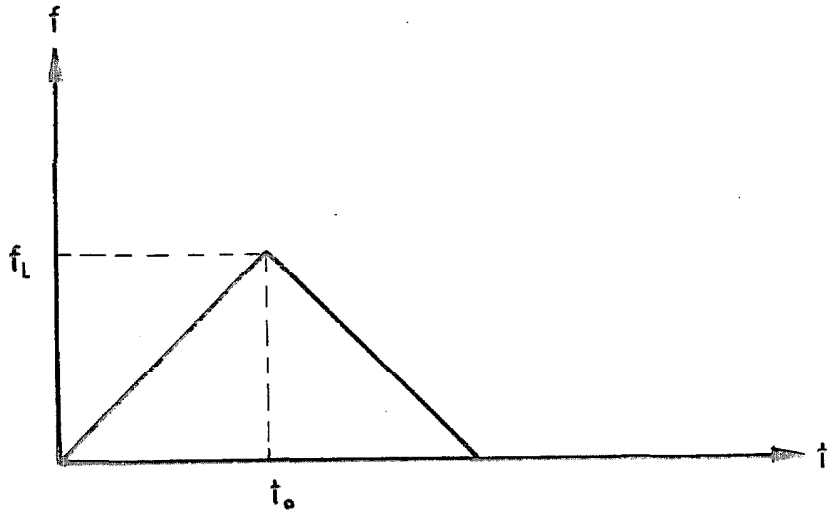

Fig. (11) Triangular distribution of port opening versus time

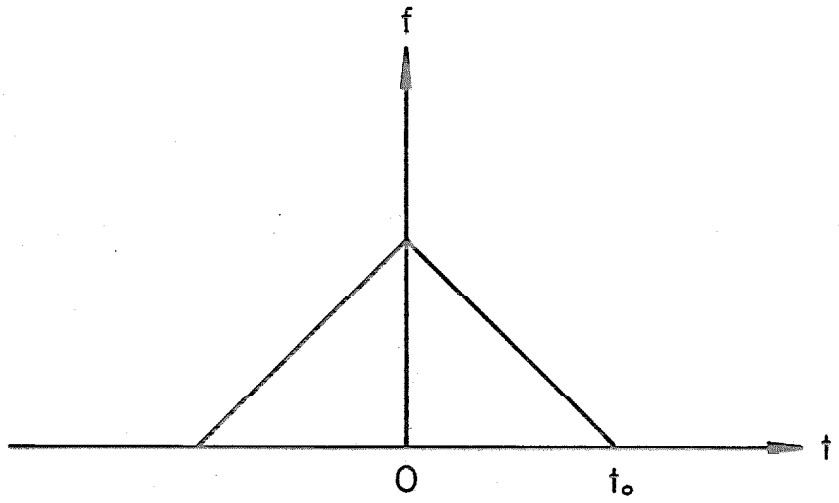

Fig. (12) New coordinates for the port closing period

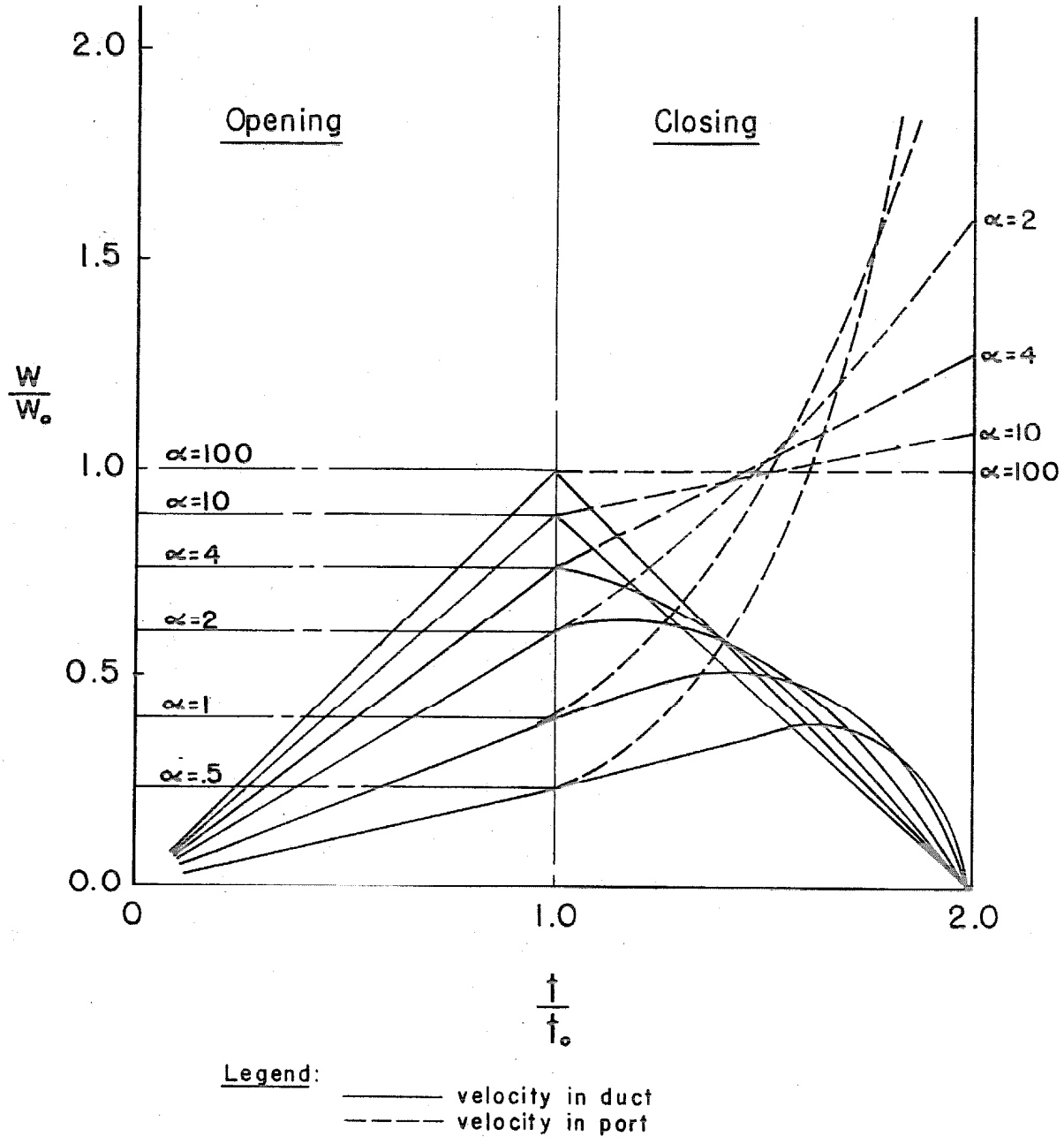

Fig. (13) Dimensionless plot of velocity in duct and port as a function of dimensionless time parameter

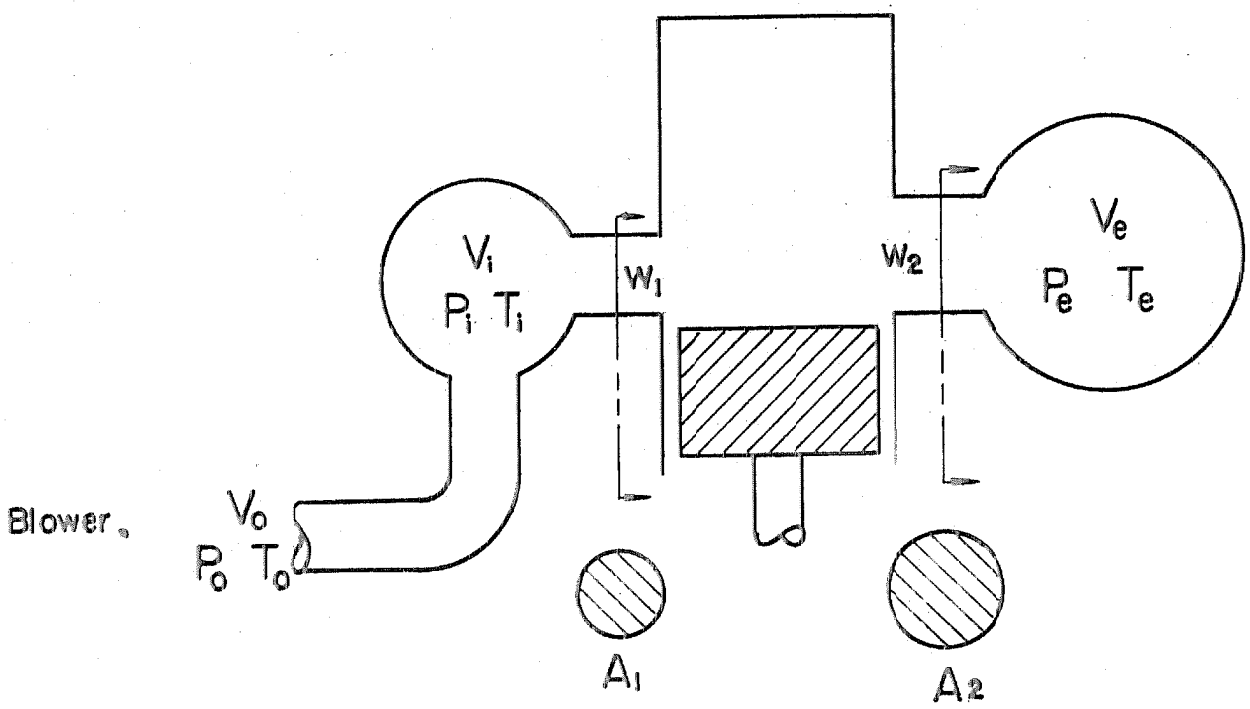

Fig. (14) Notation used in analyzing flow through engine from intake receiver to exhaust collector

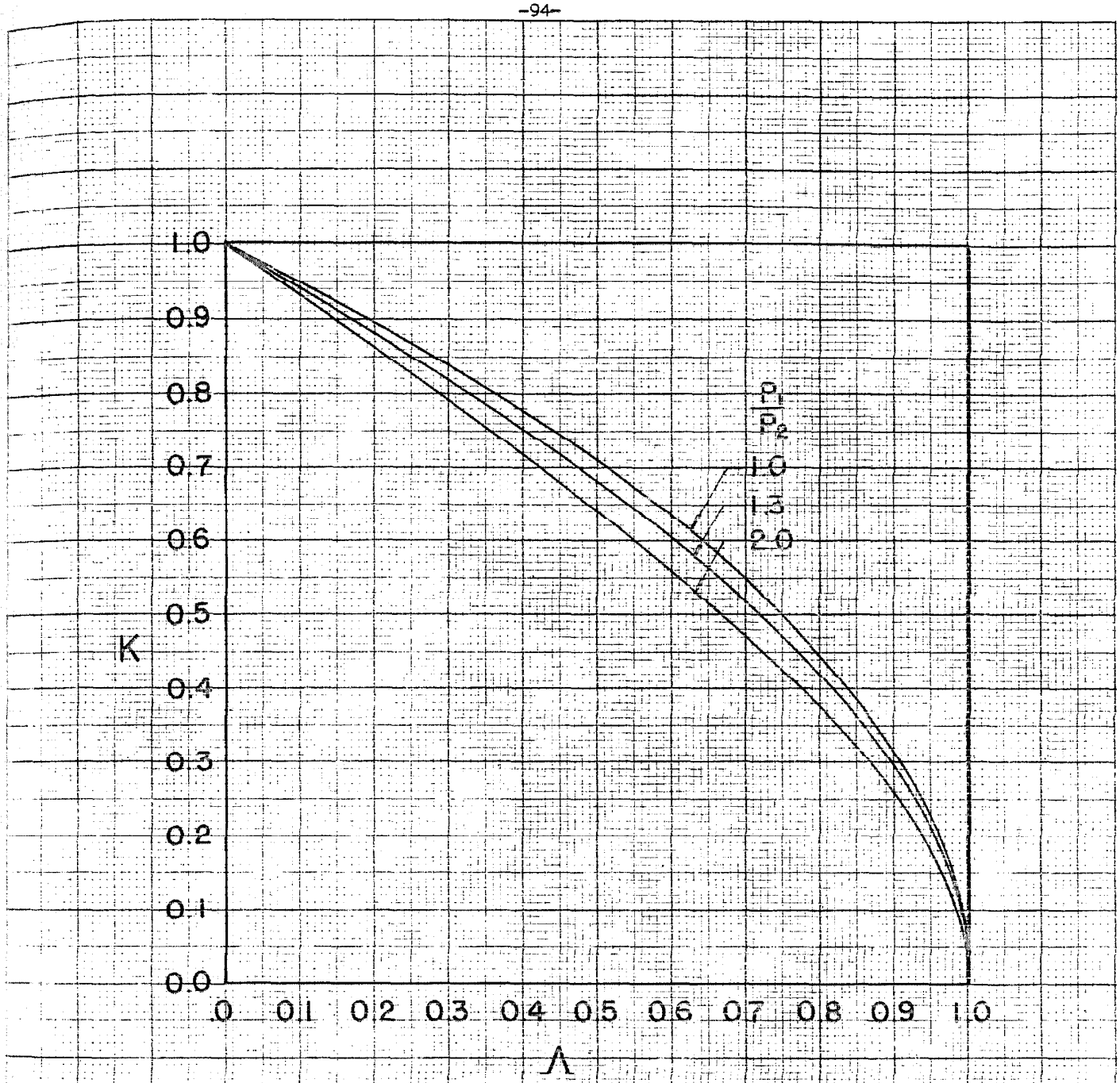

Fig. (15) Flow Coefficient vs. Loss Parameter for Different Pressure Ratios

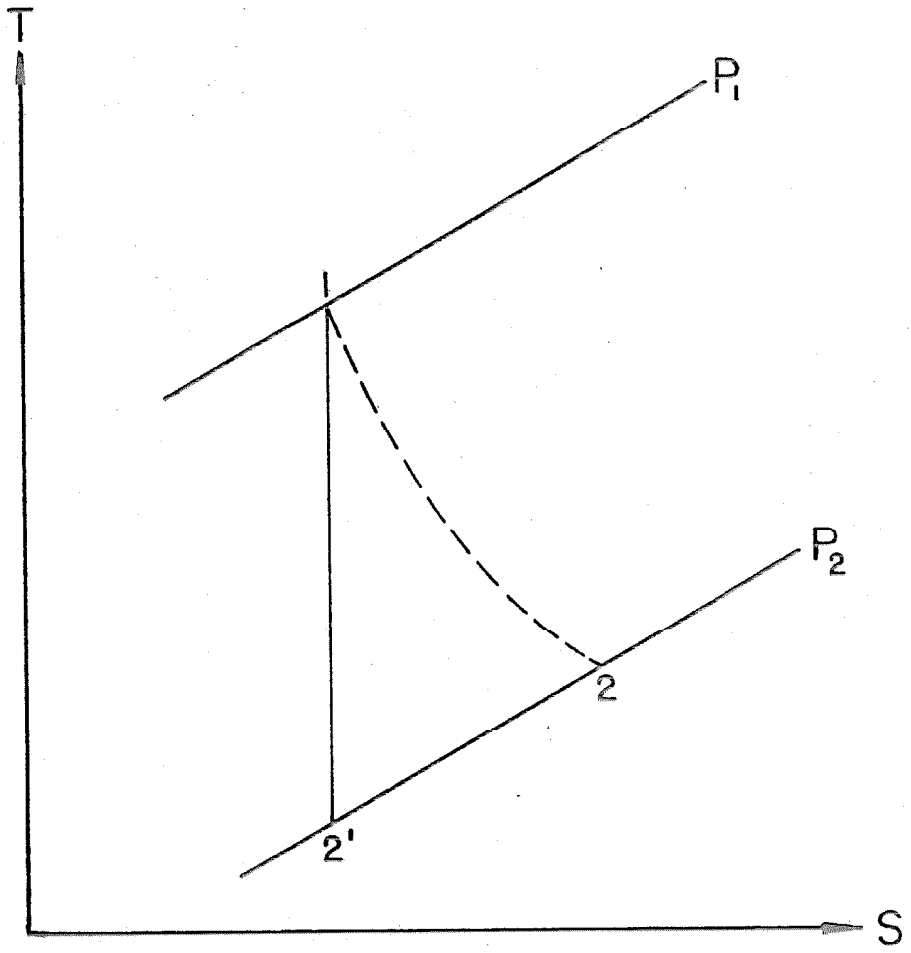

Fig. (16) Temperature—Entropy diagram for flow through engine

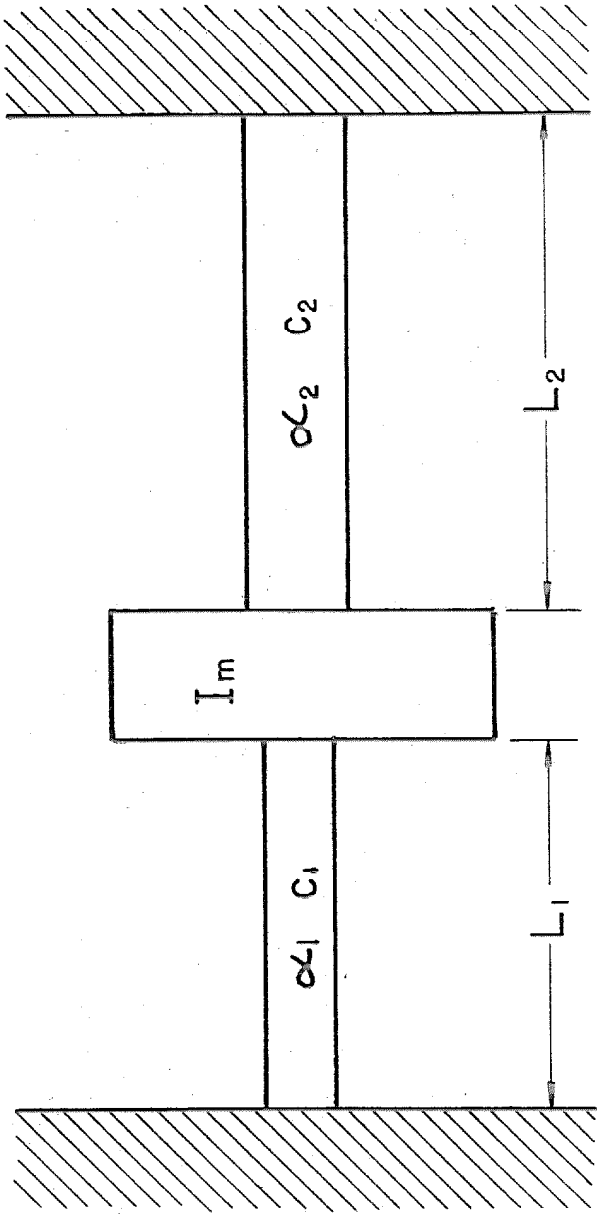

Fig. (17) Torsional vibration as an analogy to gas vibration in a pipe

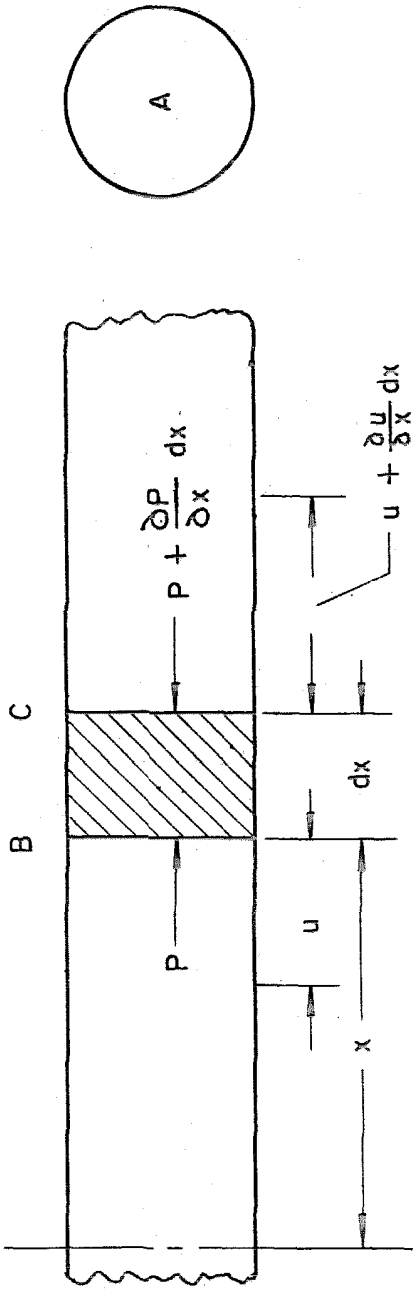

Fig. (18) Notation for analysis of longitudinal vibrations of an elastic bar

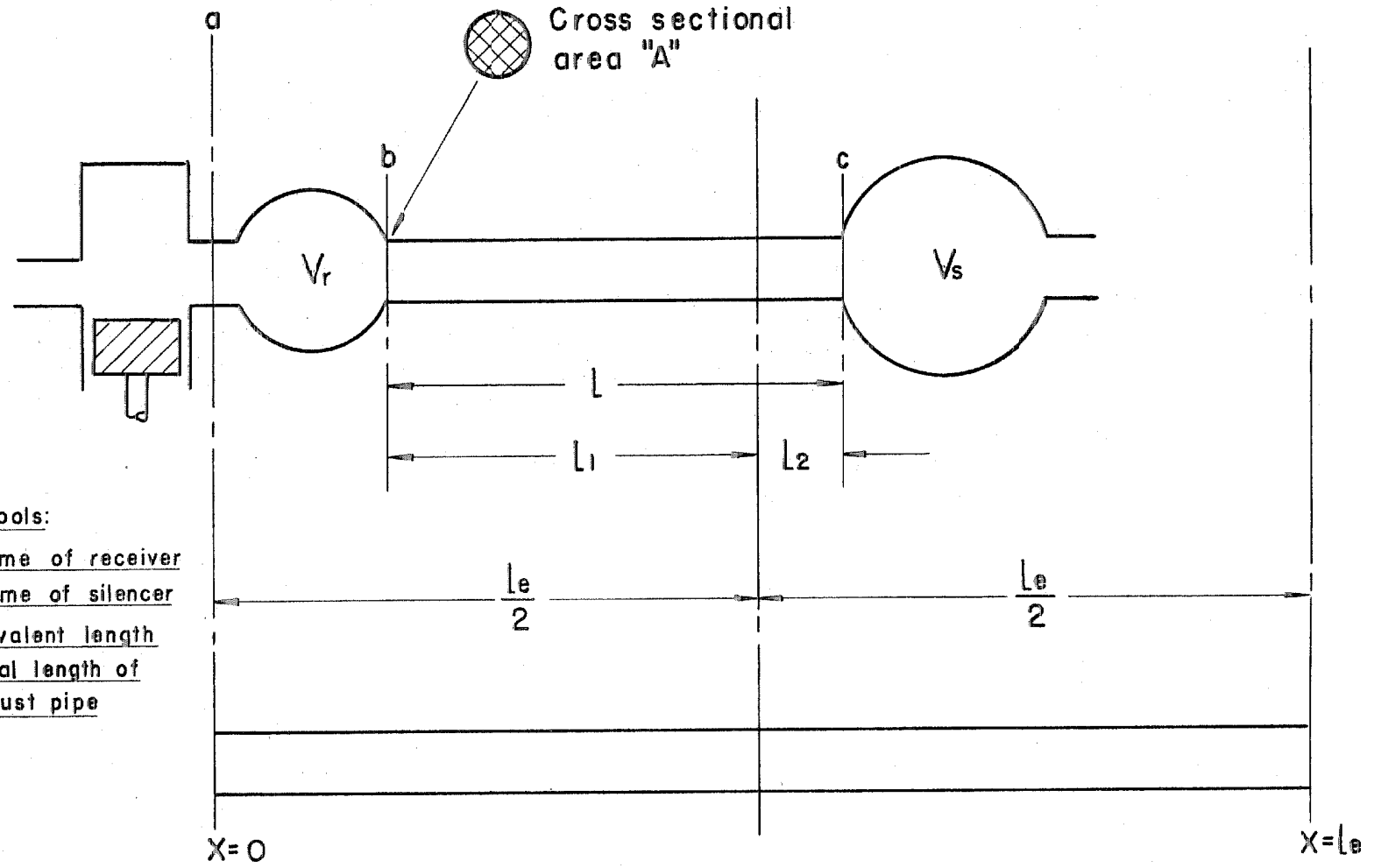

Symbols:

V_r = Volume of receiver

V_s = Volume of silencer

l_e = Equivalent length

l = Actual length of exhaust pipe

Fig. (19) Notation for analysis of equivalent length of system

(1) Assume $l_e = 20$ ft. and solve equation (76) for l
Result: $l = 15.4$ ft.

(2) Assume $l_e = 15$ ft. and repeat calculation
Result. $= 10.65$ ft.

(3) Assume $l_e = 17.5$ ft and repeat calculation
Result: $l = 13.05$ ft.

(4) Plot and with given $l = 12.3$ ft. find $l_e = 17$ ft.

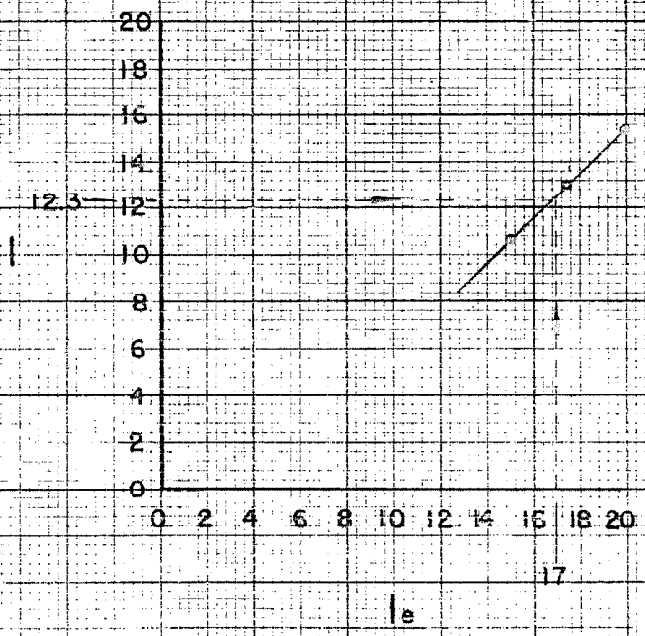

Fig. (20) Example solution of equation for equivalent length

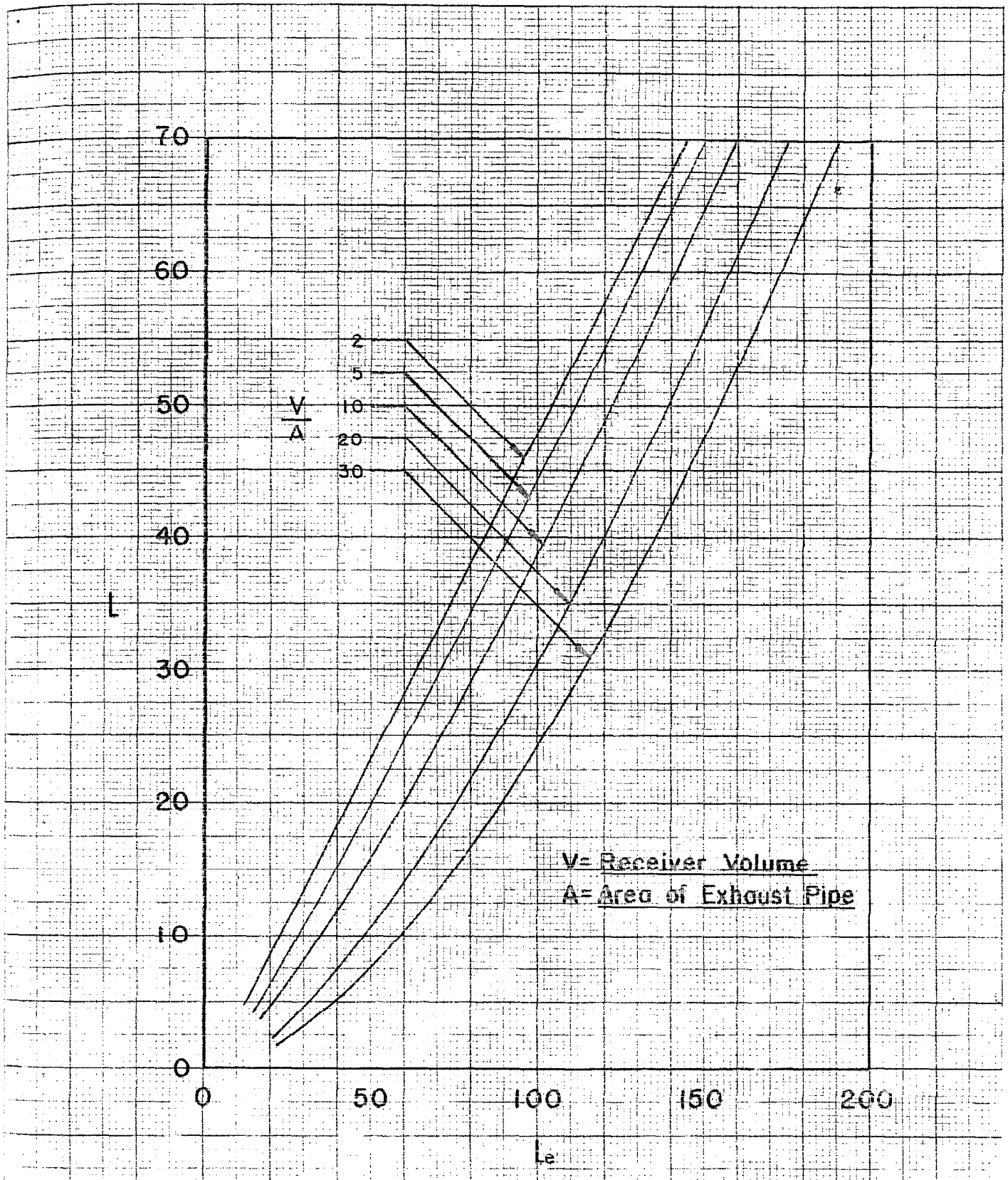

Fig. (21) Effective length vs. actual length with V/A as a parameter

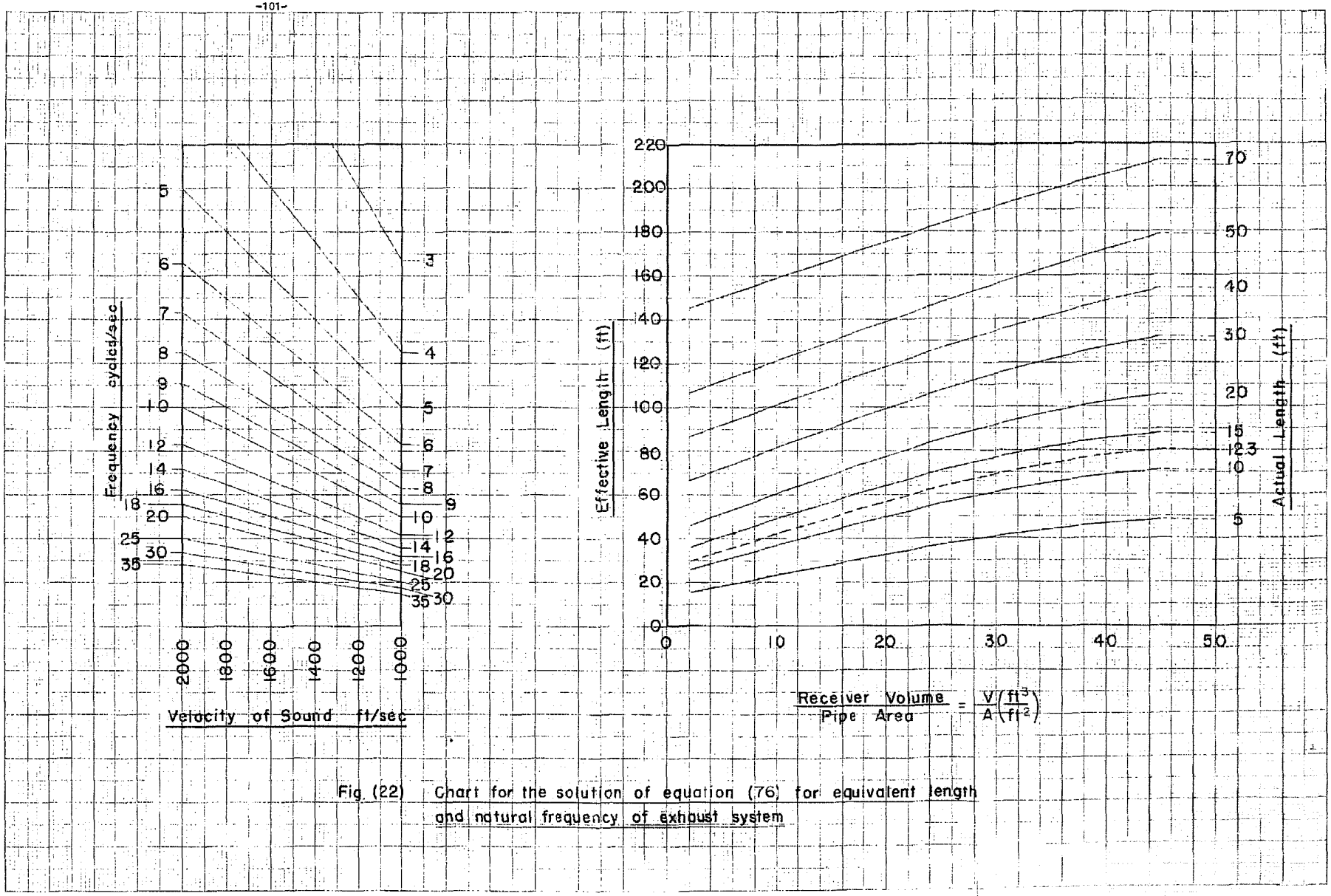

Fig. (22) Chart for the solution of equation (76) for equivalent length and natural frequency of exhaust system

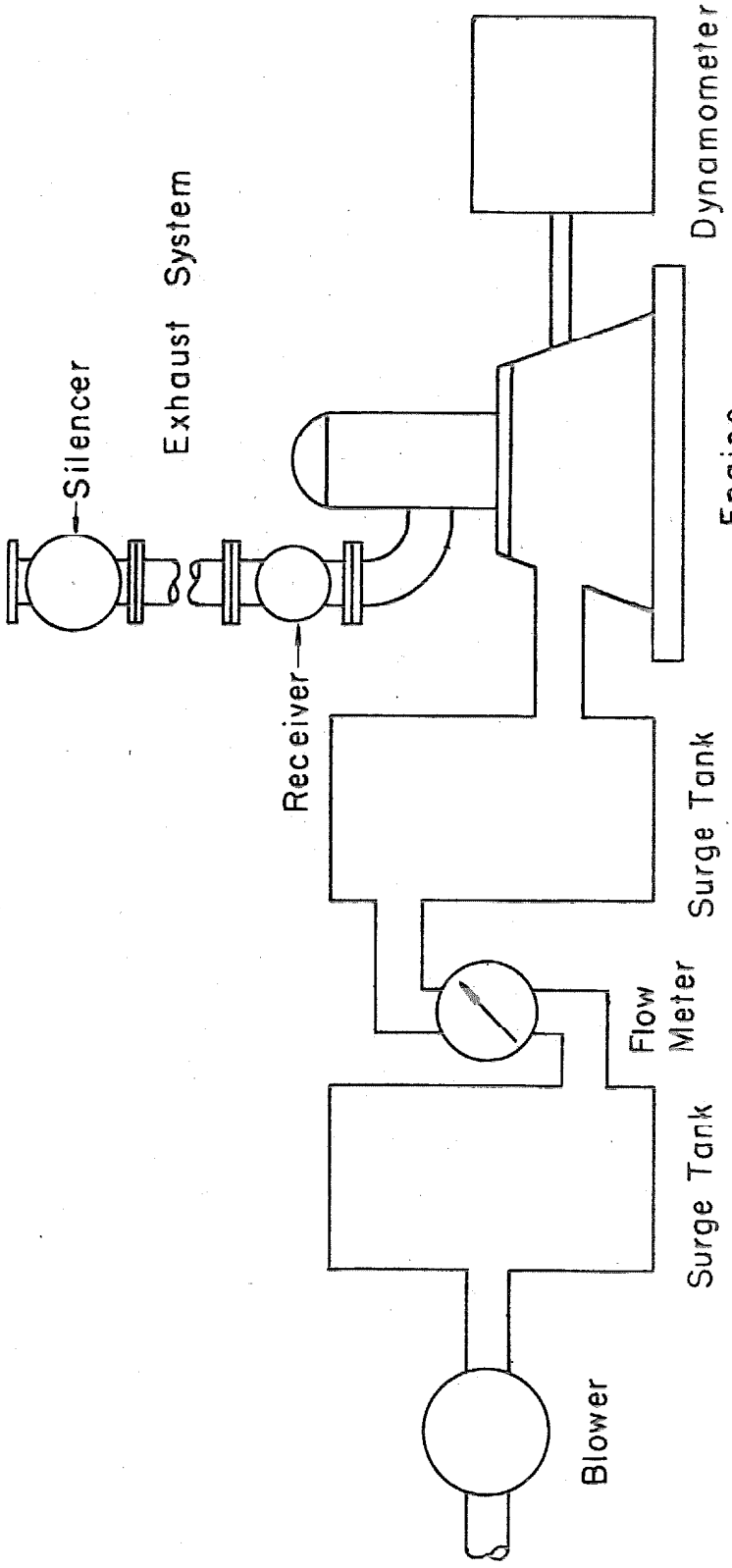

Fig.(23) Schematic Diagram of Test Setup
(Mechanical Apparatus)

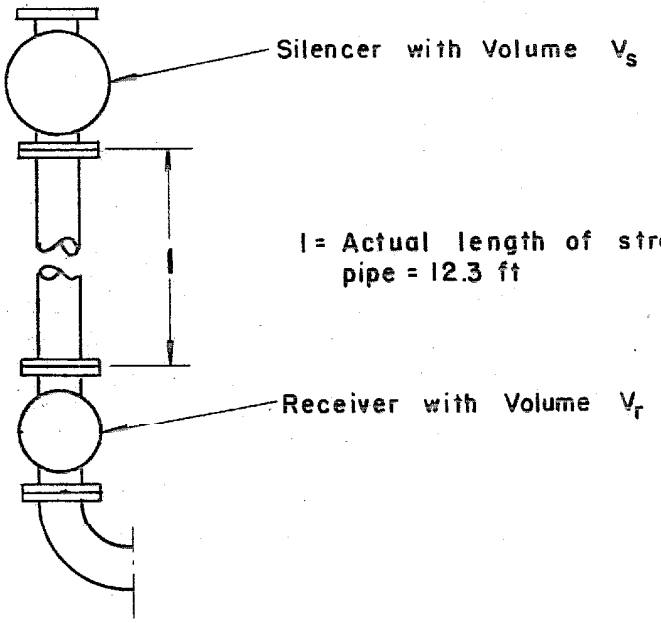

Exhaust Pipe Diameter = 4 inch (nominal size)

Dimensions of Tanks

Tank No.	Diameter inches	Length inches	Volume ft^3	Ratio = Volume / Pipe area	Volume V_D*
1	6.13	12.00	0.204	2.3	1.145
1A	6.13	12.00	0.204	2.3	1.145
2	10.13	18.00	0.840	9.5	4.71
3	12.13	24.00	1.600	17.8	9.00
4	15.63	18.63	2.070	23.5	11.60
5	15.63	33.00	3.660	41.5	20.60

* V_D = Engine displacement volume = 0.178 ft^3

Fig (24) Dimensions of Exhaust System Components of Test Setup

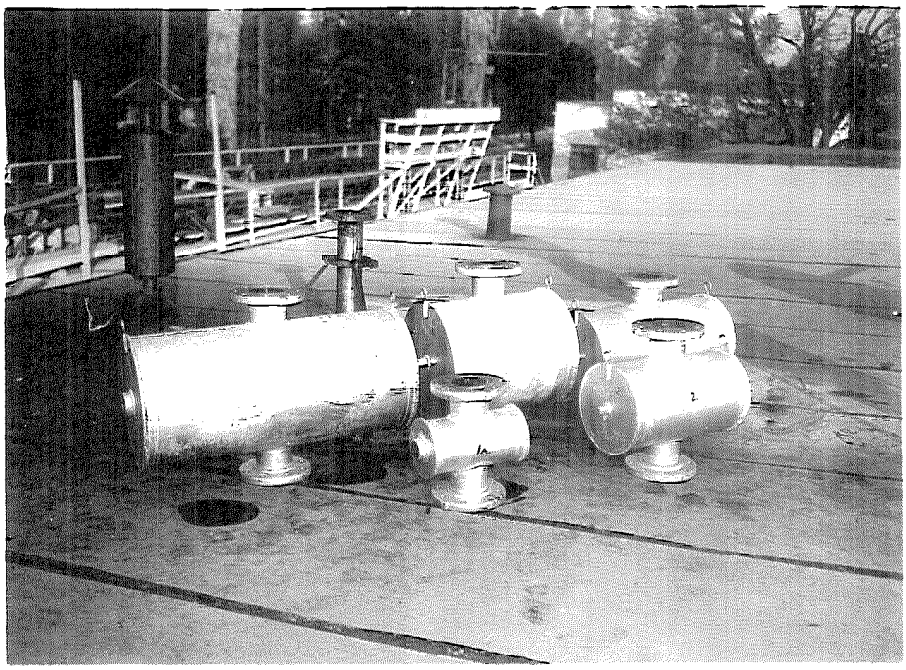

FIGURE (25)

RECEIVER AND SILENCER TANKS.

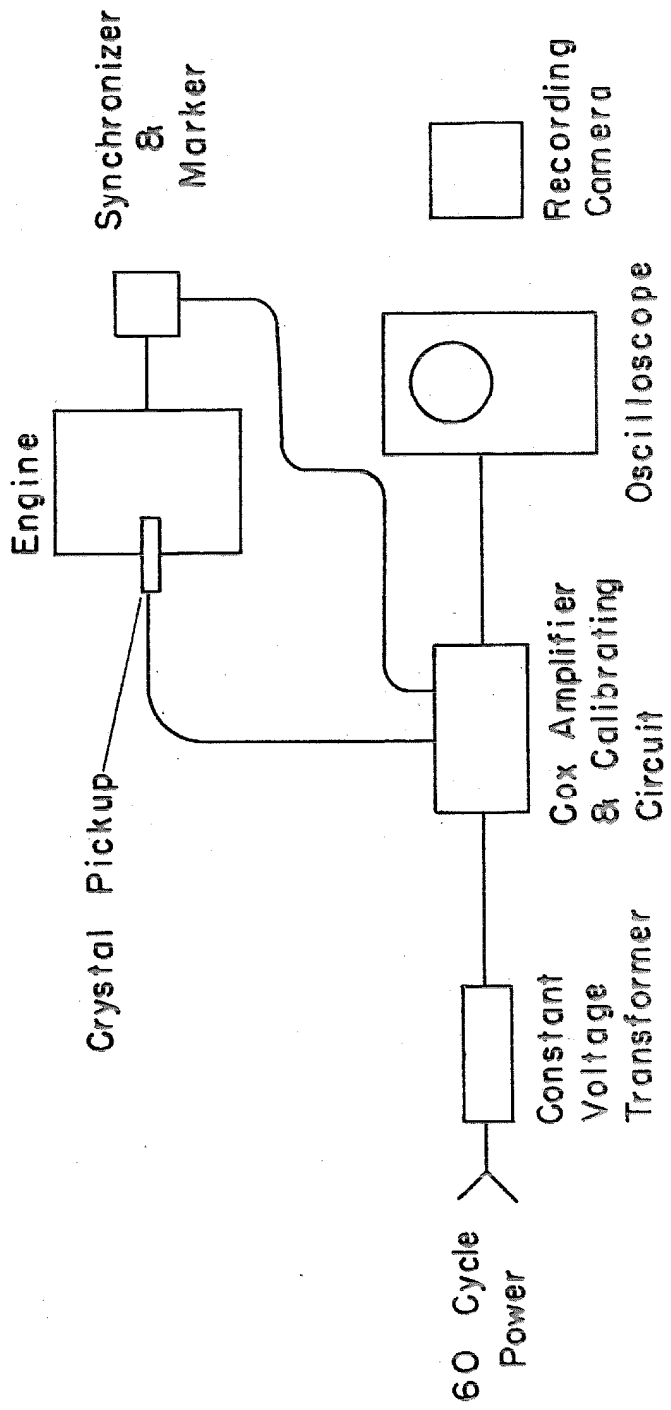

Fig.(26) Schematic Diagram of Test Setup
(Electronic Apparatus)

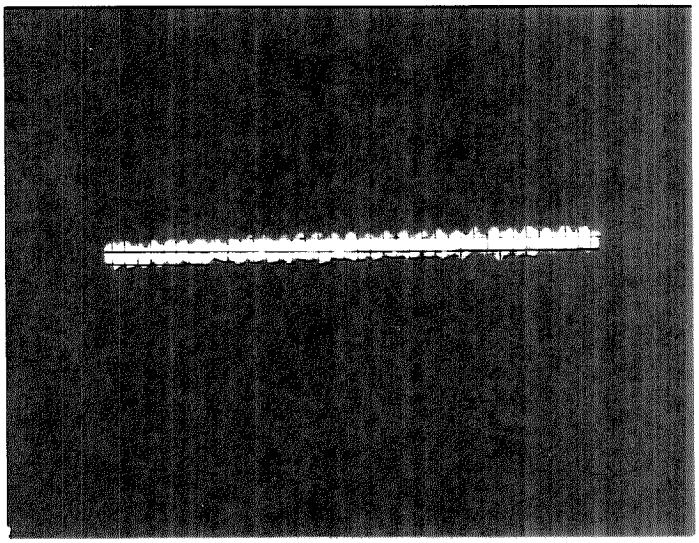

FIGURE (27)

RESIDUAL DISTURBANCE OF OSCILLOSCOPE TRACE DUE TO VIBRATION AND PICKUP.

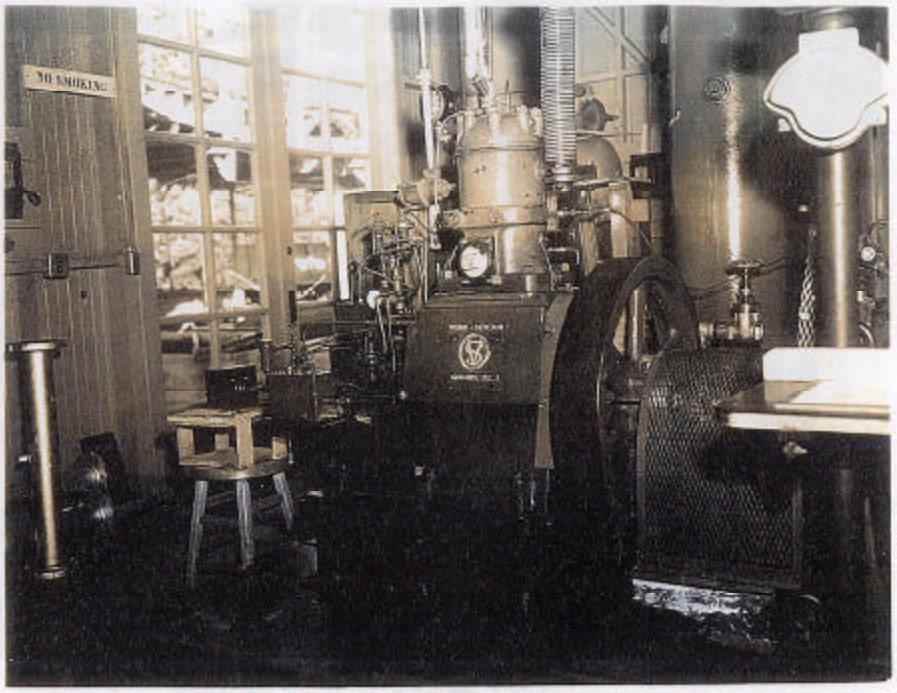

FIGURE (28)

TEST ENGINE ON DYNAMOMETER BED PLATE

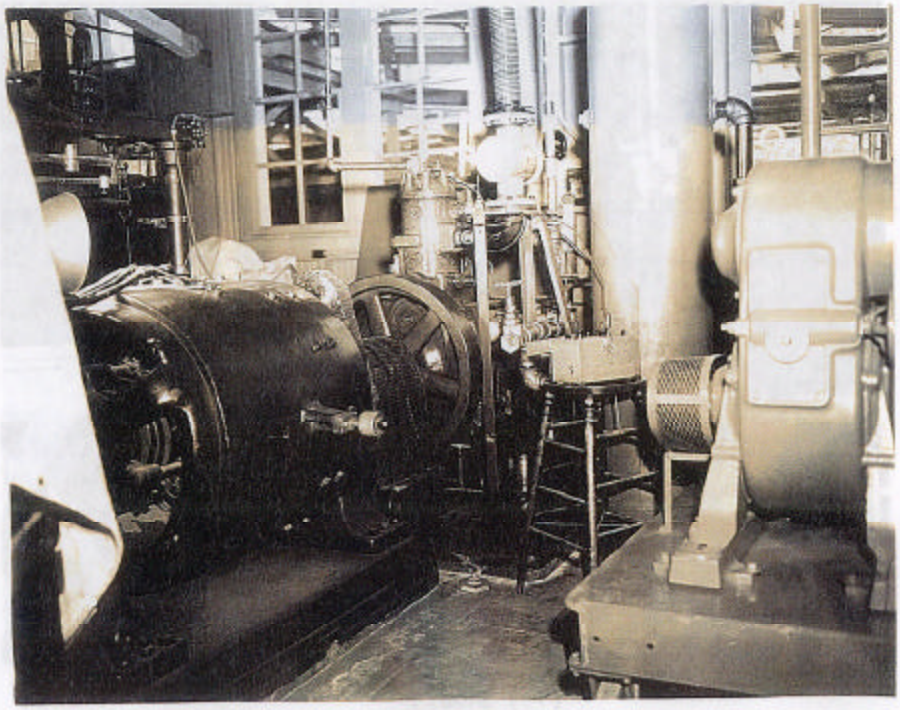

FIGURE (29)

TEST ENGINE WITH RECEIVER TANK NO. 1 IN POSITION.

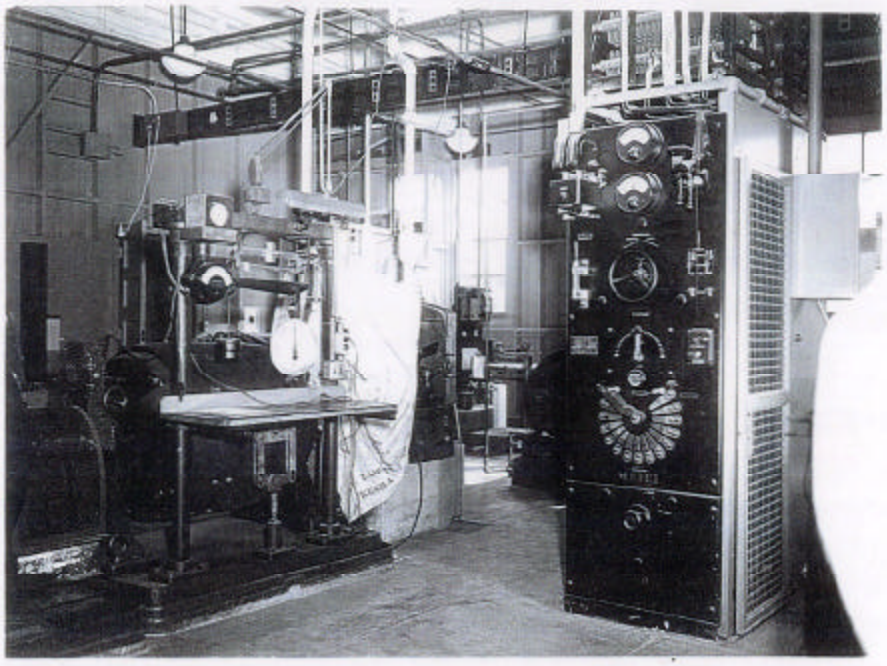

FIGURE (30)

DYNAMOMETER AND CONTROL PANEL.

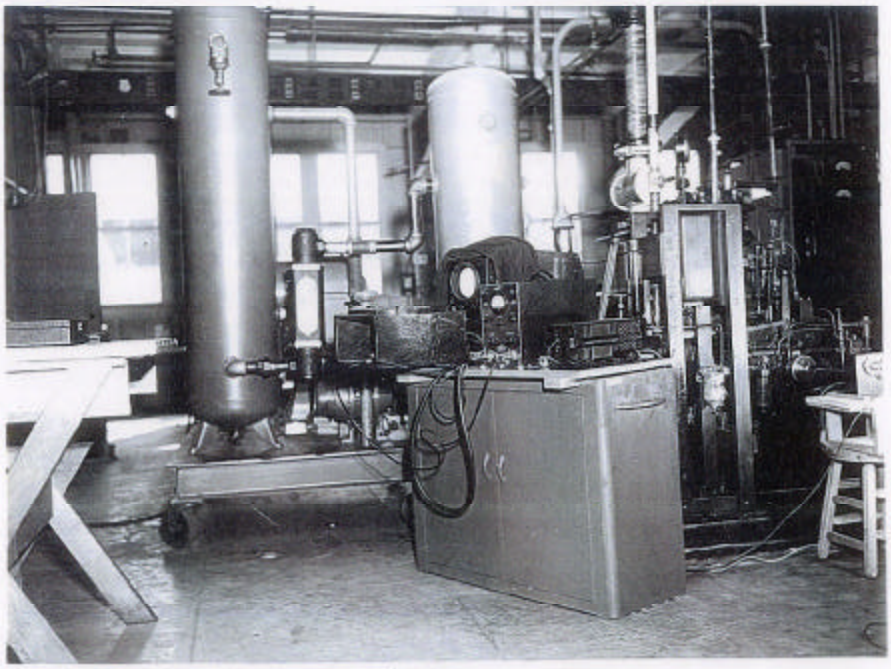

FIGURE (31)

AIR SUPPLY SYSTEM, FLOW METER AND ELECTRONIC INSTRUMENTS.

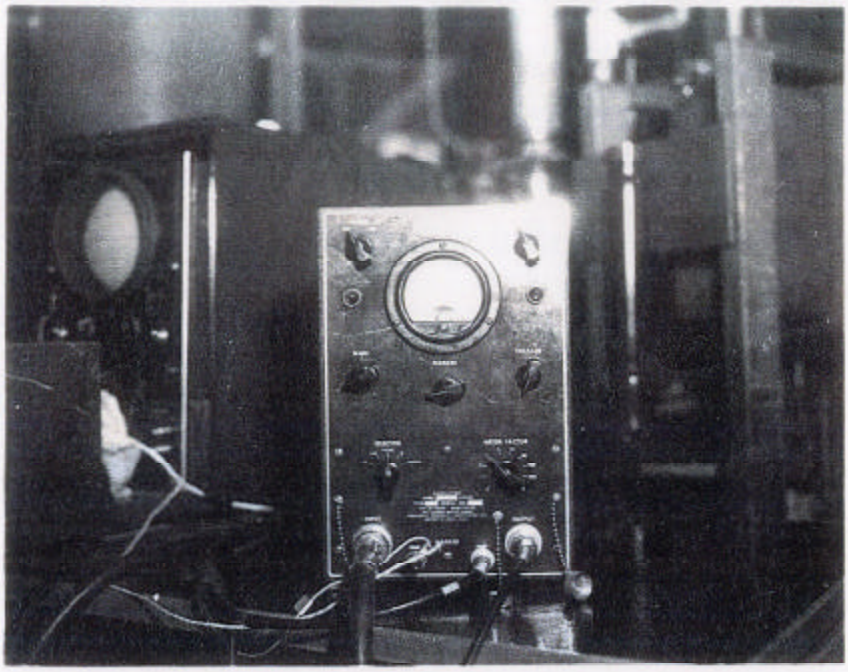

FIGURE (32)

AMPLIFIER AND CALIBRATING CIRCUIT.

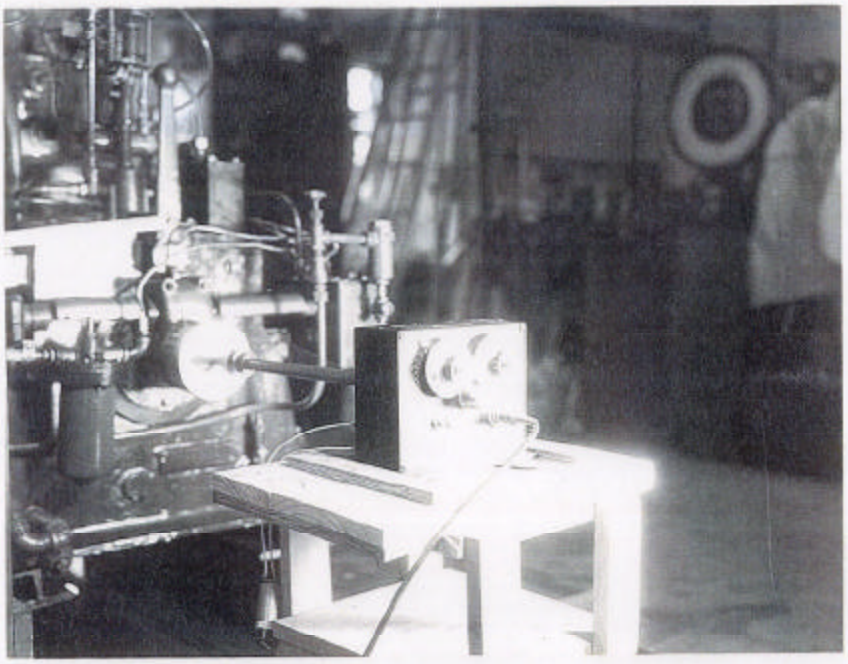

FIGURE (35)

MARKER AND SYNCHRONIZER UNIT.

FIGURE (33) AND (34) FOLLOW THIS PAGE.

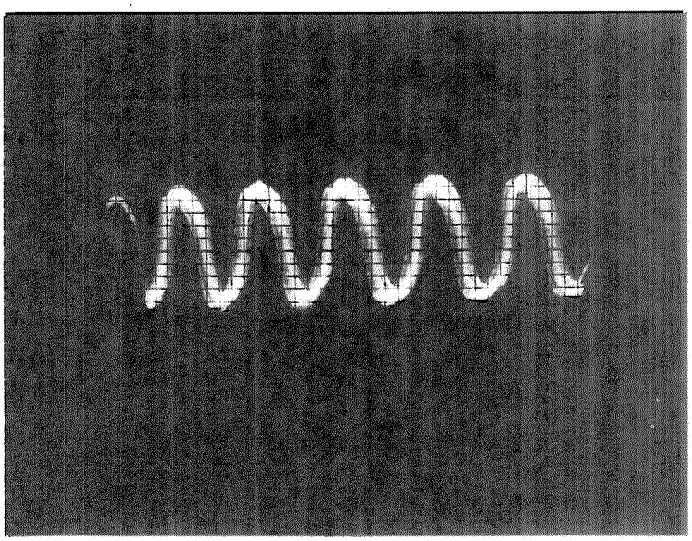

FIGURE (33)
CALIBRATION TRACE:
1 MILLIVOLT PER INCH DEFLECTION ON OSCILLOSCOPE SCREEN.

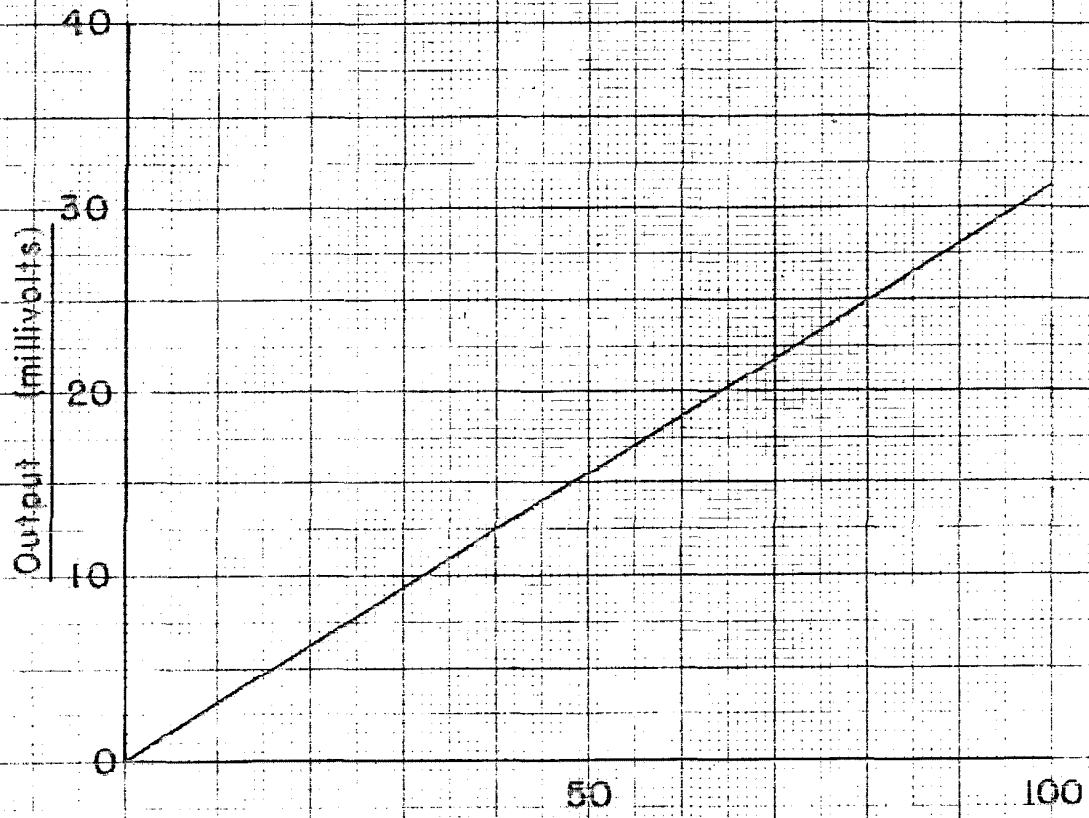

Fig. (34) Calibration of quartz crystal element

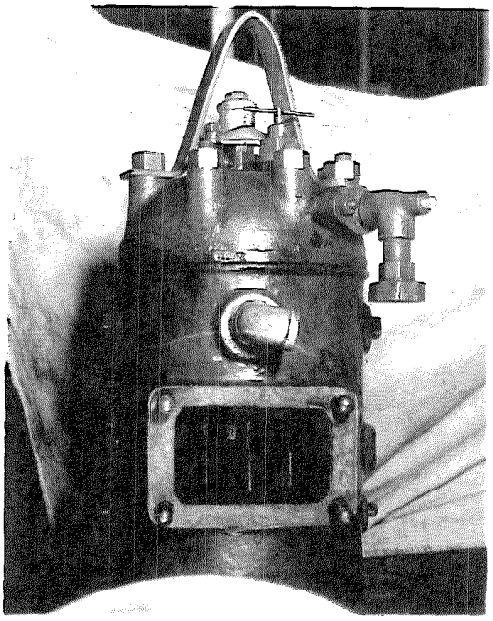

FIGURE (36)

TEST ENGINE CYLINDER AND EXHAUST PORT.

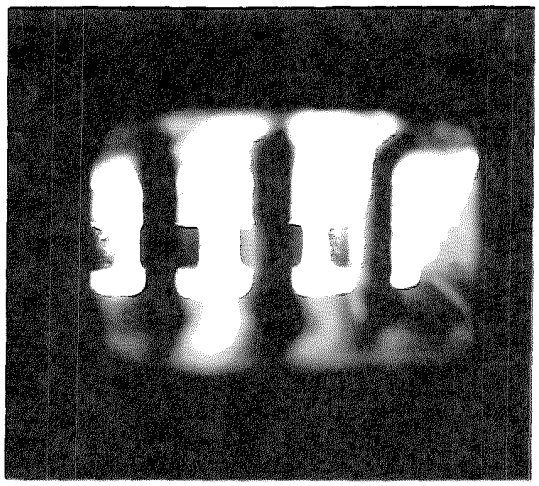

FIGURE (37)

VIEW INTO CYLINDER THROUGH EXHAUST PORT, SHOWING INTAKE PORTS.

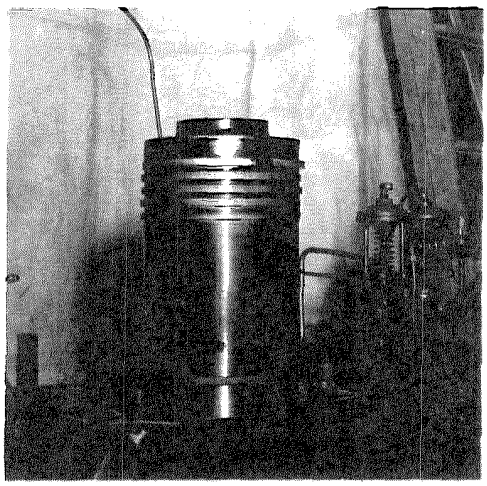

FIGURE (38)

TEST ENGINE PISTON WITH DEFLECTOR CROWN.

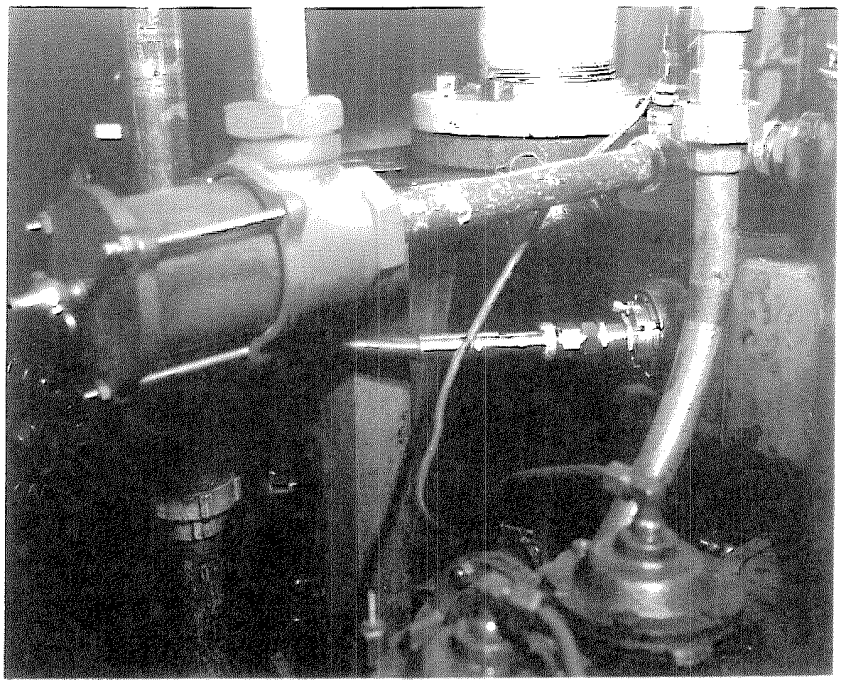

FIGURE (39)

CLOSE-UP OF CRYSTAL PICKUP MOUNTED IN EXHAUST.

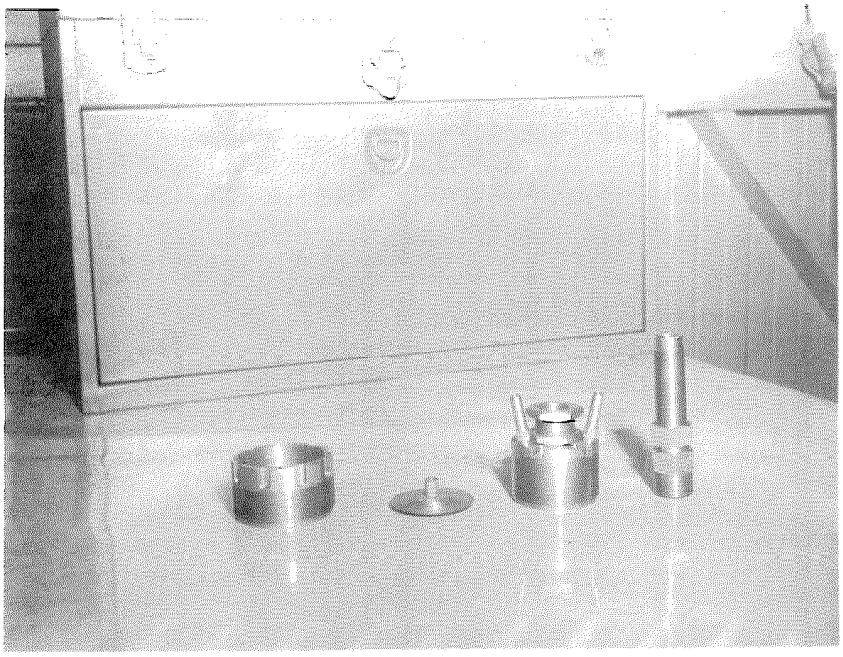

FIGURE (40)

LOW PRESSURE MULTIPLIER DISASSEMBLED AND QUARTZ CRYSTAL PICKUP ELEMENT.

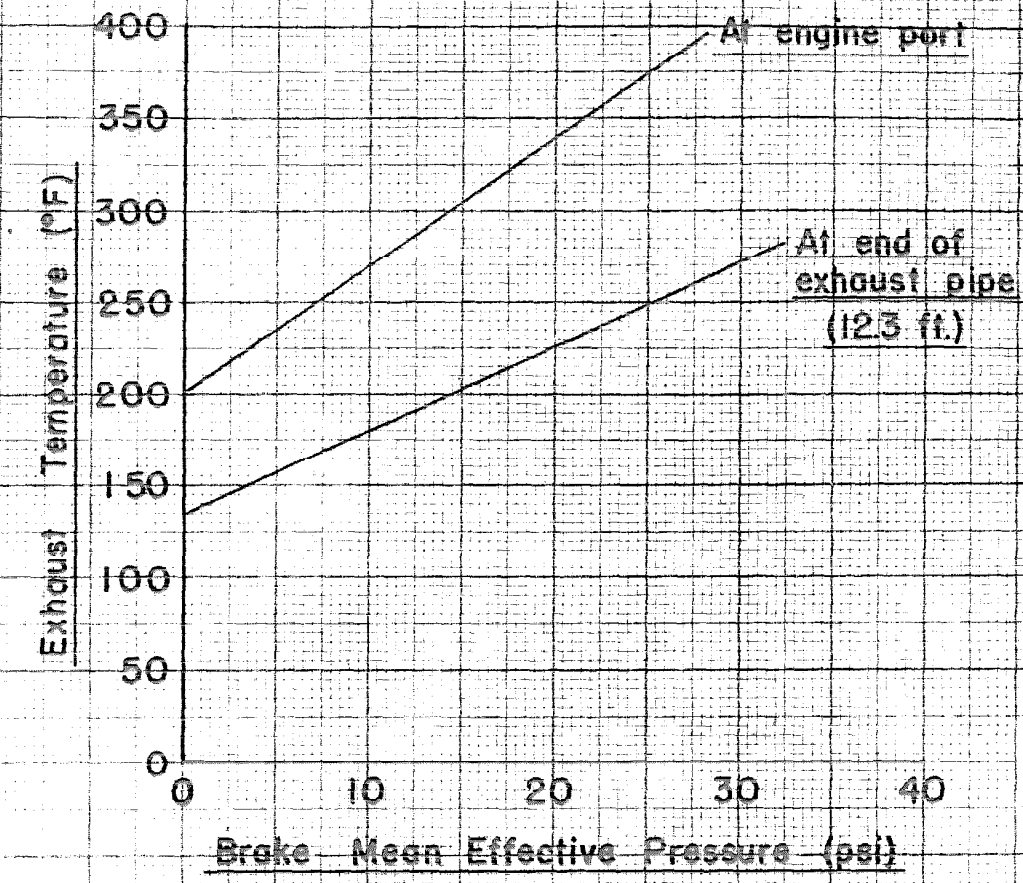

Fig.(41) Exhaust temperature as a function of brake mean effective pressure for two locations in test setup

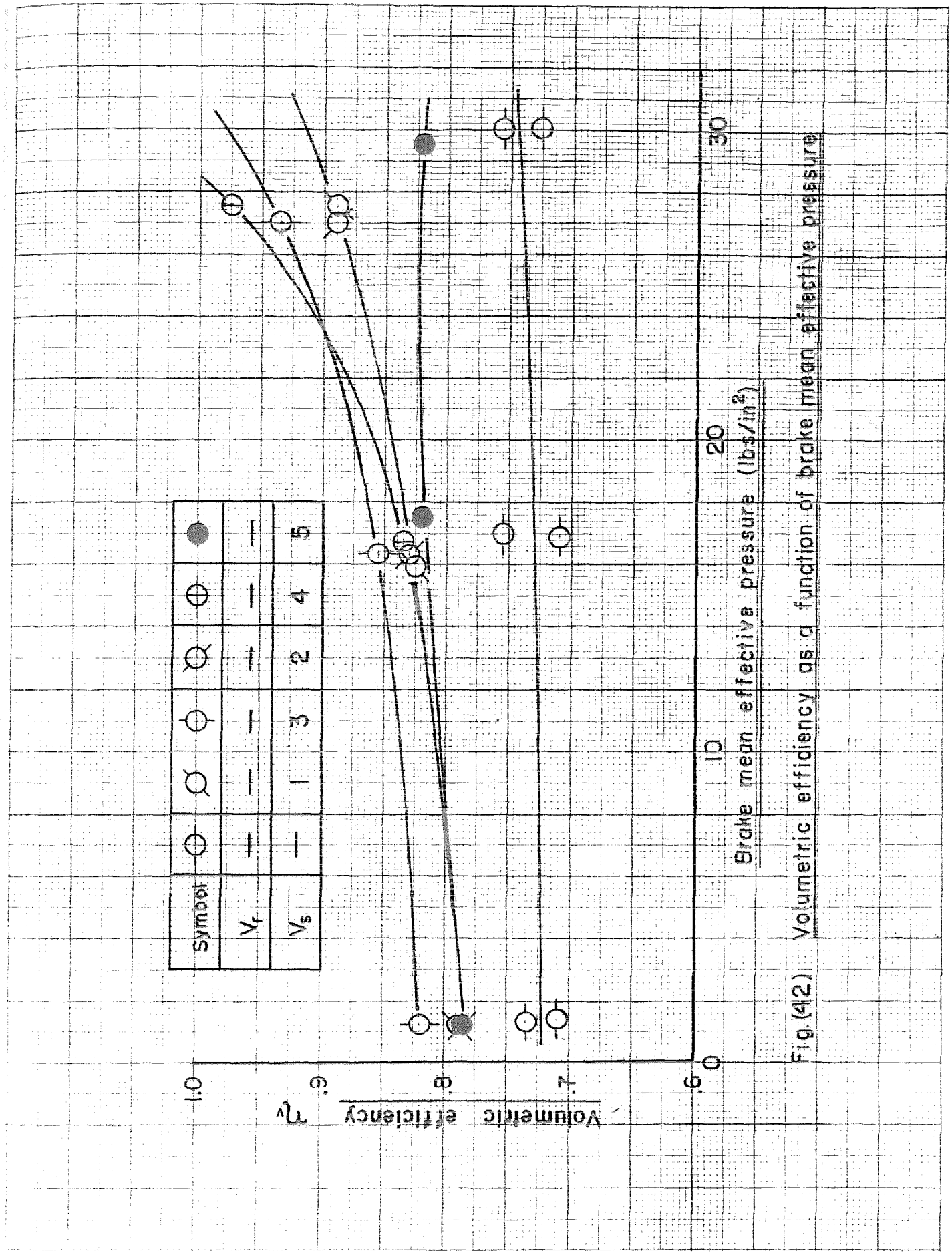

Fig. (42) Volumetric efficiency as a function of brake mean effective pressure

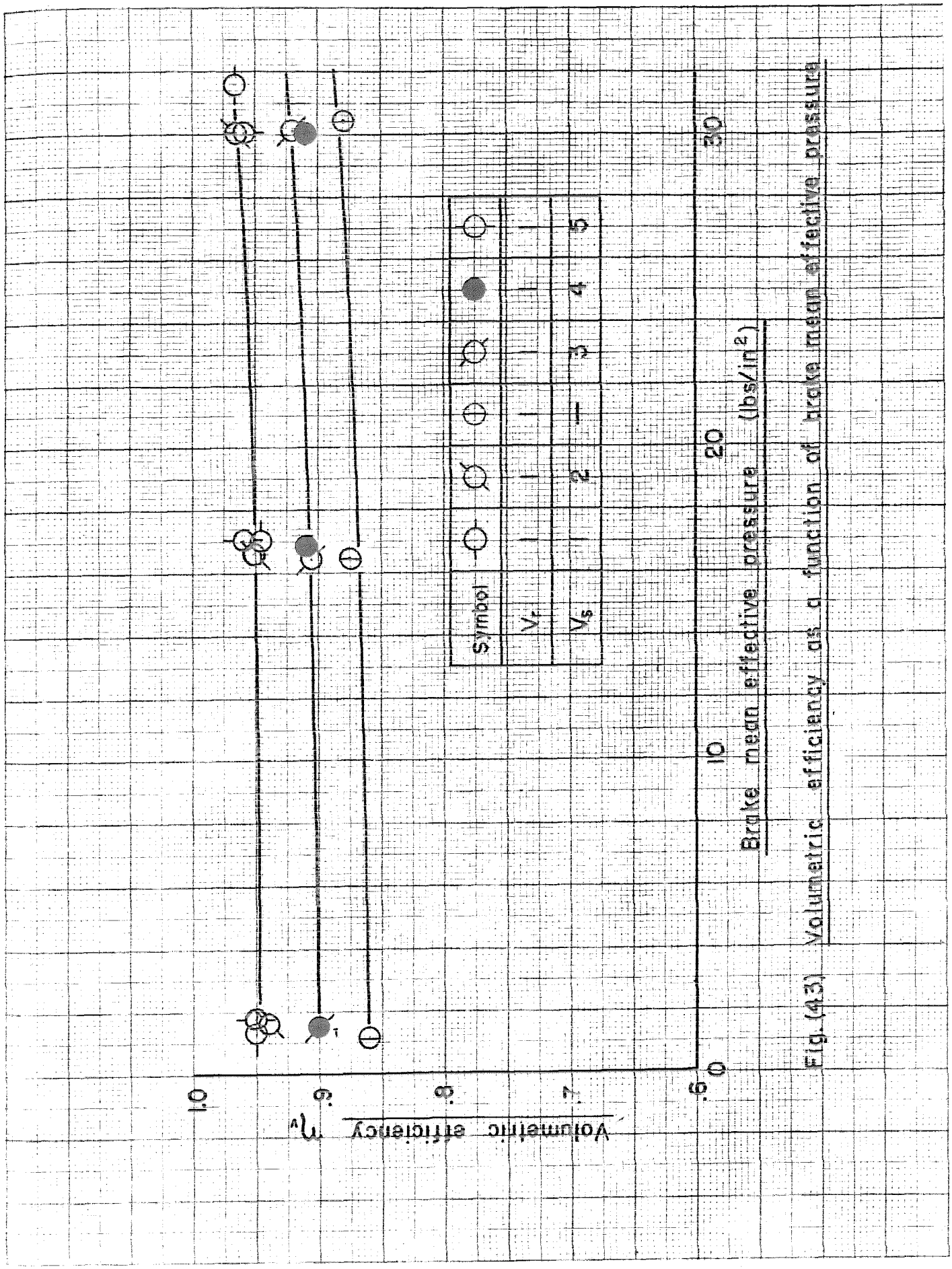

Fig. (43) Volumetric efficiency as a function of brake mean effective pressure

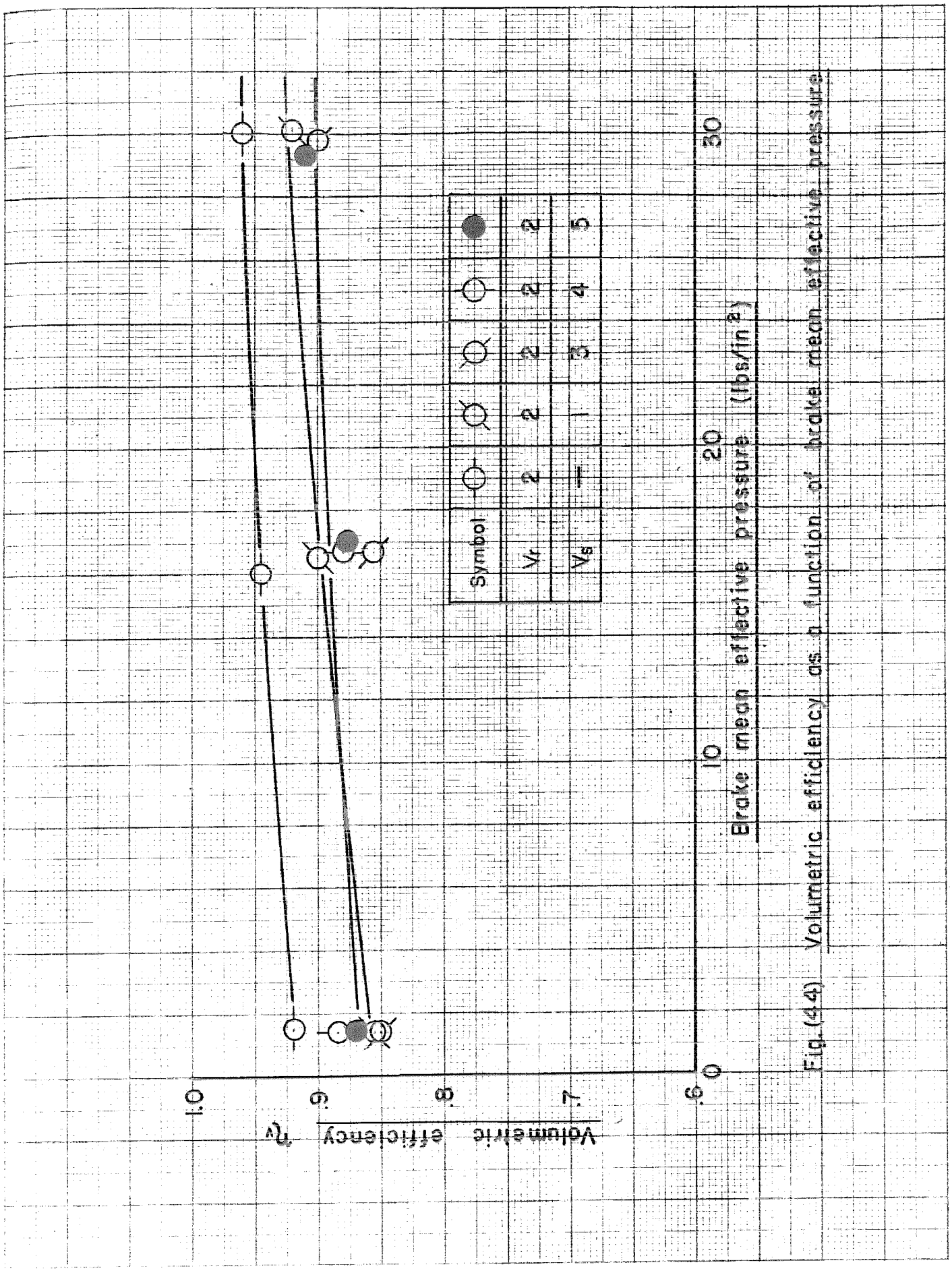

Fig. (44) Volumetric efficiency as a function of brake mean effective pressure

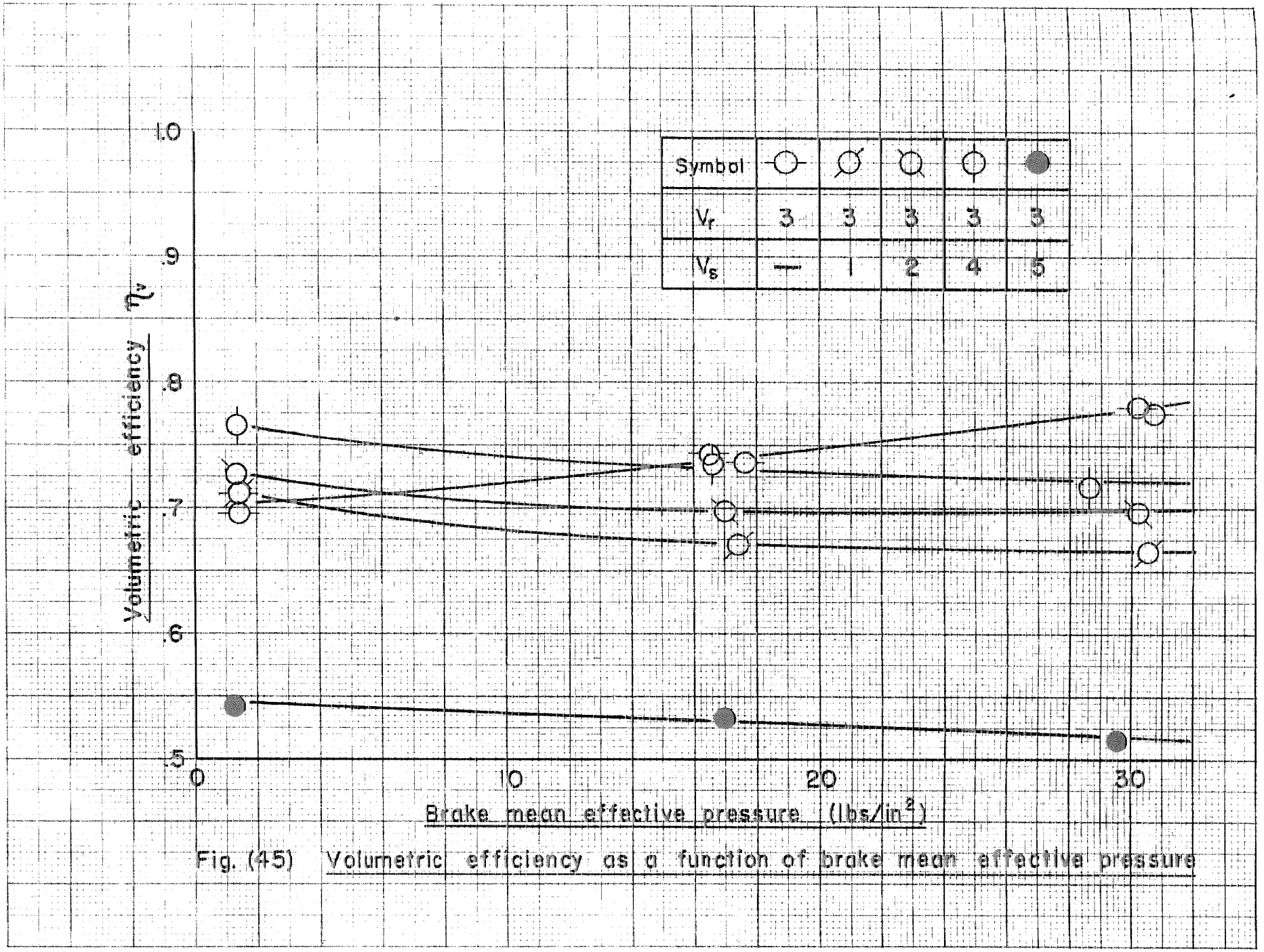

Fig. (45) Volumetric efficiency as a function of brake mean effective pressure

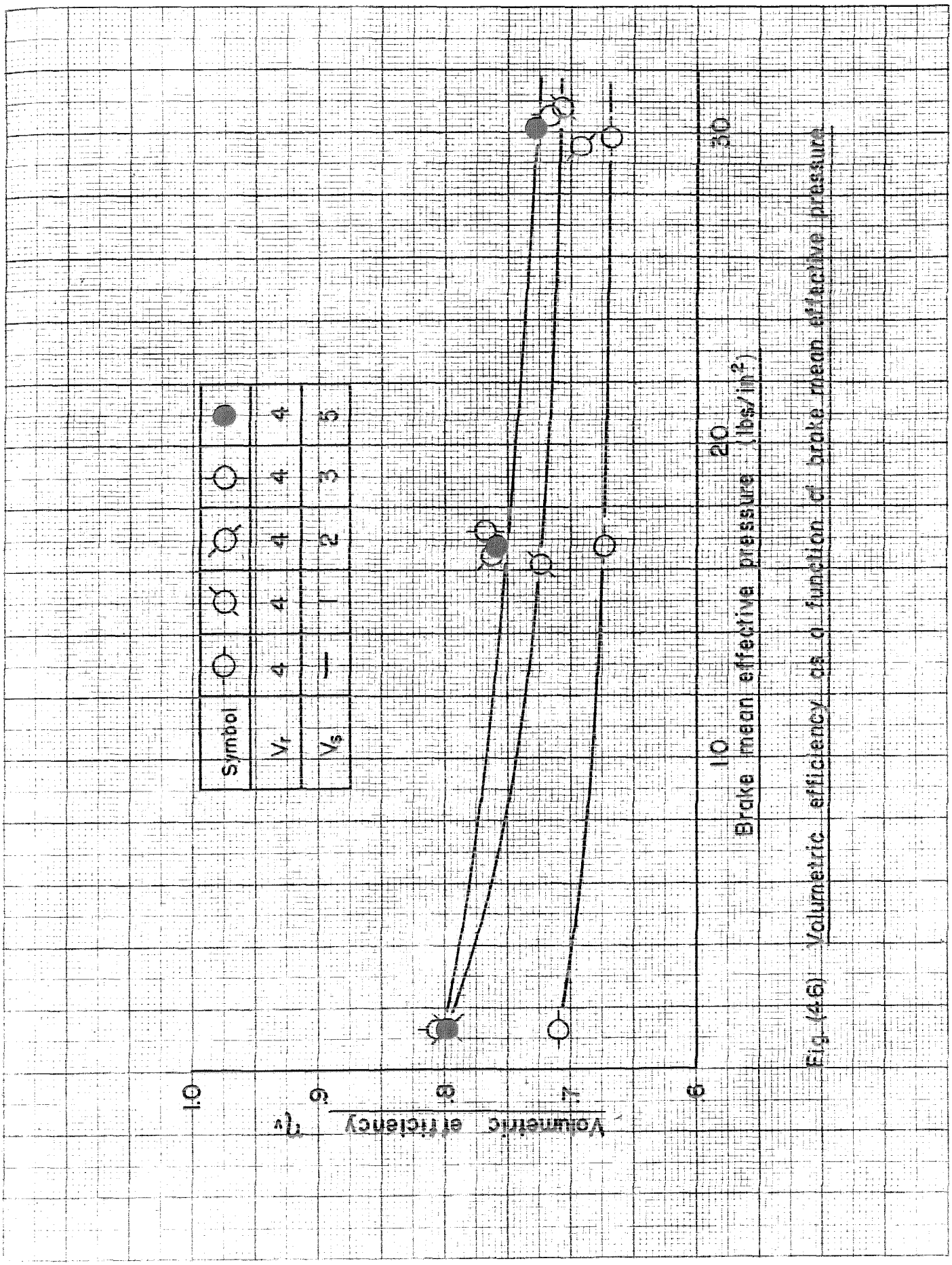

Fig. (4.6) Volumetric efficiency as a function of brake mean effective pressure

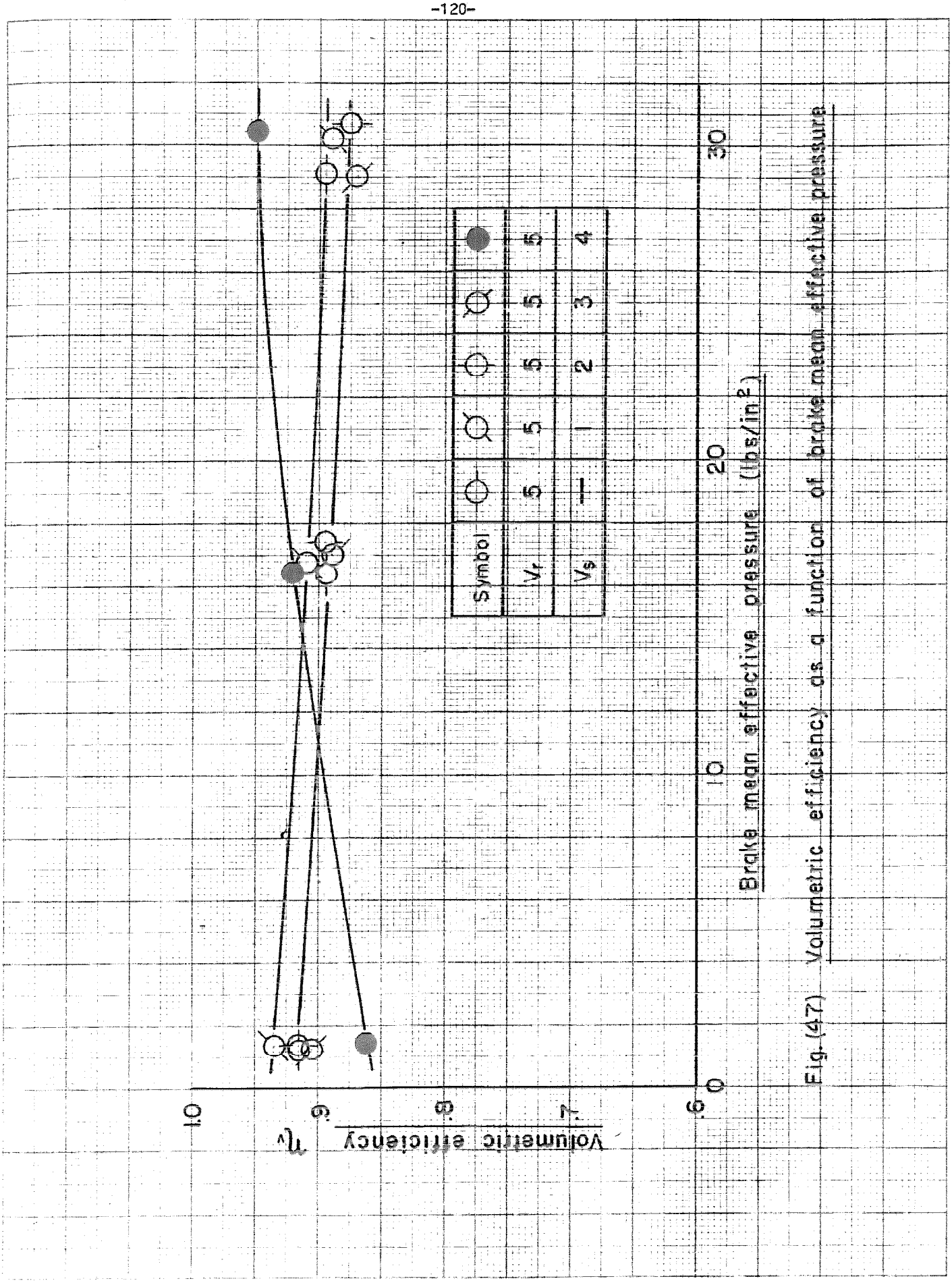

Fig. (47) Volumetric efficiency as a function of brake mean effective pressure

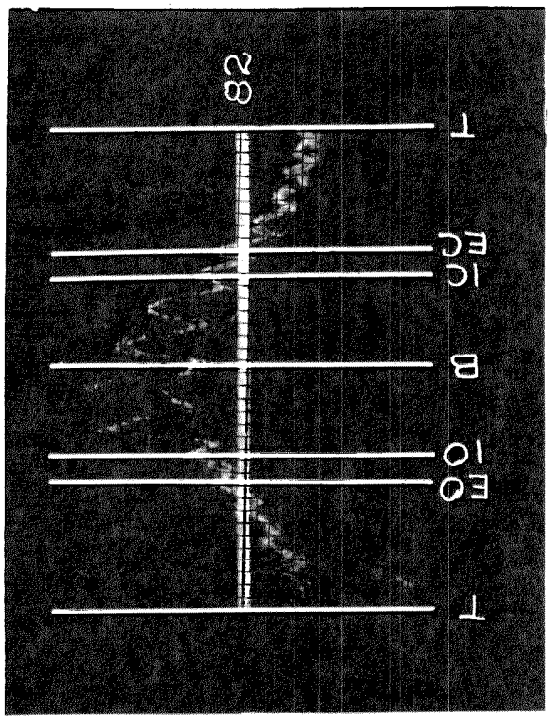
82
T
EC
IC
B
IO
EO
T

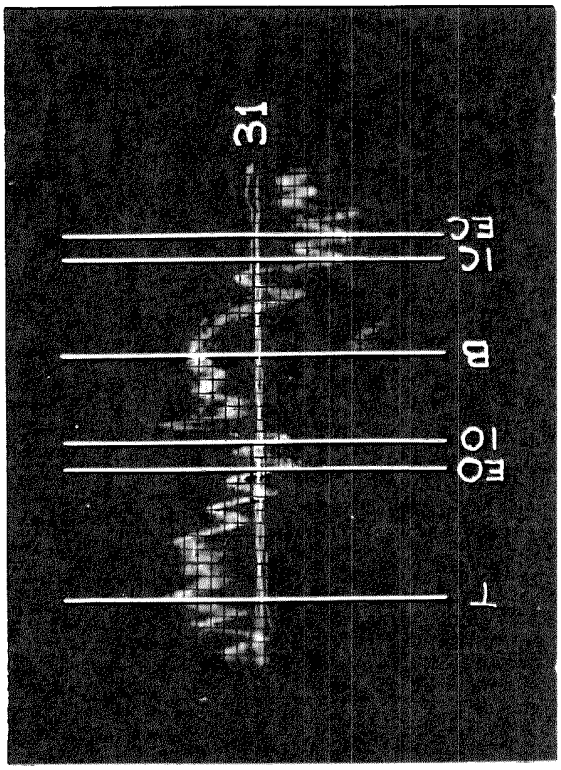
31
EC
IC
B
IO
EO
T

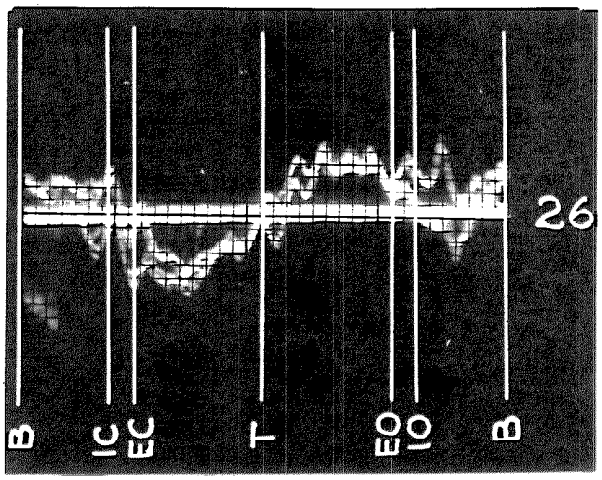
26
B
IC
EC
T
EO
IO
B

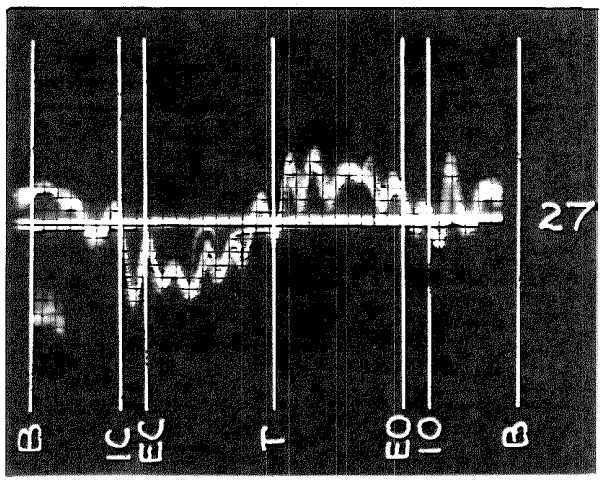
27
B
IC
EC
T
EO
IO
B

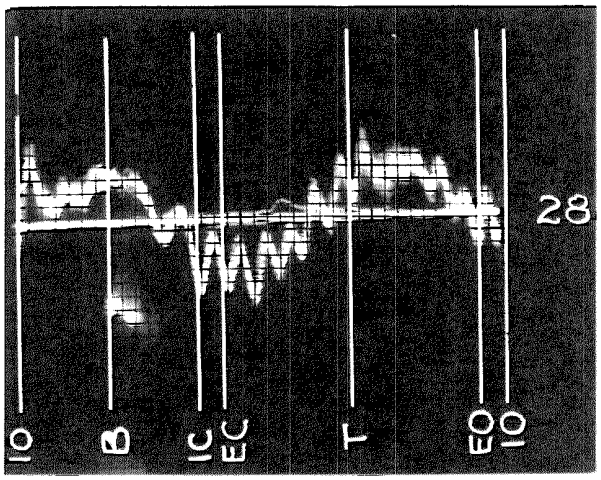
28
IO
B
IC
EC
T
EO
IO

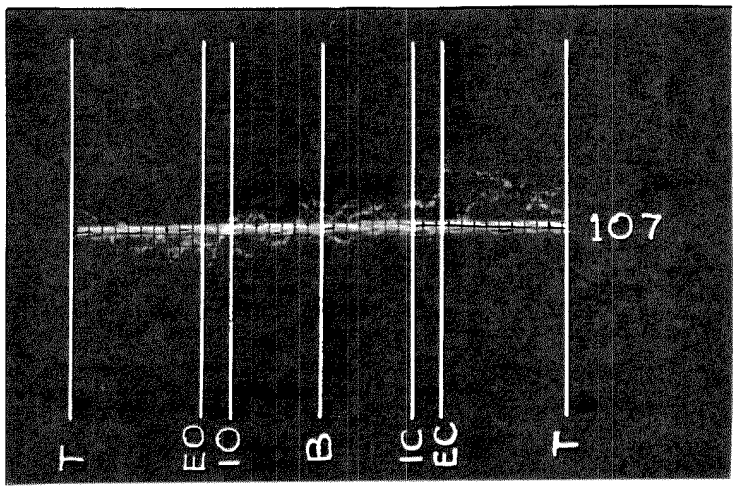
T
EO
IO
B
IC
EC
T
107

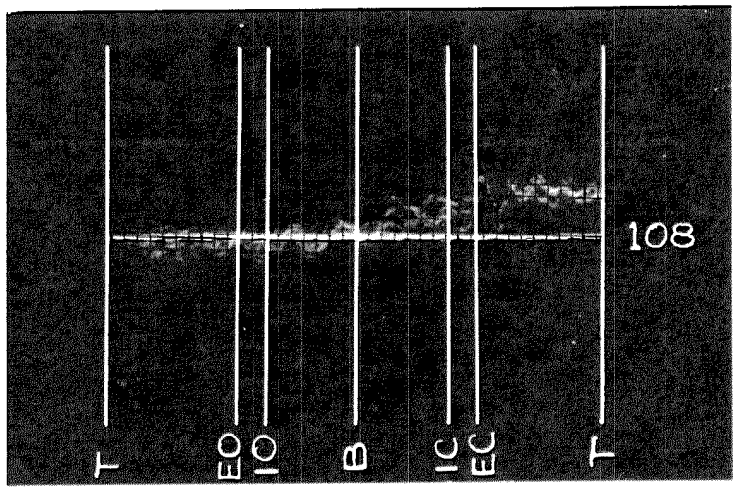
T
EO
IO
B
IC
EC
T
108

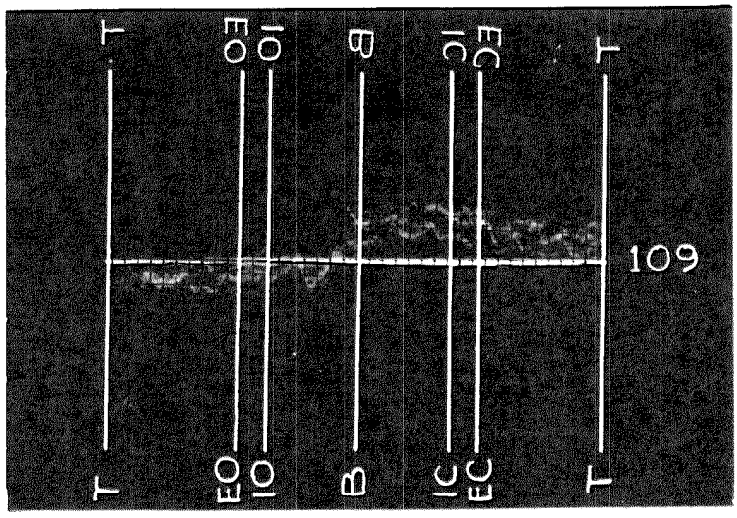
T
EO
IO
B
IC
EC
T
109

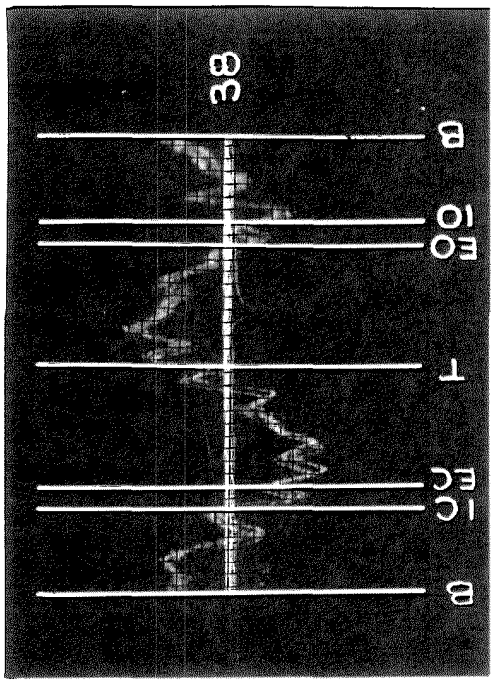
38
B
EO
T
EC
IC
B

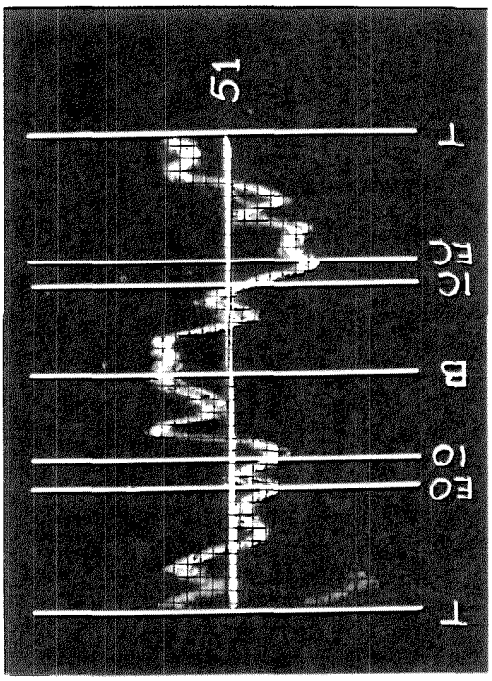
51
T
EC
IC
B
EO
T

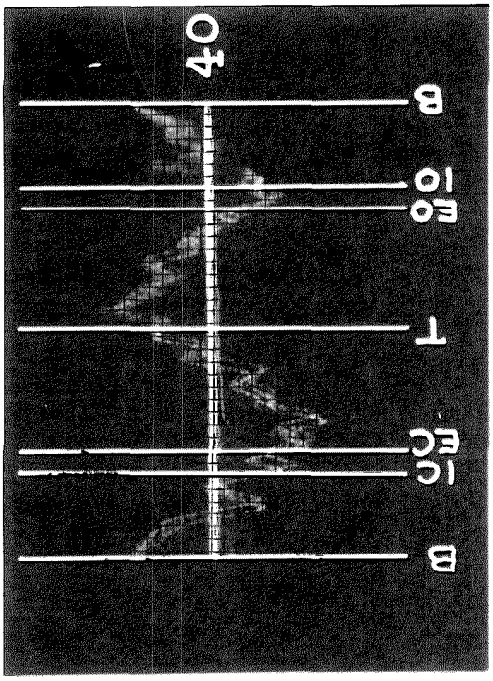
40
B
EO
T
EC
IC
B

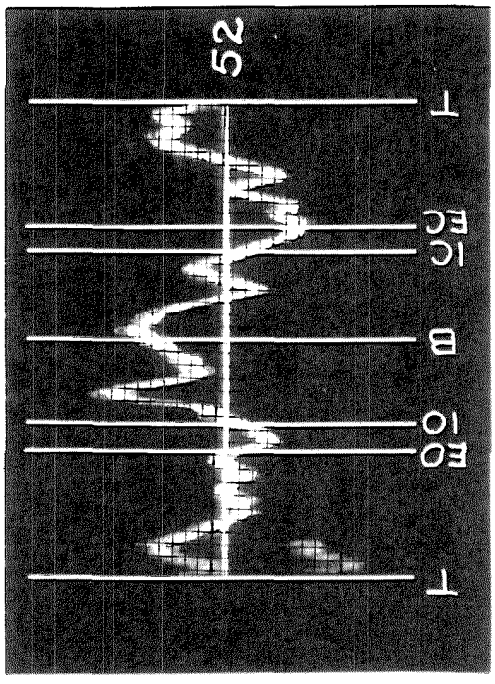
52
T
EC
IC
B
EO
T

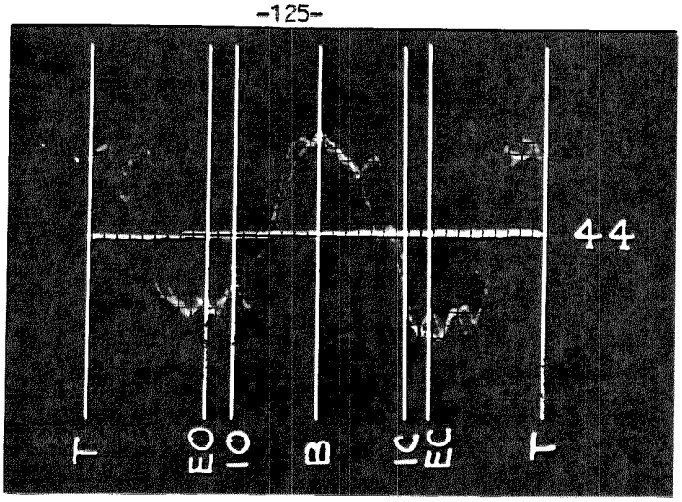
44
T
EO
IO
B
IC
EC
T

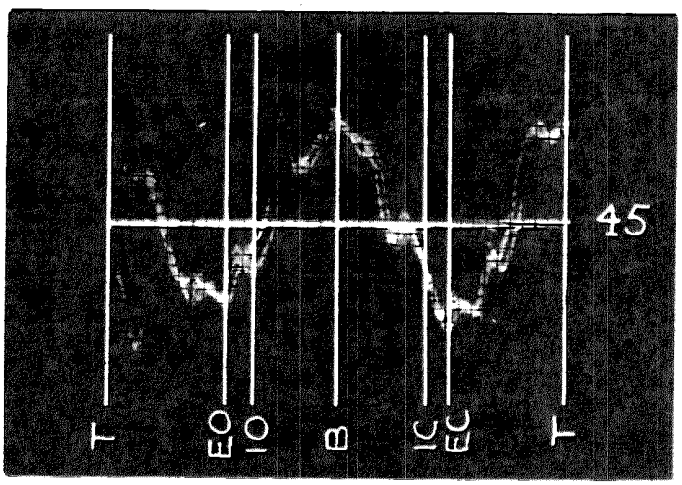
45
T
EO
IO
B
IC
EC
T

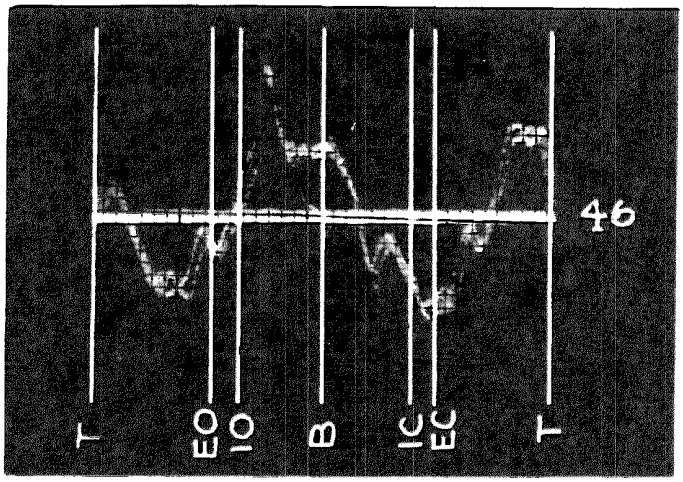
46
T
EO
IO
B
IC
EC
T

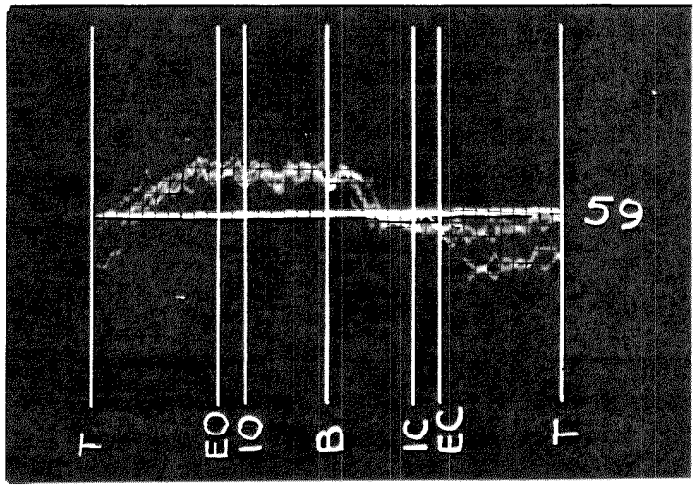
59
T
EO
IO
B
IC
EC
T

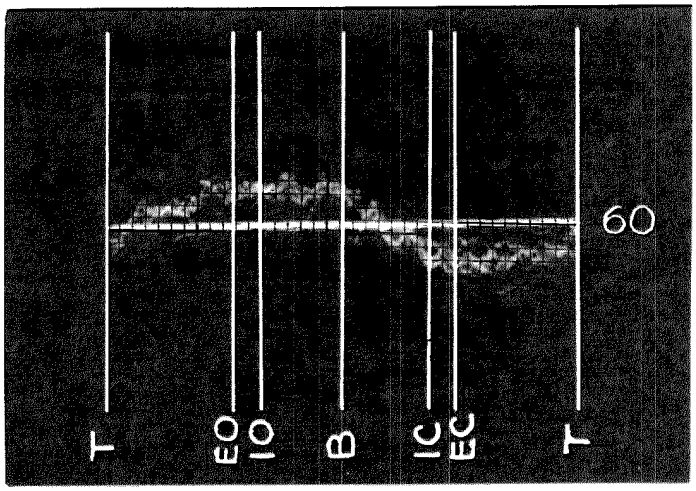
60
T
EO
IO
B
IC
EC
T

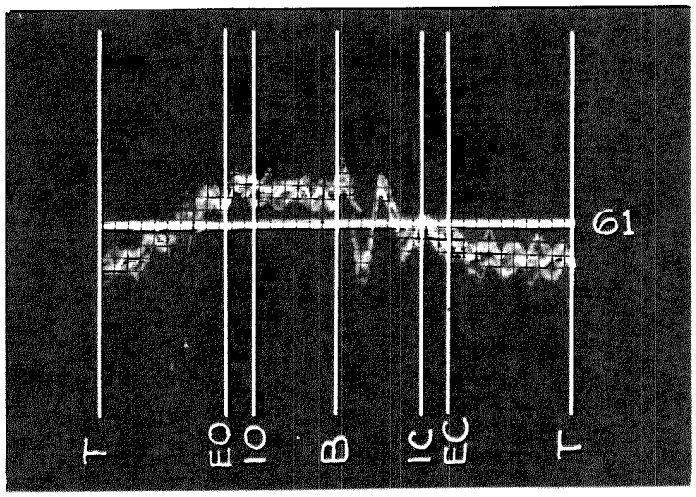
61
T
EO
IO
B
IC
EC
T

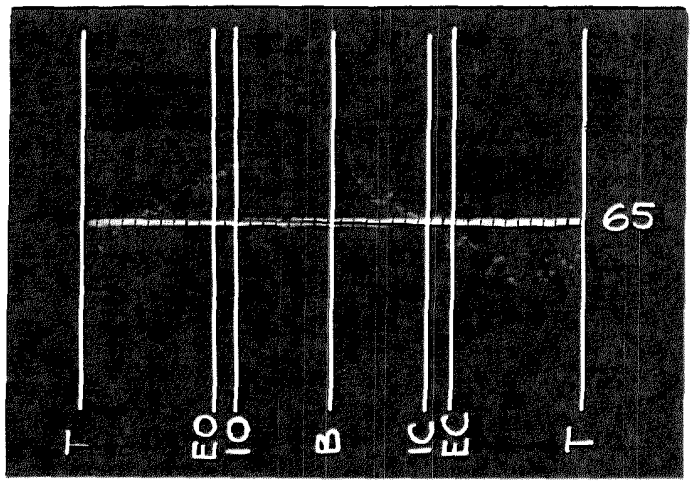
65
T
EO
IO
B
IC
EC
T

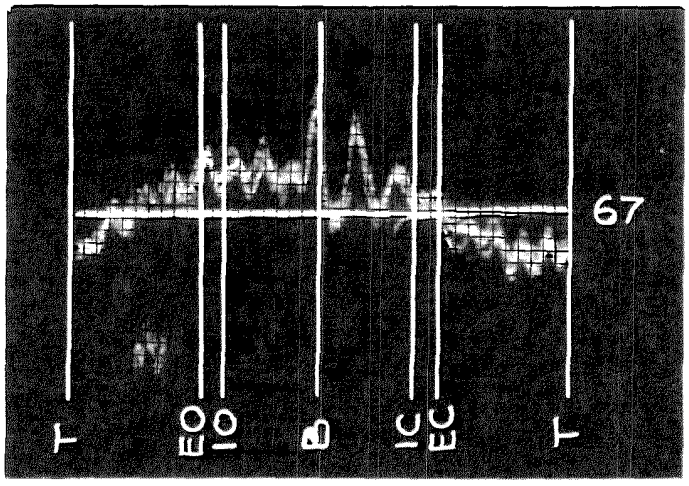
67
T
EO
IO
B
IC
EC
T

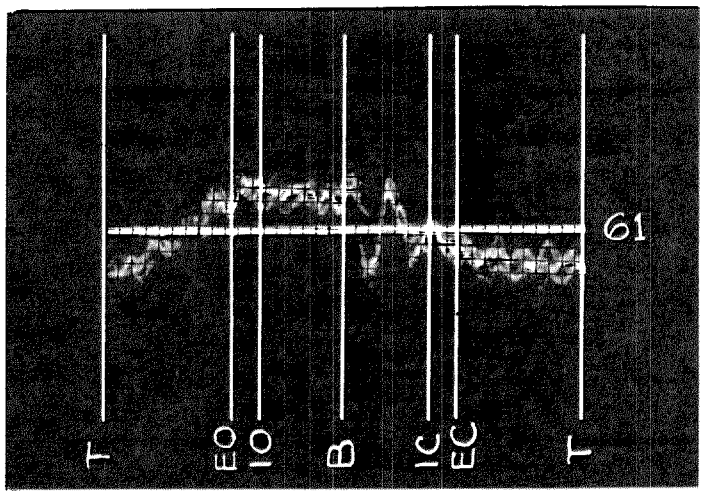
61
T
EO
IO
B
IC
EC
T

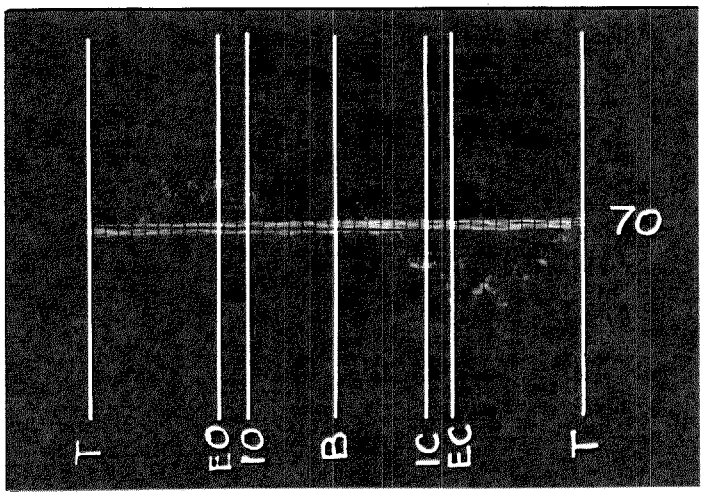
70
T
EO
IO
B
IC
EC
T

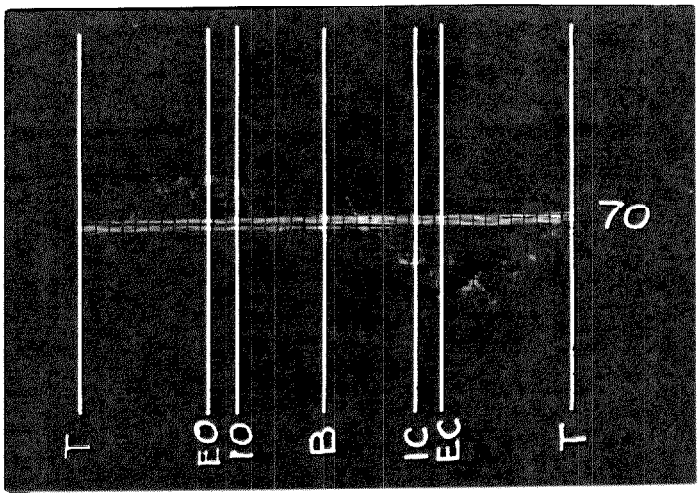
T
EO
IO
B
IC
EC
T
70

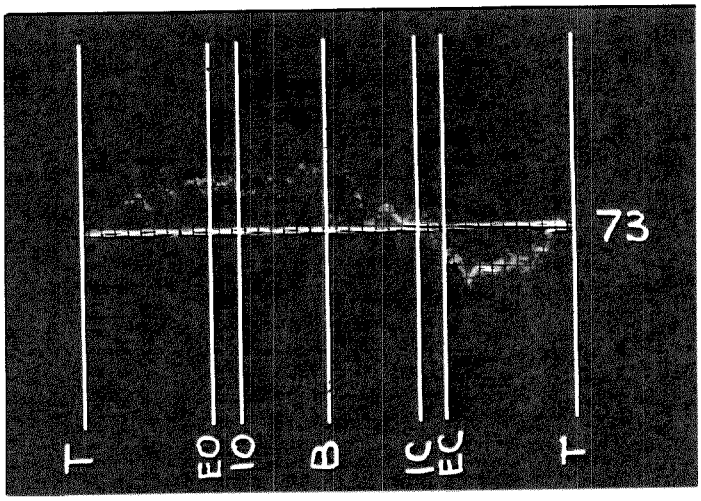
T
EO
IO
B
IC
EC
T
73

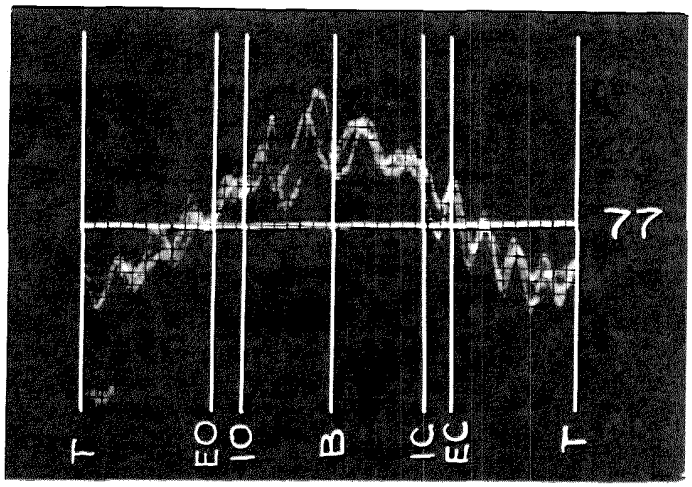
77
T
EO
IO
B
IC
EC
T

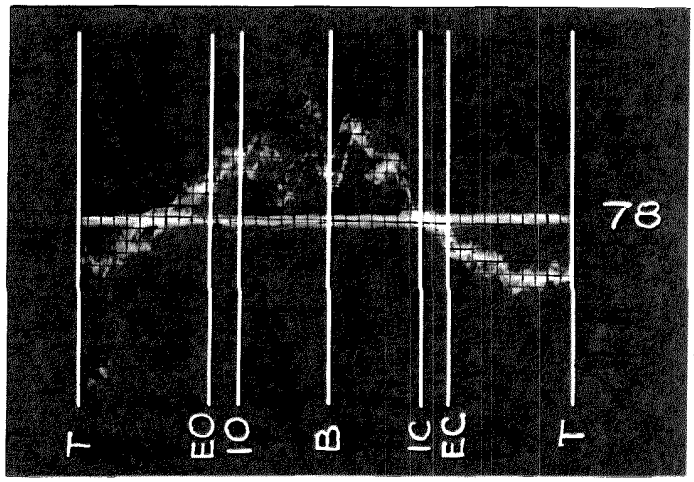
78
T
EO
IO
B
IC
EC
T

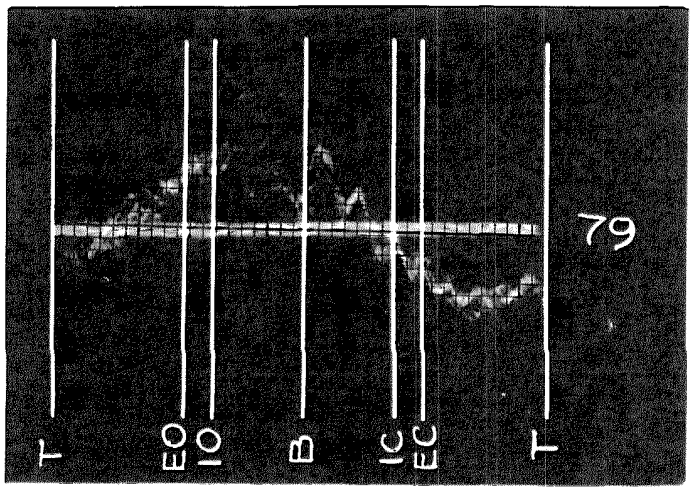
79
T
EO
IO
B
IC
EC
T

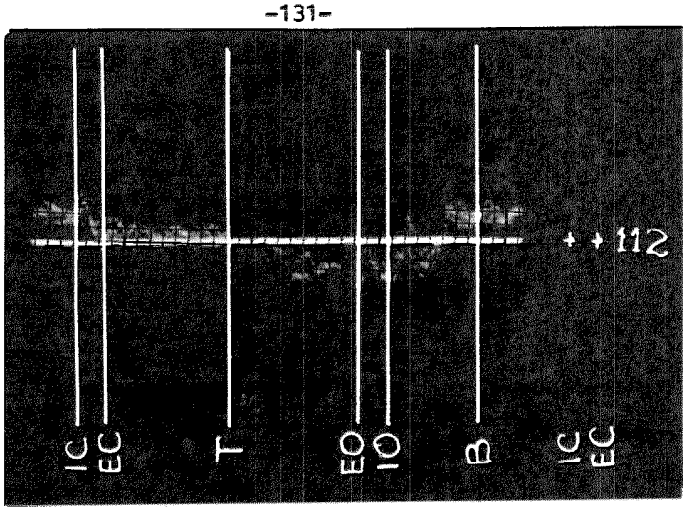
112
IC
EC
T
EO
IO
B
IC
EC

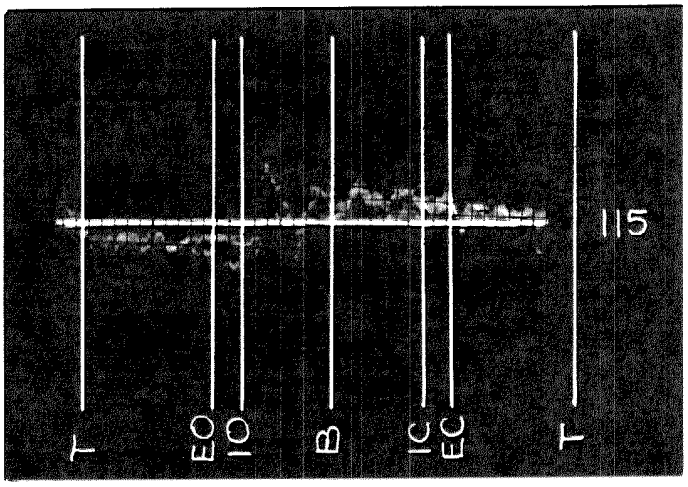
115
T
EO
IO
B
IC
EC
T

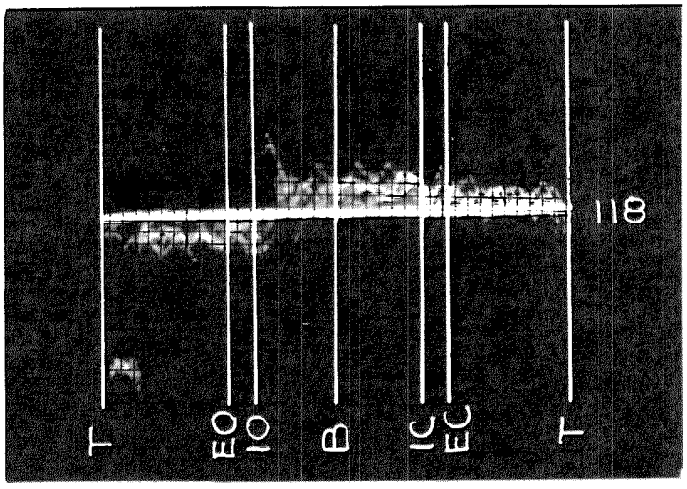
118
T
EO
IO
B
IC
EC
T

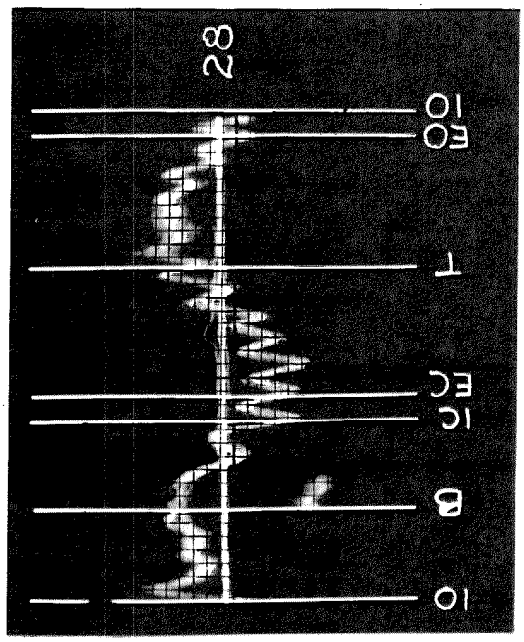
28
IO
EO
T
EC
IC
B
IO

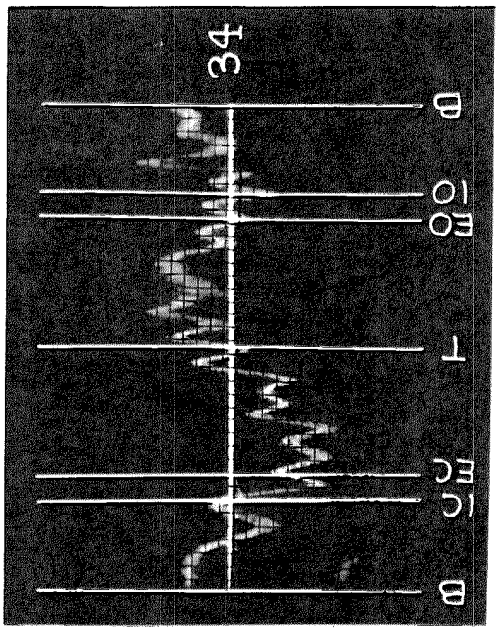
34
B
IO
EO
T
EC
IC
B

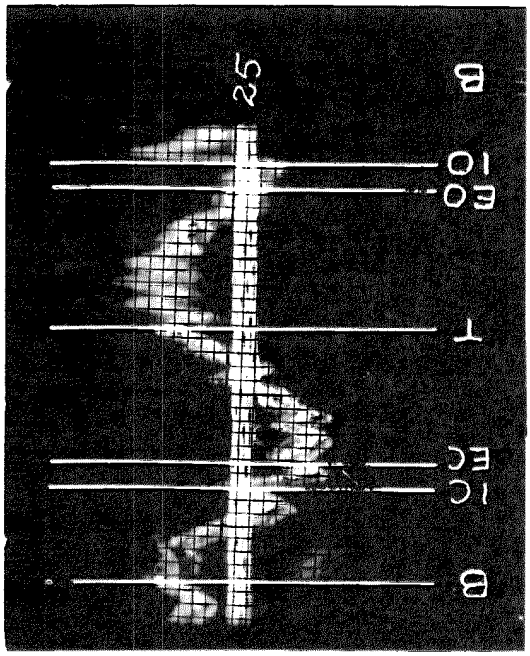
25
B
IO
EO
T
EC
IC
B

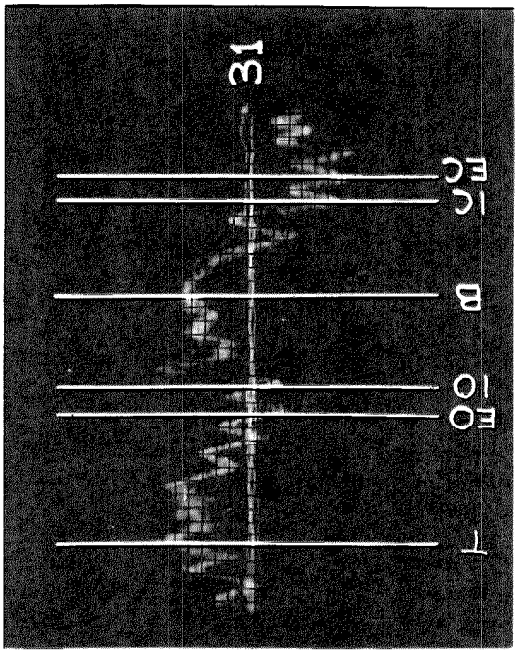
31
EC
IC
B
IO
EO
T

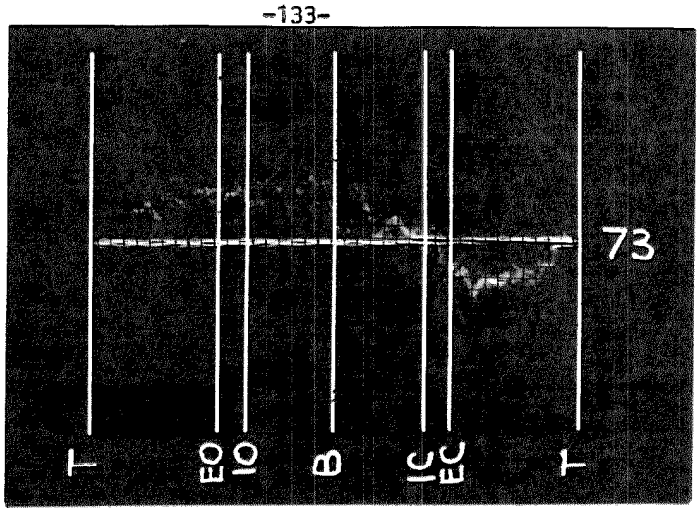
73
T
EO
IO
B
IC
EC
T

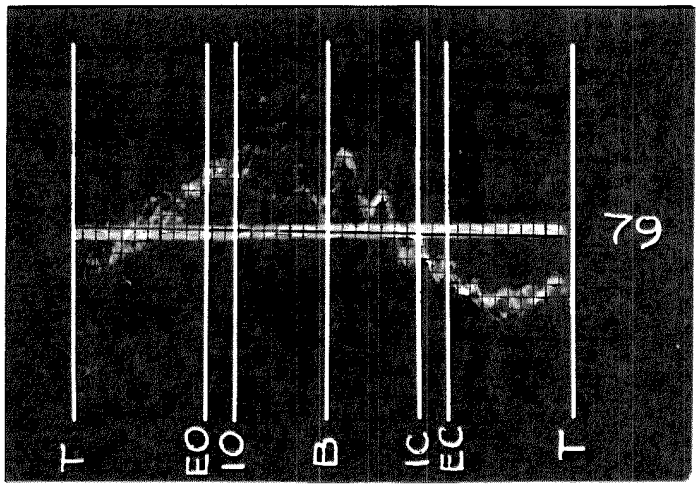
79
T
EO
IO
B
IC
EC
T

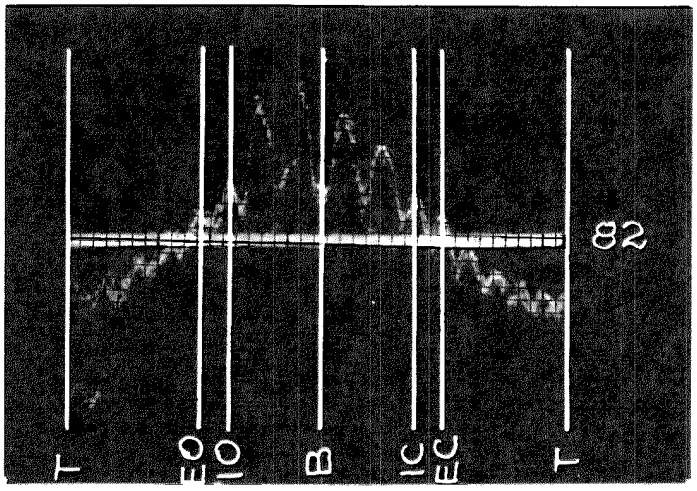
82
T
EO
IO
B
IC
EC
T

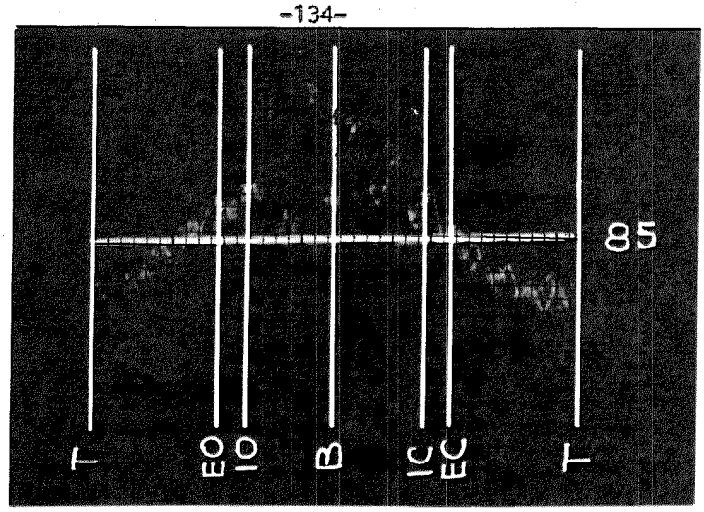
85
T
EO
IO
B
IC
EC
T

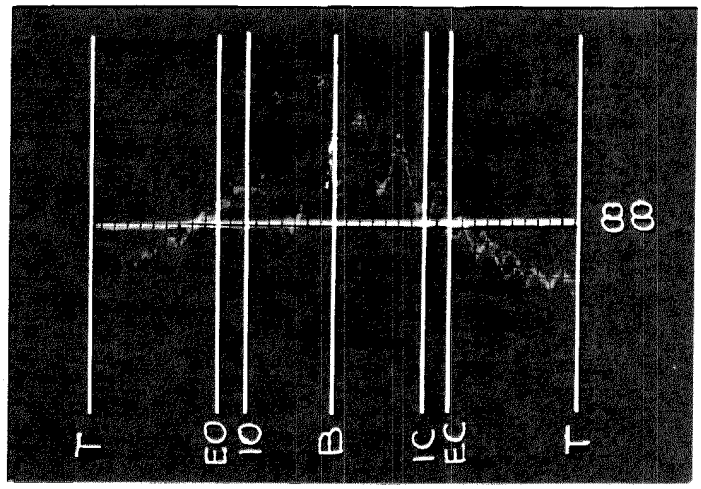
88
T
EO
IO
B
IC
EC
T

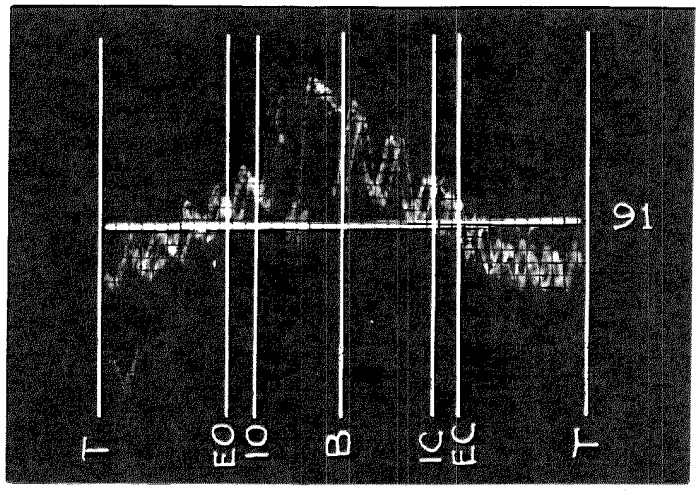
91
T
EO
IO
B
IC
EC
T

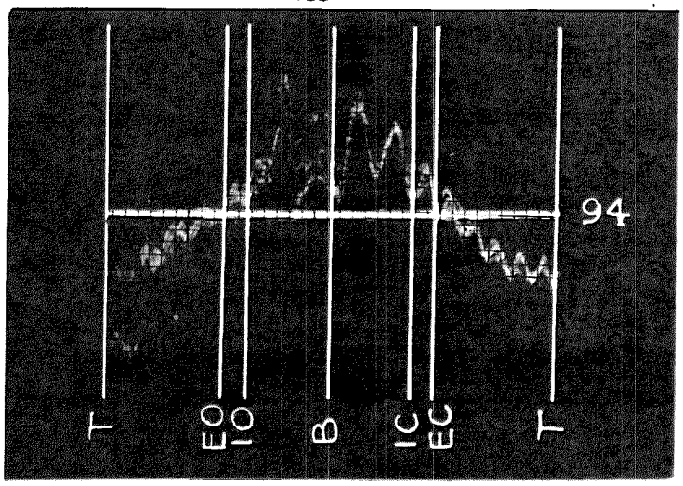
94
T
EO
IO
B
IC
EC
T

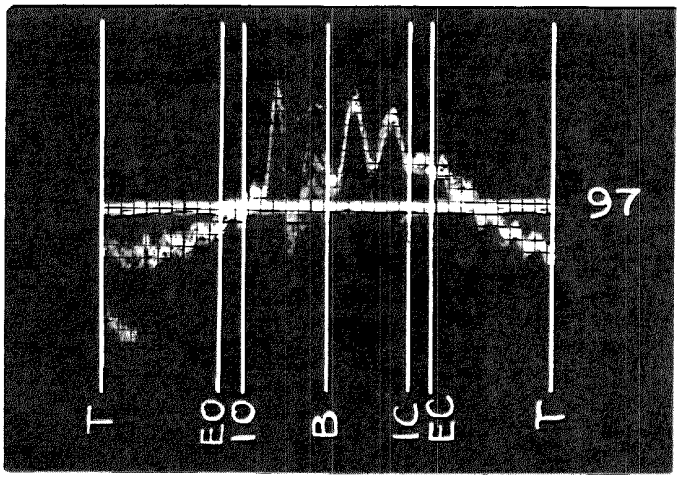
97
T
EO
IO
B
IC
EC
T

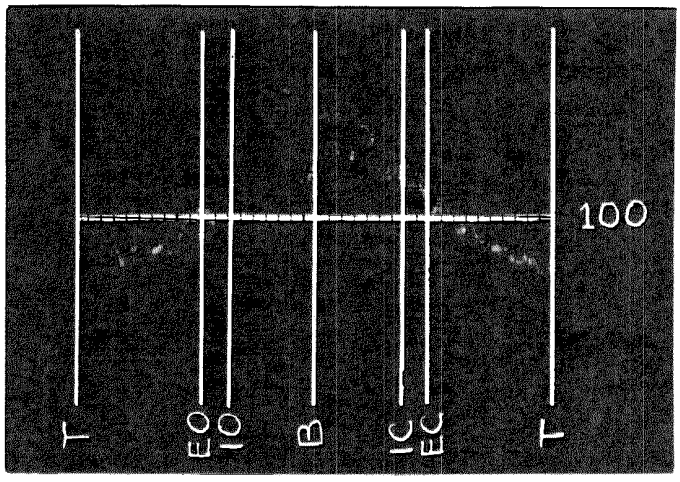
100
T
EO
IO
B
IC
EC
T

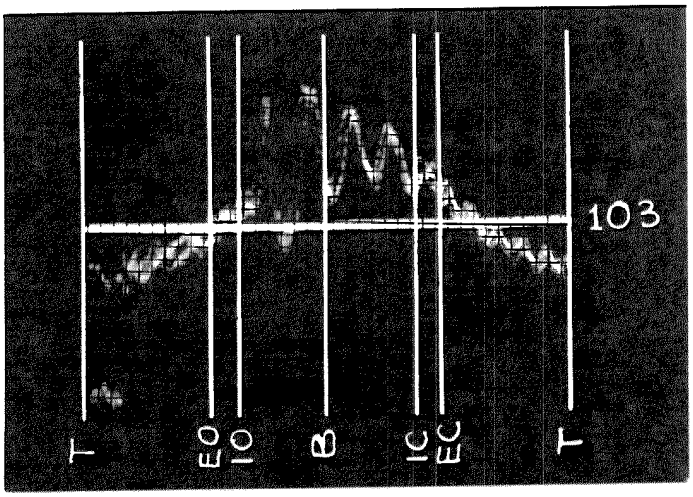
103
T
EO
IO
B
IC
EC
T

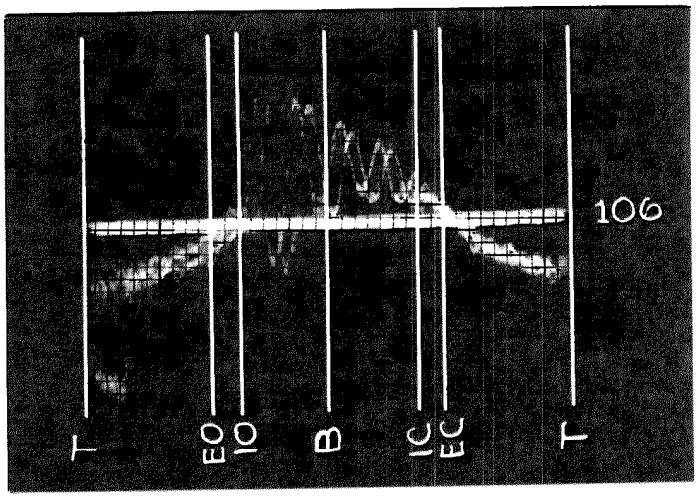
106
T
EO
IO
B
IC
EC
T

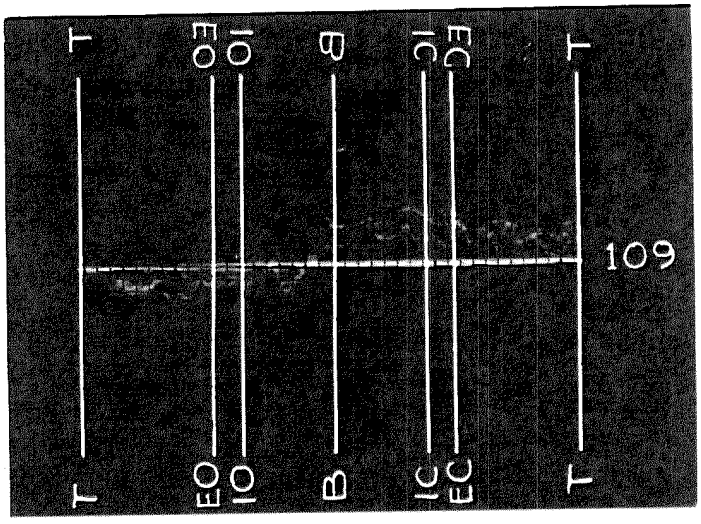
109
T
EO
IO
B
IC
EC
T

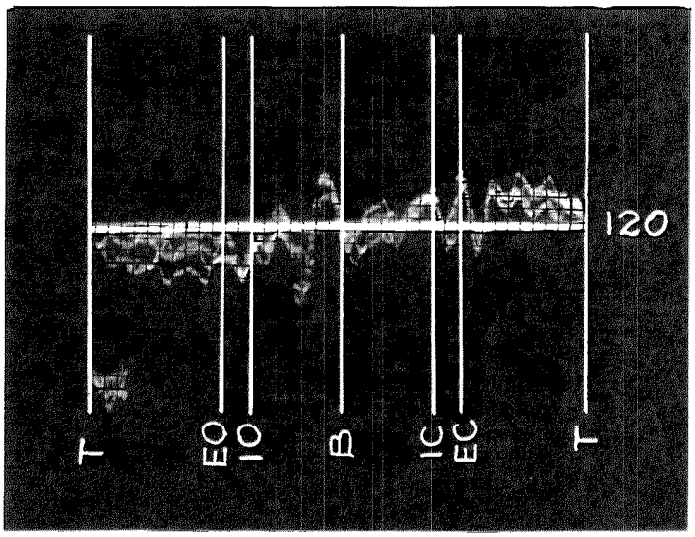
T
EO
IO
B
IC
EC
T
120